TECHNISCHE UNIVERSITÄT MÜNCHEN

Fakultät Wissenschaftszentrum Weihenstephan für Ernährung, Landnutzung und Umwelt

Lehrstuhl für Entwicklungsgenetik

Fox transcription factors in adult neurogenesis

Iris Schäffner

Vollständiger Abdruck der von der Fakultät Wissenschaftszentrum Weihenstephan für Ernährung, Landnutzung und Umwelt der Technischen Universität München zur Erlangung des akademischen Grades eines

Doktors der Naturwissenschaften

genehmigten Dissertation.

Vorsitzender: Univ.-Prof. Dr. S. Scherer

Prüfer der Dissertation: 1. Univ.-Prof. Dr. W. Wurst

2. Univ.-Prof. Dr. D. C. Lie,
Friedrich-Alexander-Universität Erlangen-Nürnberg

Die Dissertation wurde am 08.01.2014 bei der Technischen Universität München eingereicht und durch die Fakultät Wissenschaftszentrum Weihenstephan für Ernährung, Landnutzung und Umwelt am 19.02.2014 angenommen.

meinen Eltern

I Abstract

It is now well accepted that adult neural stem cells produce new functional neurons in discrete regions of the adult brain – the dentate gyrus of the hippocampal formation and the subventricular zone of the lateral ventricles. Neurogenesis in the adult hippocampus contributes to learning and memory; moreover there are indications that impaired hippocampal neurogenesis contributes to cognitive dysfunction in ageing and in neurodegenerative and neuropsychiatric diseases. The molecular regulation of adult hippocampal neurogenesis is not fully understood. FoxO proteins are key transcriptional regulators of proliferation, DNA damage repair, and cellular detoxification across multiple tissues. Moreover, FoxO factors have been linked to ageing processes and neurodegenerative processes. The first aim of this thesis was to determine whether FoxO transcription factors fulfill functions in adult hippocampal neurogenesis. To this end, a triple conditional KO mouse model was used to specifically delete FoxO1, FoxO3 and FoxO4 in adult neural stem cells. Loss of FoxOs resulted in a transient increase in proliferation and neurogenesis in young adult mice and a depletion of FoxO-deficient cells over time. Furthermore, FoxO-deficient cells showed a delayed maturation and significant morphological alterations of the mitochondrial compartment. Interestingly, analysis of potential FoxO downstream targets in adult hippocampal neurogenesis revealed a conspicuous dysregulation of Notch target genes, indicating that FoxO modulates the Notch signaling pathway to regulate stem cell maintenance. Additionally, the GPR17 signaling pathway was identified as putative mediator of FoxO signaling.

Mutations of FoxG1 - another member of the Fox superfamily of transcription factors - were recently described to be responsible for the congenital variant of Rett syndrome. FoxG1 was further shown to be involved in telencephalic development and developmental hippocampal neurogenesis. The second goal of this thesis was to understand the role of FoxG1 in adult hippocampal neurogenesis with a particular focus on the effects of FoxG1 mutations associated with the congenital variant of Rett syndrome. Retroviral timeline and stage specific marker analysis revealed a distinct temporal expression pattern of FoxG1 in the adult hippocampal neurogenic lineage with highest expression levels in immature newborn neurons. Retrovirus mediated expression of FoxG1 gain of function mutants associated with the congenital variant of Rett syndrome resulted in massive defects in fate determination,

survival, and morphological development of adult-born hippocampal neurons, strongly indicating that FoxG1 dosage and timing are essential for survival and maturation of adult-born neurons in the dentate gyrus. Most intriguingly, retrovirus mediated expression of FoxG1 gain of function mutants associated with the congenital variant of Rett syndrome did not elicit any obvious phenotypic changes in SVZ neurogenesis, suggesting that neurogenesis of different neuronal subtypes may show differential sensitivity to FoxG1 mutations.

In summary, this thesis demonstrates that members of the Fox superfamily, namely FoxO transcription factors and the FoxG1 transcription factor, are key regulators of adult hippocampal neurogenesis. Given the importance of FoxOs in ageing and the role of FoxG1 in the pathophysiology of Rett syndrome, these insights may contribute to the understanding of the molecular mechanisms underlying cognitive dysfunction in ageing and Rett syndrome.

II Zusammenfassung

Adulte neurale Stammzellen produzieren in bestimmten Regionen des adulten Gehirns neue funktionelle Neurone. Diese Regionen sind der Gyrus dentatus des Hippokampus und die Subventrikulärzone des lateralen Ventrikels. Die adulte hippokampale Neurogenese wird mit Lern- und Gedächtnisprozessen in Verbindung gebracht. Außerdem gibt es Hinweise, dass eine Beeinträchtigung der adulten hippokampalen Neurogenese mit kognitiven Dysfunktionen während des Alterungsprozesses sowie mit neurodegenerativen und neuropsychatrischen Erkrankungen in Zusammenhang steht. Die molekulare Regulation der adulten hippokampalen Neurogenese ist noch nicht vollständig verstanden.

Die Proteine der FoxO-Familie sind wichtige transkriptionale Regulatoren in Bezug auf Proliferation, DNA-Reperaturprozesse und zelluläre Detoxifikation in verschiedenen Gewebearten. Des Weiteren wurden die FoxO-Transkriptionsfaktoren mit Alterungsprozessen und neurodegenerativen Prozessen in Zusammenhang gebracht. Die erste Zielsetzung dieser Doktorarbeit war es zu untersuchen, ob die FoxO-Transkriptionsfaktoren Aufgaben in der adulten hippocampalen Neurogenese erfüllen. Hierzu wurde ein dreifach konditionales Knockout (KO) Mausmodell benutzt, in welchem FoxO1, FoxO3 und FoxO4 spezifisch in adulten neuralen Stammzellen ausgeschaltet wurden. Proliferation und Neurogenese waren aufgrund des KO der FoxOs vorübergehend erhöht in jungen adulten Mäusen. Mit der Zeit erfolgte allerdings eine Depletion der FoxO-defizienten Zellen. Außerdem zeigten die FoxO-defizienten Zellen eine verzögerte Reifung und signifikante morphologische Veränderungen der Mitochondrien. Interessanterweise wurden als potentielle FoxO-Zielgene Notch-Zielgene identifiziert. Dies deutet darauf hin, dass die FoxO-Proteine den Notch-Signalweg modulieren, um den Stammzellerhalt zu regulieren. Zusätzlich wurde der GPR17-Signalweg als mutmaßlicher Mediator des FoxO-Signalweges identifiziert.

Mutationen des FoxG1-Gens, welches für einen weiteren Transkriptionsfaktor der Fox-Familie kodiert, wurden kürzlich mit der kongenitalen Variante des Rett-Syndroms in Verbindung gebracht. Des Weiteren ist FoxG1 an der Entwicklung des Telencephalons und der Neurogenese des sich entwickelnden Hippokampus beteiligt. Die zweite Zielsetzung dieser Doktorarbeit war es, die Rolle von FoxG1 in der adulten hippokampalen Neurogenese zu verstehen, insbesondere in Bezug auf

die Auswirkungen der Mutationen, die mit der kongenitalen Variante des Rett-Syndroms assoziiert wurden. Die Analyse einer retroviralen Zeitachse und Stadiums-spezifischer Markerexpression zeigten ein eindeutiges zeitliches Expressionsmuster für FoxG1 in der adulten hippokampalen neurogenen Zelllinie auf. FoxG1 ist am stärksten in unreifen neugeborenen Neuronen exprimiert. Retrovirale Überexpression von FoxG1-Mutanten, die mit der kongenitalen Variante des Rett-Syndroms assoziiert wurden, führten zu massiven Defekten in der Determinierung des Zellschicksals, im Überleben der Zellen und in der morphologischen Entwicklung der adult geborenen hippokampalen Neurone. Diese Ergebnisse deuten darauf hin, dass sowohl das Maß als auch der zeitliche Ablauf der FoxG1-Expression wesentlich für das Überleben und die Reifung der adult geborenen Neurone im Gyrus dentatus sind. Am bemerkenswertesten war die Beobachtung, dass eine Überexpression der FoxG1-Mutanten zu keinerlei offensichtlichen phänotypischen Veränderungen in der Neurogenese der Subventrikulärzone führten. Dies deutet darauf hin, dass die Neurogenese verschiedener neuronaler Subtypen unterschiedlich sensitiv auf FoxG1-Mutationen reagieren.

Zusammengefasst zeigt diese Doktorarbeit auf, dass Mitglieder der Fox-Superfamilie, nämlich die FoxO-Transkriptionsfaktoren und der FoxG1-Transkriptionsfaktor, wichtige Regulatoren der adulten hippokampalen Neurogenese sind. Bedenkt man die Bedeutung der FoxOs in Bezug auf Alterung und die Rolle des FoxG1 in der Pathophysiologie des Rett-Syndroms, tragen diese Erkenntnisse zum Verständnis der molekularen Mechanismen bei, die kognitiven Dysfunktionen in Alterungsprozessen und dem Rett-Syndrom zu Grunde liegen.

III Abbreviations

°C	Degree Celsius
Amp	Ampicillin
aNSC	Adult neural stem cell
APS	Ammonium persulfate
bp	Base pair
BrdU	Bromodeoxyuridine
BSA	Bovine serum albumine
c	Concentration or centi-
C57/Bl6J	Black inbred mouse strain
CAG	cytomegalovirus immediate early enhancer-chicken *β*-actin hybrid promoter
CDK	Cyclin dependent kinase
cDNA	Complementary deoxyribonucleic acid
CNS	Central nervous system
CE	Cytosolic extract
cfu	Colony forming unit
ChIP	Chromatin-immuno-precipitation
CT	cycle threshold
Cy3	Carbocyanine
Cy5	Indodicarbocyanine
d	Day
DAPI	4',6-Diamidino-2-phenylindole
DCX	Doublecortin
DG	Dentate gyrus
DMEM	Dulbecco's modified eagle medium
DNA	Deoxyribonucleic acid
dNTPs	Deoxynucleotides triphosphate
dpi	Days post injections
dpt	Days post Tamoxifen
DTT	Dithiotreithol
E.coli	*Escherichia coli*
EBSS	Earle's Balanced Salt Solution
ECL	Enhanced chemiluminescence
EDTA	Ethylene diamine tetraacetic acid
EGTA	Ethylene glycol tetraacetic acid
eSC	Embryonic stem cell
EtBr	Ethidium Bromide
EtOH	Ethanol
FACS	Fluorescence activated cell sorting
FGF	Fibroblast growth factor
FGFR	Fibroblast growth factor receptor
FITC	Fluorescein isothiocyanate
g	Gram
GABA	*γ*-aminobutyric acid
GCL	Granule cell layer
GFAP	Glial fibrillary acidic protein
GFP	Green fluorescent protein
GPC	Glial progenitor cell

gt	Goat
h	Hour
HBS	Hepes buffered saline
HBSS	Hank's balanced salt solution
HEK	Human embryonic kidney
HEPES	4-(2-hydroxyethyl)-1-piperazine-ethanesulfonic acid
HF	hippocampal fissure
HRP	Horseradish peroxidase
IHC	Immunohistochemistry
IRES	Internal ribosome entry site
kDa	Kilo dalton
KO	Knock-out
L	Liter
LB	Luria-Bertani
m	Milli-
M	Molar mass
MCL	Molecular cell layer
MeOH	Methanol
min	Minute
mitoDsred red	Fluorescent protein from Discosoma species targeting mitochondria
MOI	Multiplicity of infection
MMLV	Moloney murine leukemia virus
ms	Mouse
MW	Molecular weight
n	Nano-
NaAc	Sodium acetate
NE	Nuclear extract
NLS	Nuclear localization sequence
NMDA	*N*-methyl-D-aspartic acid
NSA	Neurosphere assay
OB	Olfactory bulb
p	Pico-
PAGE	Polyacrylamide gel electrophoresis
PBS	Phosphate buffered saline
PBST	Phosphate buffered saline Triton X-100
PCR	Polymerase chain reaction
PF	Primer forward
PFA	Paraformaldehyde
PGC	Periglomerular cell
PI3-kinase	Phosphatidylinositol 3-kinase
PK	Proteinkinase K
PMSF	Phenylmethylsulphonyl fluoride
PR	Primer reverse
PSF	Penicillin-streptomycine-fungizone
PVDF	Polyvinylidene difluoride
qPCR	Quantitative polymerase chain reaction
rb	Rabbit
rcf	Relative centrifugal force
RFP	Red fluorescent protein

RNA	Ribonucleic acid
ROS	Reactive oxygen species
rpm	Revolutions per minute
RT	Room temperature
SD	Standard deviation
SDS	Sodium dodecyl sulfate
sec	Second
SGZ	Subgranular zone
SVZ	Subventricular zone
TAE	Tris-acetate-EDTA buffer
TBS	Tris buffered saline
TBST	Tris buffered saline Triton X-100
TEMED	Tetramethylethylenediamine
Tris	Tris(hydroxymethyl)aminomethane
V	Volume
VEGF	Vascular endothelia growth factor
VSVG	Vesicular stomatitis virus G-protein
Wnt	Wingless
WT/wt	Wild type
β	Beta
λ	wavelength
µ	Micro-

VI List of Figures

V Table of Contents

1 Introduction

In 2013, the world's population reached 7.2 billion people. The population is aging rapidly – an average of over 6 % of the people are 80 years old or older (United Nations, 2013). In developed countries the aged population is larger due to better health care but emerging countries are predicted to catch up. In 2050, the world's population will reach 9 billion people and the proportion of people aged 80 years or older will have increased by a factor three to over 22 %. Brain disorders, including neurodegenerative, psychiatric and developmental diseases, represent already a tremendous disease burden and will increase in the future due to the aging society. Understanding brain function and diseases in detail is an enormous responsibility going on since decades; accomplishment of this task is essential to counter the expected health-economic problems posed by the increasing prevalence of age associated disorders of the central nervous system.

1.1 Neurogenic niches in the adult brain

For a long time it was thought that the adult mammalian brain does not produce new neurons after development and that degenerated or dying neurons cannot be replaced (Ramon y Cajal, 1928). Neuronal loss caused by injuries such as stroke or neurodegenerative diseases such as Parkinson's disease or Alzheimer's disease were considered to be permanent. Only in the 1960s Cajal's dogma was revealed to be wrong (Altman, 1962; Altman, 1963; Altman & Das, 1965; Altman & Das, 1966; Altman, 1969). The persisting proliferation in the postnatal and adult forebrain was demonstrated using [^{3}H]-thymidine autoradiography, with which proliferating cells could be tagged and their fate observed (Altman, 1969; Kaplan & Hinds, 1977). In the 1990s BrdU-labeling as a new technique to label proliferating cells provided key evidence for neurogenesis in the adult brain of primates and humans (Gould et al., 1999a; Kornack & Rakic, 1999; Eriksson et al., 1998).

In the last 20 years two main niches in the adult mammalian brain were revealed, where neurogenesis is continuously taking place during the whole life (Alvarez-Buylla & Garcia-Verdugo, 2002; Zhao et al., 2008). Neurogenic niches are defined as

microenvironments, which anatomically house stem cells and functionally control their neuronal development *in vivo*.

The two neurogenic niches of the adult mammalian brain are the dentate gyrus (DG) of the hippocampus and the subventricular zone (SVZ) of the lateral ventricles (Figure. 1.1).

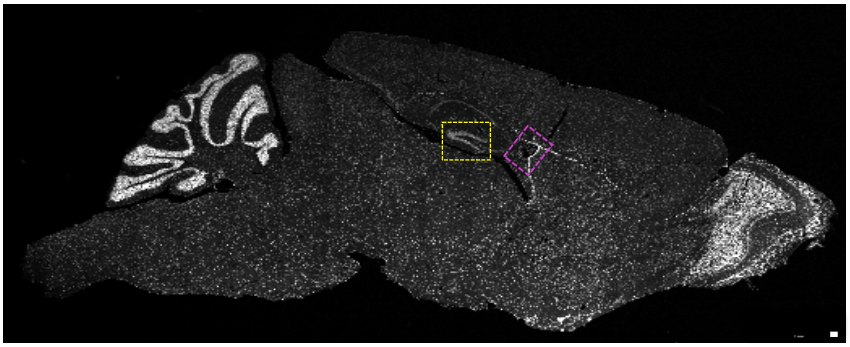

Figure 1.1: Neurogenic regions in the adult brain. Tile scan of a sagittal slice of an adult mouse brain stained with Dapi taken with a 20x objective of a confocal microscope. Scale bar 100 µm. The dentate gyrus (framed in yellow) of the hippocampus and the subventricular zone of the lateral ventricle (framed in pink) are the two main regions in mammals where neurogenesis occurs throughout lifetime.

The sources of the newly generated cells are adult neural stem cells (aNSCs). These cells have self-renewal potential and maintain the potential to generate the three major cell types of the brain - neurons, astrocytes and oligodendrocytes (Gage, 2000; Simons & Clevers, 2011).

1.1.1 Adult hippocampal neurogenesis

The hippocampal formation as part of the limbic system plays an important role in learning and memory (Andelman et al., 2010; Grasby et al., 1993; Kitamura et al., 2009; Miller et al., 2013; Scoville & Milner, 1957).

The hippocampus is subdivided into four regions - CA1, CA2, CA3 and dentate gyrus. The areas of the hippocampus are linked by unique and largely unidirectional connections through the so-called tri-synaptic hippocampal circuit (Amaral & Witter, 1989). The granule cell dendrites in the molecular cell layer of the dentate gyrus receive most of their input from the entorhinal cortex via the perforant pathway. The axons of the granule cells (mossy fibers) innervate the pyramidal neurons of the CA3. Mossy fiber synapses are large aggregations of termini with multiple transmitter release sites and post-synaptic densities (Lauri et al., 2001). Pyramidal cells of the CA3 region provide the major input to the CA1 region, the so called Schaffer

collaterals, which are the efferent projections of the CA3 pyramidal neurons (Gold & Kesner, 2005) and give rise to associational connections via collateral axons that terminate within CA3. The CA1 pyramidal neurons project finally to the subiculum, the main output of the hippocampus (Andersen, 2007).

The dentate gyrus is subdivided into four areas - the subgranular zone (SGZ), the granule cell layer (GCL), the molecular cell layer (MCL) and the hilus (Gage et al., 2008; Figure 1.2). aNSCs are located in the SGZ of the dentate gyrus. They continuously give rise to new granule cells (Seri et al., 2001). aNSCs can be identified by their radial glia like morphology and marker expression like GFAP (glial fibrillary protein), Sox2 (sex determining region Y (sry) related high mobility group (HMG) box 2) or Nestin (Zhao et al., 2006). Loss of the radial glia like cell population is associated with the loss of hippocampal neurogenesis (Deng et al. 2009, Zhao et al. 2006). The aNSCs are largely quiescent and enter proliferation at a low frequency. They give rise to transit amplifying progenitors (TAPs), which show mostly short tangentially processes and express markers like Sox2, Tbr2 (T-box brain gene 2) and Ascl1 (achaete-scute comlex like 1) but are negative for GFAP (Fukuda et al., 2003). The TAPs divide fast and differentiate further to dividing neuroblasts, which are characterized by the expression of DCX (Doublecortin) (Kempermann et al., 2004). The neuroblasts mature onwards to post-mitotic immature neurons, which still express DCX. The majority of cells reach this stage within three days after the initial division. During further maturation in the early post-mitotic stage the new neurons transiently express the immature marker Calretinin and permanently express Prox1 (Brandt et al., 2003). They start to project axons to the CA3 region and develop a clearly visible apical dendritic tree four to ten days after mitosis (Hastings & Gould, 1999). The post-mitotic neurons down-regulate the immature markers Calretinin and DCX after two to three weeks and start to express mature neuronal markers such as Calbindin, NeuN or MAP2 (Brandt et al., 2003; Kempermann et al., 2004). The development of first spines can be detected approximately 16 days after neuronal birth; the new neurons receive inputs from axosomatic, axodendritic and axospinous synapses (Ge et al., 2006; Toni et al., 2007). Mature adult-born dentate granule neurons are morphologically characterized by a complex dendritic tree that is covered with spines (Toni et al., 2008). Spine maturation continues for up to six months after neuronal birth (Toni et al., 2007). Electrophysiologically, the synaptic integration follows a stereotypical process; tonic GABA (Gamma-Aminobutyric Acid)

activation depolarizes the young neurons, followed by hyperpolarization through GABAergic inputs and finally excitation through glutamatergic synaptic inputs (Ge et al., 2006). During late maturation period, between four to six weeks after neuronal birth, the newborn neurons exhibit enhanced long-term potentiation with increased potentiation amplitude and decreased induction threshold (Ge et al., 2007).

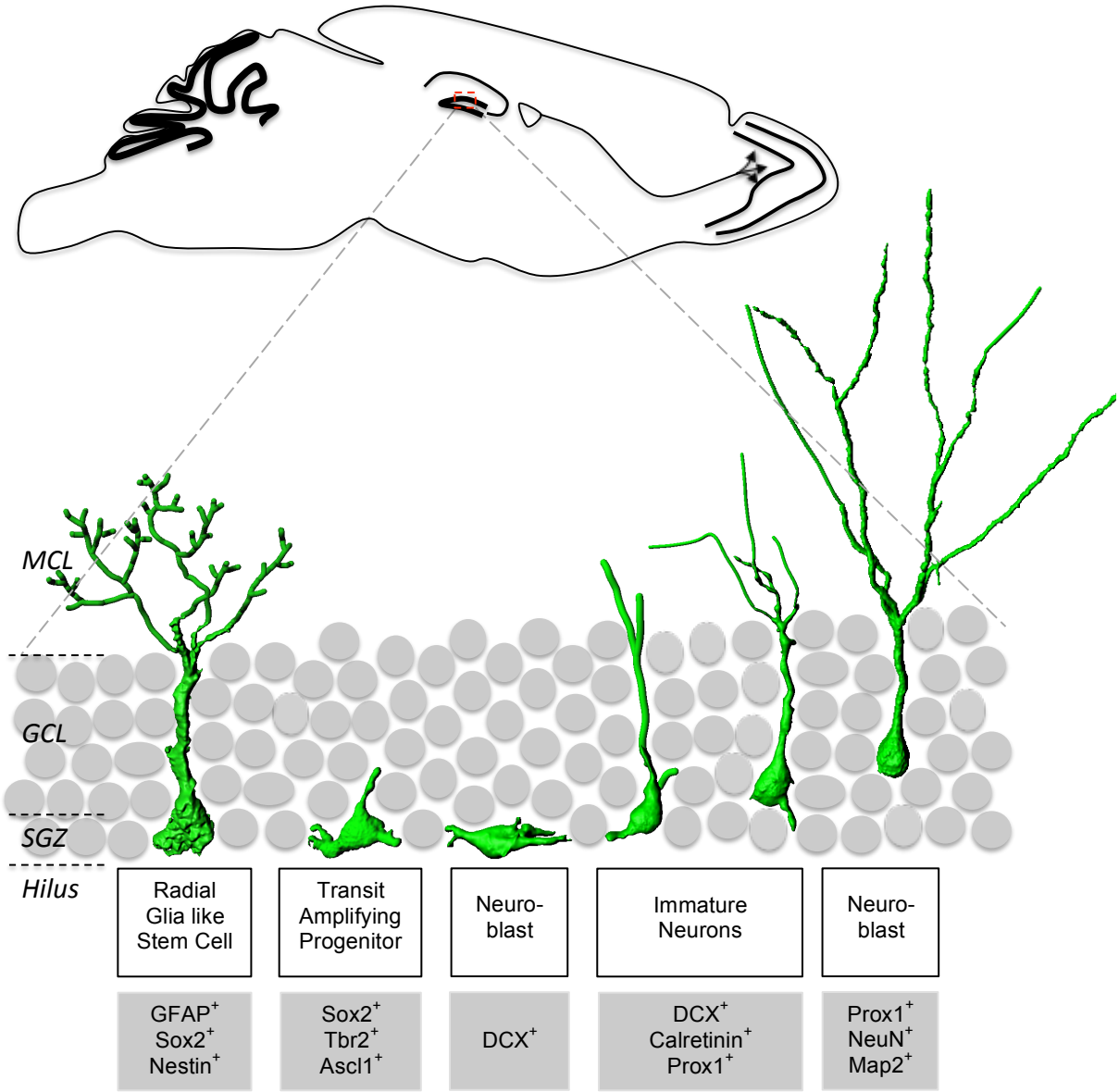

Figure 1.2: Process of adult hippocampal neurogenesis.
The developmental stages of adult hippocampal neurogenesis are identified by cell morphology, proliferative ability and marker expression. Radial glia like stem cells with astrocytic properties (expression of GFAP and Sox2) give rise to transient amplifying neural progenitors (expression of Sox2, Tbr2, Ascl1). These develop to neuroblasts and further to immature neurons (expression of DCX, Calretinin, Prox1), which finally differentiate to mature neurons - the granule cells of the dentate gyrus (expression of Prox1, NeuN, Map2).

1.1.2 Adult subventricular zone neurogenesis

The subventricular zone (SVZ) is the second neurogenic region in the adult rodent brain and is located at the lateral walls of the lateral ventricles (Altman, 1963; Doetsch & Alvarez-Buylla, 1996; Eriksson et al., 1998). In the adult rodent brain distinct cell types can be found in the SVZ – ependymal cells, niche astrocytes, stem cells, transit amplifying cells (TAPs) and neuroblasts (Beckervordersandforth et al., 2010; Doetsch et al., 1997; Ihrie & Alvarez-Buylla, 2011). Figure 2.2 illustrates neurogenesis in the adult SVZ.

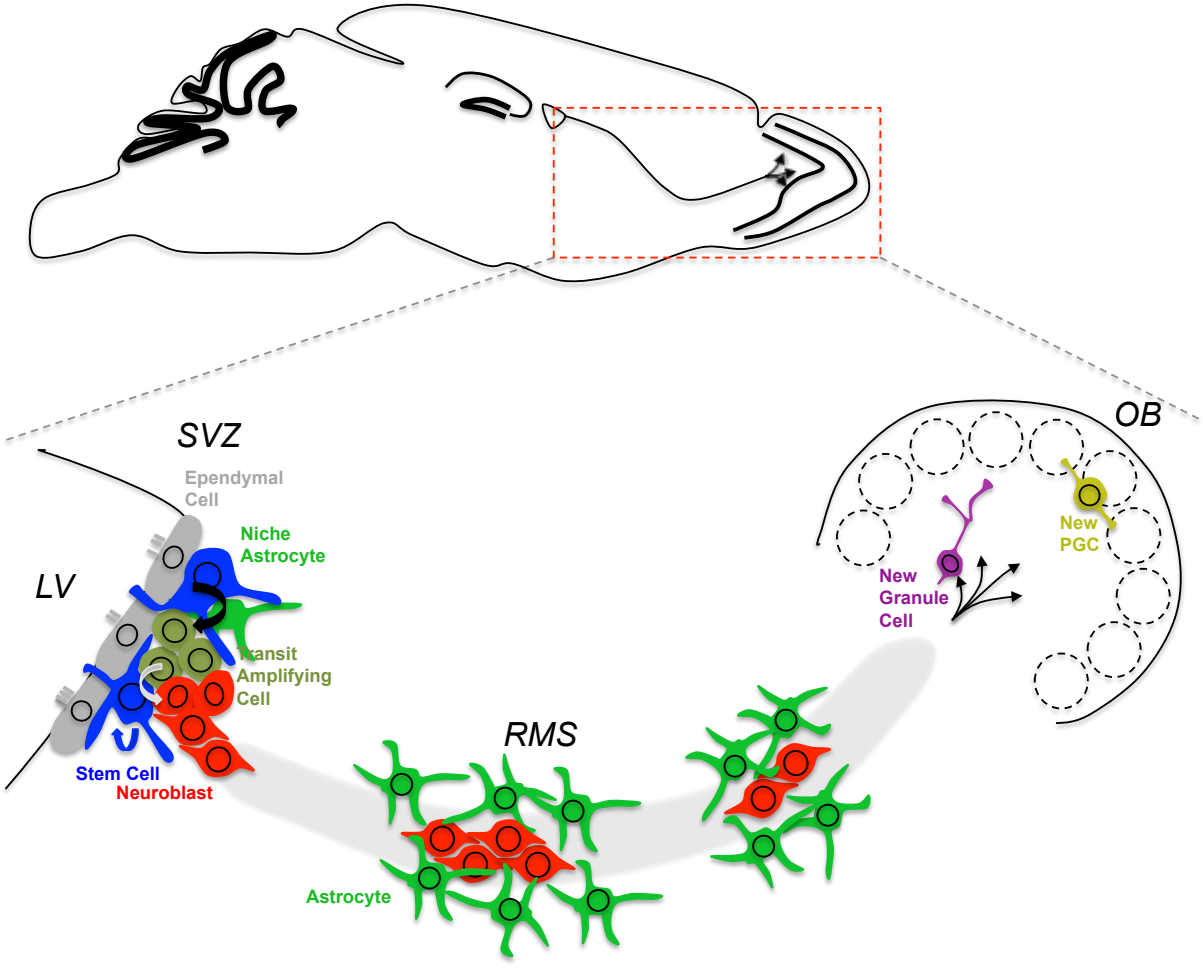

Figure 1.3: Adult neurogenesis in the adult SVZ/OB system.
Slowly proliferating neural stem cells residing in the SVZ of the lateral ventricle give rise to rapidly proliferative transient amplifying cells, which give rise to neuroblasts. Neuroblasts migrate towards the olfactory bulb (OB) through the rostral migratory stream (RMS). Within the OB the immature neurons differentiate into two types of interneurons - the granule cells and the periglomerular cells (PGC).

Stem cells in the SVZ are characterized among others by expression of the markers GFAP, Sox2 and Nestin. The stem cells have an astrocytic morphology and proliferate very slowly. *In vitro*, these cells exhibit the two distinct characteristics of stemness – multipotency and self-renewal (Beckervordersandforth et al., 2010). In vivo, SVZ stem cells have been demonstrated to generate new neurons and oligodendrocytes *in vivo* (Menn et al., 2006). SVZ Stem cells generate rapidly proliferating transient amplifying progenitors, which differentiate into immature neurons, the so-called neuroblasts. Adjacent ependymal cells promote differentiation to immature neurons by expressing inhibitors for gliogenesis (Lim et al., 2000). The neuroblasts migrate in chains through the rostral migratory stream (RMS) towards the olfactory bulb (OB) (Lois et al., 1996; Jankovski & Sotelo, 1996). In the RMS, the neuroblasts migrate along glial tubes (Peretto et al., 1997). After reaching the OB the neuroblasts migrate out radially and differentiate into two types of interneurons - granule cells and periglomerular cells (Belluizzi et al., 2003; Kato et al., 2001). The majority of newly generated neurons in the SVZ/OB system are GABAergic granule neurons. The continuous generation of new interneurons, which modulate spatial and temporal coding of olfactory information, might provide a cellular substrate for adaptation to environmental changes (Cecchi et al., 2001; Doetsch & Hen, 2005).

1.1.3 Functional relevance and significance of adult neurogenesis in health and disease

Most recently, Spalding et al. were able to show that around one-third of the neurons in the human hippocampus is exchanged during lifetime (Spalding et al., 2013). Their data suggests a daily turnover rate of 0,004 %, which corresponds to around 700 new neurons per day per hippocampus. In adult mice the daily turnover rate was estimated to be around 0,03 to 0,06 % (Kempermann et al., 1997b). While these turnover rates may appear quite low, studies manipulating the rate of neurogenesis have provided strong evidence that neurogenesis is highly relevant for hippocampal information processing, indicating that even a small number of newly generated neurons has tremendous impact on the hippocampal circuitry.

Adult hippocampal neurogenesis has been suggested to be important for cognition and mood regulation (Deng et al., 2009). Conditional deletion, e.g., of FGF receptor

in adult hippocampal stem cells negative impacts on stem cell proliferation and was shown to result in defects in memory consolidation (Zhao et al., 2007). Other studies described impairments in the long-term but not the short-term retention of spatial memory as a consequence of reduced adult neurogenesis (Deng et al., 2009; Jessberger et al., 2009; Snyder et al., 2005; Winocur et al., 2006). It has also been proposed that new neurons may contribute to pattern separation (Clelland et al., 2009; Creer et al., 2010; Nakashiba et al., 2012; Sahay et al., 2011a, 2011b) - the distinct encoding of very similar events (Gilbert et al., 2001; Leutgeb et al., 2007).

Neurogenesis declines with age in both neurogenic niches (Molofsky et al., 2006; Rossi et al., 2008). Decreased neurogenesis in the hippocampal niche due to aging or stress was shown to be correlated with cognitive deficits, anxiety and depression (Mirescu & Gould, 2006; Rossi et al., 2008). Data from animal models of anxiety and depression indicate that neurogenesis is required for some of the effects of antidepressants (David et al., 2009; Santarelli et al., 2003).

Disturbance of adult neurogenesis was found to accompany brain injuries, neurodegenerative disease and neurological disorders. For example, precursor proliferation was found to be increased for days to weeks following aberrant neuronal activity in mouse models (Ma et al., 2009). Seizures lead to mis-migration of newborn neurons, aberrant dendritic growth and mossy fiber recurrent connections in the adult SGZ (Kron et al., 2010). It was further shown in adult rats that aberrant adult neurogenesis due to seizures can be inhibited by an antiepileptic drug, which – most strikingly - also protected the animals from seizure associated impairments in hippocampus-dependent cognition (Jessberger et al., 2007). Adult neurogenesis was also examined in Alzheimer's and Parkinson's disease models with differing results. Transgenic mouse models with mutations in the amyloid precursor protein showed decreased neurogenesis due to impaired survival of newborn neurons, while presenilin mutations (risk gene for early-onset familial Alzheimer's disease) lead either to increased or decreased neurogenesis, depending on the mouse model and genetic background (Jankowsky et al., 2005; Verret et al., 2007; Wang et al., 2004). Transgenic mouse models for Parkinson's disease, in which overexpression of endogenous α-synuclein was applied, revealed varying impairments in adult neurogenesis. Winner and colleagues showed an impairment of the survival of newborn neurons in the dentate gyrus and the SVZ (Winner et al., 2004), while Tani and colleagues demonstrated that proliferation and migration velocity was reduced

but survival of newborn neurons was not affected (Tani et al., 2010). Furthermore hippocampal neurodegeneration, neurochemical changes and impaired motor performance upon ageing were revealed (Nuber et al., 2008). Animal models with mutations in the LRRK2 (Leucin-rich repeat kinase 2) gene, which are the most frequent cause of autosomal dominant Parkinson's disease, showed reduced proliferation and survival, severe alterations in axon guidance and dendritic development of newborn adult progenitors and abnormal exploratory behaviors (Melrose et al., 2010; Winner et al, 2011). Given the importance of adult neurogenesis in physiological conditions and the significant negative impact of disturbance of neurogenesis on hippocampal processing, it has been hypothesized that disease-induced disturbances of hippocampal neurogenesis significantly contribute to cognitive deficits in ageing, neurodegenerative diseases and injury.

Another interesting observation is that risk genes for human neuropsychiatric diseases such as FMRP, MECP2, and DISC1, were shown to regulate adult neurogenesis. FMRP (fragile X mental retardation protein) deficient mice have increased proliferation and glial fate commitment of neural precursor cells in the adult SGZ (Luo et al., 2010). MECP2 (Methyl-CpG-binding protein 2), which is mutated in Rett Syndrom, is critical for maturation and spine formation of adult-born neurons in the dentate gyrus (Smrt et al., 2007). DISC1 (Disrupted-in-schizophrenia 1) was shown to have several functions in adult hippocampal neurogenesis. It promotes progenitor proliferation through GSK3β/β-catenin pathway and limits on the other site dendritic growth and synapse formation through AKT/mTor signaling (Duan et al., 2007; Kim et al., 2009). The importance of risk genes for human neuropsychiatric diseases raise the intriguing possibility that disturbance of adult neurogenesis contributes to the neuropsychiatric deficits in these diseases.

1.1.4 Regulation of adult neural stem cell homeostasis

Tissue homeostasis is the equilibrium that balances cell loss and cell regeneration, and that serves to maintain cell mass and function. Adult stem cells as the cellular origin of new cells are crucial for tissue homeostasis. The regulation of the balance between stem cell quiescence, proliferation and differentiation in the adult brain is essential for maintaining adult neurogenesis throughout life. Dysbalance between

stem cell quiescence, proliferation and differentiation will result in premature termination of neurogenesis. Next to maintenance of stem cells and their proliferation capacity, tight regulation of the differentiation and functional integration of newborn neurons is essential to ensure the hippocampal function.

Generally, adult hippocampal neurogenesis is controlled by the interplay of extrinsic signals provided by the neurogenic niche with cell-intrinsic regulators. The influence of extrinsic signals is illustrated by the observation that physical exercise and environmental enrichment (Brown et al., 2003; Kempermann et al., 1997a, 1997b: van Praag et al., 1999a; 1999b) potently stimulate adult neurogenesis. A number of niche derived growth factors, cytokines and morphogens have been identified that affect many steps of neurogenesis including proliferation, neuronal differentiation, and survival (Kandasamy et al., 2010; Kuhn et al., 1997; Mira et al., 2010; Zhao et al., 2007).

Adult neural stem cell maintenance and proliferation

BMPs (bone morphogenic proteins), as an example of niche depending extrinsic factors, are critical to maintain the balance between quiescence and proliferation of adult neural stem cells. Loss of BMP-induced signaling leads to enhanced recruitment of quiescent neural stem cells into cell cycle, which leads finally to depletion of neural stem cells, precursors, and newborn neurons (Mira et al., 2010). Another potent extrinsic factor to control adult neural stem cell maintenance is Notch signaling. It has been shown that loss of Notch1 or of RBPJ, which is the transcriptional effector of Notch signaling, leads to premature neuronal differentiation and rapid depletion of the neural stem cell pool (Ables et al., 2010; Ehm et al., 2010; Imayoshi et al., 2010). VEGF, FGF-2, Shh, and IGF have been suggested as potent niche derived and circulation derived proliferation signals (Gómez-Pinilla et al., 1997; Lai et al., 2003; Palmer et al., 2000; Trejo et al., 2001). Interneurons in the SGZ release GABA to activate the self-renewal mode of quiescent adult neural stem cells and precursor cell proliferation (Song et al., 2012; Song et al., 2013).

Cell intrinsic regulators of stem cell maintenance comprise cell cycle regulators, transcription factors and epigenetic regulators. Cell cycle inhibitors like p21 or p53 are critical to maintain the quiescence of adult neural stem cells and precursors (Gil-Perotin et al., 2011; Kippin et al., 2005; Marqués-Torrejón et al., 2013). Their loss leads to the depletion of the neural stem cell pool. Kippin and colleagues suggested

that the uncontrolled proliferation in the SVZ of $p21^{-/-}$ animals, which first results in an increase in progenitor cells, leads finally to a premature depletion of the proliferation capacity due to a finite proliferation potential.

Different transcription factors were correlated with neural stem cell quiescence and proliferation. The transcription factor Sox2 was intensely analyzed regarding its role in stem cell maintenance and proliferation, since it is expressed both in radial glia like stem and precursor cells. Loss of Sox2 results in reduction of stem cells and loss of precursor proliferation in the adult dentate gyrus (Ferri et al., 2004; Favaro et al., 2009). Analysis of Sox2 targets revealed a subset of genes, which implement the effects of Sox2 on stem cell maintenance and progenitor proliferation. The orphan nuclear receptor tailless (TLX) is positively regulated by Sox2 (Shimozaki et al., 2011). TLX was shown to be critical for the stimulation of the self-renewal of neural stem cells and by keeping SVZ and SGZ stem cells in an undifferentiated state (Liu et al., 2008; Niu et al., 2011; Qu et al., 2010; Shi et al., 2004; Zhang et al., 2008). Loss of TLX leads to a decrease in the proliferation of neural stem and precursor cells. TLX was suggested to operate by suppressing pathways, which promote stem cell quiescence, including cell cycle inhibition by p21 or PTEN mediated inhibition of the PI3K signaling (Niu et al., 2011; Zhang et al., 2006). Further was TLX suggested to activate canonical Wnt signaling to promote neural stem cell proliferation and self-renewal (Qu et al., 2010). Another target of Sox2 in neural stem cells is the morphogen sonic hedgehog (Shh) (Favaro et al., 2009). Shh was shown to promote proliferation in the postnatal hippocampus; most intriguingly Shh is able to compensate at least partially the proliferation and self-renewing defects in Sox2-deficient postnatal neural stem cells (Ahn & Joyner, 2005; Favaro et al., 2009; Lai et al., 2003). Sox2 also has major function in controlling multipotency of adult neural stem cells. Kuwabara and colleagues demonstrated that Sox2 prevents neuronal differentiation and keeps stem cells in a multipotent state by inhibiting the transcriptional activation of the pro-neuronal transcription factor NeuroD1 through Wnt-signaling (Kuwabara et al., 2009). Next to Sox2 the transcription factor REST (Repressor element 1-silencing transcription factor) was associated with the maintenance of neural stem cells (Gao et al., 2011). REST is expressed in neural stem cells and transit amplifying progenitors. Loss of REST leads to a transient mild increase in proliferation followed by mild decrease in proliferation and neurogenesis at later time points *in vivo* in the adult dentate gyrus, while cultured REST-deficient

neural stem cells show self-renewing deficits *in vitro* (Gao et al., 2011). REST is proposed as a negative regulator of neuronal differentiation by repressing neuronal differentiation genes like ASCL1 and NeuroD1, thereby keeping adult neural stem cells in an undifferentiated state.

Next to classical signaling pathways and transcription factors, epigenetic mechanisms, like DNA methylation, histone modifications or non-coding RNAs, are emerging regulators of adult neural stem cell maintenance and proliferation (reviewed by Sun et al., 2011), which coordinate gene expression programs: the expression of the stem cell proliferation factor FGF2 and several miRNAs was for example shown to be suppressed by the Methyl-CpG-binding domain protein 1 (Mbd1) to equilibrate proliferation and differentiation in adult hippocampal neurogenesis (Liu et al., 2010).

Regulation of neuronal differentiation and integration

The newly generated cells have to differentiate in the accurate neurotransmitter phenotype and integrate into the existing circuitry to contribute to the plasticity of the adult brain. Differentiation and integration are key factors influencing the survival of newborn neurons.

Neurotransmitter systems like GABA and NMDAR (N-Methyl-D-Aspartate Receptor) were shown to be critical for activity-dependent differentiation and maturation in adult hippocampal neurogenesis. GABA signaling is essential for dendritic development and synaptic integration of newborn neurons (Ge et al., 2006; Jagasia et al., 2009; Song et al., 2012; Song et al., 2013; Tashiro et al., 2006a; Tozuka et al., 2005). NMDAR signaling controls survival of immature neurons and is required for enhanced synaptic plasticity of newborn granule neurons in the adult dentate gyrus (Ge et al., 2007; Snyder et al., 2001; Tashiro et al., 2006a).

Survival and maturation of new dentate gyrus neurons was shown to depend on the precise expression of specific transcription factors like Prox1 (prospero-related homeobox gene 1), CREB (cAMP response element binding protein) and NeuroD1 (neurogenic differentiation 1) in the adult dentate gyrus (Gao et al., 2009; Jagasia et al., 2009; Lavado et al., 2010). CREB signaling is active in immature neurons and was shown to be critical for dendritic growth, maturation, survival and integration of newly generated cells. NeuroD1 was also found as a cell-intrinsic factor, required for the survival and differentiation of newborn neurons both in the adult SGZ and SVZ

(Gao et al., 2009; Kuwabara et al., 2009). Loss of NeuroD1 leads to the loss of new mature neurons while the stem cell and progenitor populations are not affected. Prox1 is suggested to post-mitotically define the granule cell identity and maintains thereby the neuronal identity of mature neurons in the dentate gyrus (Iwano et al., 2012; Lavado et al., 2010).

With techniques such as the generation of conditional KO mice targeting specific cell types at chosen timepoints (Glast::CreER^{T2}; Nestin-CreER^{T2}; Frizzeled9-CreER^{TM}; CamKII-Cre; etc.) and retrovirus-mediated genetic manipulation of precursor cells in situ, powerful tools exist to further decode regulators and the functional role of adult neurogenesis. In the end the ensuing perceptions might help to develop new treatments for mood disorders and neurodegenerative and neurological diseases.

1.2 Fox transcription factors

The first member of the superfamily of winged helix/forkhead class of transcription factors was discovered in 1989 in drosophila (Weigel et al., 1989). The human Fox family consists of 50 members, while the murine Fox family consists of 44 members. They are characterized by a 110-amino-acid, monomeric DNA binding domain termed the “forkhead box” or “Fox” (Kaestner et al., 2000). The canonical winged helix/forkhead DNA binding domain is highly conserved in genes from yeast to humans and all proteins having sequence homology are considered members of the Fox superfamily. Subclasses are defined from FoxA to FoxS based on additional conserved domains or motifs. Forkhead factors were shown to be involved in diverse biological process, such as cell cycle regulation (FoxM1, FoxO, FoxA1, FoxG1, FoxK1), survival (FoxO), metabolism (FoxA, FoxC, FoxO), immunoregulation (FoxP3, FoxJI, FoxN1, FoxO, FoxD2, FoxP1) and embryonic development (all except FoxB, FoxG, FoxK, FoxO, FoxQ, FoxS) (reviewed by Tuteja & Kaestner, 2007a, 2007b). The Fox family comprises five risk genes for diseases in humans – FoxC1 mutations lead to glaucoma phenotypes, FoxC2 mutations cause lymphoedema-distichiasis syndrome, FoxG1 mutations are associated with congenital variants of Rett syndrome, FoxP2 deficiency elicit language acquisition defects and FoxP3 mutations are associated with severe autoimmune disorders (Ariani et al., 2008; Hannenhalli &

Kaestner, 2009). Further, it was shown that deregulation of the expression of Fox genes through mechanisms such as gene amplification, chromosomal translocation, or impaired transcriptional regulation can lead to the development of metabolic diseases and cancer (reviewed by Lehmann et al., 2003). In this study the subclasses FoxO and FoxG1 were analyzed regarding their role in adult neurogenesis.

1.2.1 FoxO transcription factors

The family of FoxO transcription factors consists of 4 members - FoxO1, FoxO3a (termed below as FoxO3), FoxO4 and FoxO6. FoxOs appear to recognize the same consensus sequence and, except for FoxO6, are expressed in a wide range of tissues. FoxO6 expression is restricted to the CNS in mammals. FoxO6 is mainly expressed in the CA1 and CA3 regions of the hippocampus in adult mice, but not in the dentate gyrus. Genetic studies revealed that FoxO transcription factors have partially redundant functions. Except for FoxO1 null mice, which die at embryonic day 10.5 because of incomplete vascular development, FoxO3, FoxO4 and FoxO6 null mice do not develop major obvious phenotypes (Furuyama et al., 2004; Hosaka et al., 2004; Salih et al., 2012), suggesting functional redundancy between the different FoxO family members.

Two evolutionary conserved signaling pathways – PI3K-Akt [phosphatidylinositol 3-kinase-Akt; Akt is also known as PKB (protein kinase B)] and JNK (Jun N-terminal kinase) - regulate FoxOs. FoxOs are negatively regulated by the canonical PI3K-Akt - signaling pathway (Biggs et al., 1999; Brunet et al., 1999; Kops et al., 1999; Rena et al., 1999; Tang et al., 1999) and positively regulated in the presence of oxidative stress through JNK (Essers et al., 2004; Wang et al., 2005; Wang et al., 2012). The activation of PI3-kinase by insulin and growth factors leads to an increased level of phosphatidylinositol-3-phosphate, which acts as second messenger to activate PDK1 (phosphoinositide-dependent kinase 1) and PKB (Akt). The activation of PKB (Akt) leads to its translocation to the nucleus, where it phosphorylates FoxOs at three conserved residues. This results in an increased binding of FoxOs to 14-3-3 proteins and the cytoplasmic localization of both. Binding to 14-3-3 proteins inhibits the interaction between FoxOs and target DNA and prevent the nuclear re-import after export to the cytoplasm by masking their nuclear localization signal. The actual

inactivation of FoxOs, following phosphorylation by PDB (Akt), is the export out of the nucleus (reviewed by van der Heide et al., 2004). Under cellular stress, particularly when high levels of reactive oxygen species (ROS) are generated, FoxOs translocate into the nucleus in response to JNK signaling and cause increased transcription of target genes. JNK inhibits insulin signaling and induces the release of FoxOs to 14-3-3 proteins, thereby overriding growth factor induced FoxO inhibition (reviewed by van der Horst & Burgering, 2007). Additionally, other kinases were shown to regulate FoxO activity via phosphorylation. AMP-activated protein kinase is proposed to regulate FoxOs under energy stress (Greer et al., 2007), while CDKs, ATMs and MAPKs were shown to control FoxOs activity under genotoxic stress like DNA damage (Kress et al., 2011; Tsai et al., 2008; Yuan et al., 2008). Some further posttranslational modifications on FoxO proteins, i.e., monoubiquitination and acetylation, are known, which regulate FoxO activity (Kitamura et al, 2005; van der Horst et al., 2006). Both modifications are involved in FoxO activity regulation in response to oxidative stress.

FoxO transcription factors mainly act as transcriptional activators. The nuclear localization of FoxOs is indicative for their transcriptional activity. They can bind to many sites within the genome since their conserved consensus core recognition motif is only eight base pairs long (Furuyama et al., 2000).

FoxO transcription factors were shown to regulate many cellular functions that are central to stem cell homeostasis such as cell cycle regulation, detoxification of ROS, DNA damage repair or tumor suppression. One of the functions, to which FoxO activation was first linked to, was regulation of cell cycle progression. G1-S phase and G2-M phase transition were shown to be regulated by FoxOs via controlling the coordinate expression of cell cycle regulators including p21, p27 or p57 (reviewed by Besson et al., 2008 and Ho et al., 2008). It was shown that FoxOs promote cell cycle arrest in response to oxidative stress (Furukawa-Hibi et al., 2002; 2005) or DNA damage (Lei & Quelle, 2009; Tsai et al., 2008).

FoxOs were proposed to protect cells from oxidative damage by increasing transcription of genes regulating elimination of ROS such as MnSOD (Manganese Superoxide Dismutase) (Kops et al., 2002). MnSOD protects against oxidative damage through conversion of superoxide, which is formed as a by-product during generation of ATP in mitochondria, into hydrogen peroxide. FoxOs also induce repair of damaged DNA through the Gadd45 protein (Tran et al., 2002). FoxOs were

attributed functions in the induction of apoptosis. FoxOs activate the intrinsic apoptotic pathway by upregulation of pro-apoptotic genes of the Bcl-2 family like Bim and p53 (Dijkers et al., 2000; You et al., 2006). FoxOs directly activate Bim gene expression and promote apoptosis in sympathetic neurons after nerve growth factor deprivation (Gilley et al., 2003). There is also evidence for a tumor suppressive effect of FoxO transcription factors (reviewed by Arden, 2007), which appears to be conferred through the promotion of cell cycle arrest and pro-apoptotic activity. Regulation of cell differentiation by FoxOs was demonstrated for various tissues including blood, muscle and adipose tissue (Bakker et al., 2004; Nakae et al., 2003; Tothova et al., 2007;). FoxOs were as well assigned a role in ageing. The first indication for a function in ageing was provided by the observation that mutations of FoxO lead to an increased lifespan in *C. elegans* (Kenyon et al., 1993). Later on, SNP's (single nucleotide polymorphisms) in FoxO1 and FoxO3 were found in longevity phenotypes in Japanese, German, South Italian and Han Chinese populations (Anselmi et al., 2009; Flachsbart et al., 2009; Li et al., 2009). The FoxO-dependent extension of lifespan is proposed to be partially a result of the induced resistance to oxidative stress (Calnan & Brunet, 2008).

Finally, FoxOs were shown to have a crucial role in adult stem cells in the hematopoietic and nervous system. FoxOs maintain self-renewal of hematopoietic stem cells (Miyamoto et al., 2007; Tothova et al., 2007; Yalcin et al., 2008) and were also proposed to be important for quiescence and proliferation of postnatal/adult neural stem cells (Paik et al., 2009; Renault et al., 2009).

1.2.2 FoxG1 transcription factor

The FoxG family consists of two members FoxG1 and FoxG2, formerly termed as BF-1 and BF-2 (brain factor 1 and 2) (Tao & Lai 1992; Hatini et al., 1994). Except for some indications for its participation in the regulation of mesoderm, forebrain and neural crest development (Gómez-Skarmeta et al., 1999; Hatini et al., 1996), little is known about the function of FoxG2.

FoxG1 was first described in the telencephalon of the developing rat brain (Tao & Lai, 1992). Its expression in mouse and rat embryo and human fetal brain is restricted to neuronal cells in the telencephalon with strong expression in the

developing dentate gyrus and hippocampus (Murphy et al., 1994). Studies in Xenopus, zebrafish, chick and mice revealed an evolutionary conserved role of FoxG1 in brain development. FoxG1 plays an important role in controlling neural precursor function and identity. FoxG1 null mice die perinatal due to deletion of neural progenitor populations and consequently loss of ventral telencephalic structures (Xuan et al., 1995). Loss of FoxG1 results in premature cell cycle exit and neuronal differentiation of neocortical progenitors in the cerebral cortex (Xuan et al., 1995; Hanashima et al., 2002). FoxG1 is also important at later stages of neurogenesis. FoxG1 was found to play a role in cell migration (Tian et al., 2012). Miyoshi and Fishell showed that dynamic expression of FoxG1 is necessary to control morphology of migrating pyramidal neuron precursors and to coordinate their integration into the cortical plate (Miyoshi & Fishell, 2012). FoxG1 fulfills important functions in patterning of the developing brain (Danesin et al., 2009; Manuel et al., 2010; Roth et al., 2010). The proper formation of the inner ear is depending on FoxG1 (Pauley et al., 2006) as well as formation of the ventral olfactory system (Duggan et al., 2008; Kawauchi et al., 2009a; 2009b). Finally, FoxG1 may also have direct functions in neuronal survival (Dastidar et al., 2011).

The key function of FoxG1 in brain development is illustrated by the fact that mutations in the human FoxG1 gene are associated with the congenital form of Rett syndrome, a severe neurodevelopmental disorder. The core phenotype of the congenital form of Rett syndrome consists of postnatal microcephaly, epilepsy, sever mental retardation, absent language, dyskinesia, corpus callosum hypogenesis, simplified gyral pattern and reduced white matter volume (Guerrini & Parrini, 2012; Kortüm et al., 2011). FoxG1 mutations associated with the congenital form of Rett syndrome include disruptions of the DNA binding domains of FoxG1 (Ariani et al., 2008), duplications of FoxG1 (Brunetti-Pierri et al., 2011), microdeletions and deletions within the FoxG1 gene (Jacob et al., 2009; Papa et al., 2008; Perche et al., 2013; Takagi et al., 2013), haploinsufficiency (Kumakura et al., 2013), frameshift mutations (Le Guen et al., 2011a), truncating and missense mutations (Mencarelli et al., 2010) including one point mutation, which affects the nuclear localization of FoxG1 (Le Guen et al., 2011b).

FoxG1 is broadly expressed throughout the developing brain. In the adult brain, its expression is highly restricted. In situ hybridizations revealed very weak expression throughout the telencephalon but high expression levels within the two adult

neurogenic niches – the SVZ of the lateral ventricles and the hippocampus (Shen et. al., 2006), strongly suggesting a key role for FoxG1 in the regulation of adult neurogenesis. Indeed, two studies in mice revealed an important role for FoxG1 in postnatal development of the dentate gyrus. Haploinsufficiency of FoxG1 leads to disturbed neurogenesis in the postnatal hippocampus due to impaired survival, proliferation and differentiation of postnatally born dentate granule neurons (Shen et al., 2006). Tian and colleagues showed that prenatal and postnatal conditional deletion of FoxG1 in the hippocampal primordium and its derivatives leads to the disruption of the dentate gyrus, loss of the SGZ and impaired migration of granule cells (Tian et al., 2012).

The role of FoxG1 in adult neurogenesis has not been explored in detail. Considering the strong existing data about FoxG1's critical role in neural embryonic and postnatal development, a major impact of FoxG1 in neuronal development in the adult neurogenic niches can be assumed.

1.3 Aims of the study

FoxO transcription factors were shown to play major roles in cell biological functions such as cell cycle regulation, DNA damage repair, and detoxification, which may pertinent to stem cell homeostasis and neurogenesis. The first aim of this thesis was to investigate the function of FoxO transcription factors in adult neurogenesis. For this purpose the impact of the loss of FoxO1, FoxO3 and FoxO4 was analyzed both *in vitro* and *in vivo* regarding stem cell maintenance, proliferation, differentiation and maturation of adult born neurons. Another objective of this study was to identify signaling pathways that operate downstream of FoxO transcription factors in adult neurogenesis.

The transcription factor FoxG1 was shown to be critical for telencephalon development and postnatal development of the hippocampus. In the second part of this thesis the role of FoxG1 in adult neurogenesis was explored. Retroviral injections simulating FoxG1 gain of function were applied into the neurogenic regions of adult mice. The purpose of these experiments was to gain insights into both the FoxG1-depending processes in adult neurogenesis and the development of the congenital variant of Rett syndrome due to Foxg1 mutations.

2 Results

2.1 FoxO transcription factors in adult neurogenesis

Previous studies have shown that deletion of FoxO transcription factors during embryonic development results in the increased proliferation of neural stem/progenitor cells and transiently increased neurogenesis, followed by a depletion of the neural stem cell pool and a decrease in neurogenesis in the adult hippocampal and subventricular zone (Paik et al., 2009, Renault et al., 2009). Ablation of FoxO transcription factors specifically in NSCs of the adult CNS has not been performed and the exact role of FoxO transcription factors in adult hippocampal neurogenesis remains to be determined.

Four different mouse lines were used in this study to analyze the effects of the triple FoxO1, FoxO3 and FoxO4 (FoxO1/3/4) conditional knock out (KO) on adult neurogenesis.

For all *in vitro* experiments a FoxO1/3/4$^{fl/fl}$ mouse model was used (previously described by Paik et al., 2009, see 4.2.7). LoxP sites in this mouse line flank the exons of FoxO1, FoxO3 and FoxO4 coding for the DNA binding domains. Recombination of the conditional alleles was induced via Cre-recombinase mediated by retroviral transduction.

The *in vivo* experiments addressing the questions about proliferation and neurogenesis of adult neural stem cells (aNSCs) deficient for FoxO1, FoxO3 and FoxO4 were performed using Tamoxifen-inducible Cre-recombinase (CreER^{T2}) under the Glast (Glutamate-aspartate transporter) promoter combined with a conditional β-galactosidase reporter (Glast::CreER^{T2}/β-gal(Rosa26)/FoxO1/3/4$^{fl/fl}$, termed in the following as FoxO1/3/4 KO mice). Mice that were carrying the Glast::CreER^{T2} and the β-gal(Rosa26) transgene but were wildtype for the FoxO1/3/4 alleles (termed in the following as FoxO1/3/4 control mice) served as controls (Mori et al., 2006, Nakamura et al., Paik et al., 2007, see 4.2.7). KO of FoxO1/3/4 was induced specifically in cells with Glast promoter activity via i.p. injections of Tamoxifen. In the mouse brain GLAST::CreER^{T2} induced recombination targets neural stem cells and astrocytes (Mori et al., 2006; DeCarolis et al., 2013).

In vivo experiments analyzing the morphology of FoxO1/3/4 KO cells versus FoxO1/3/4 WT cells in the adult dentate gyrus were performed using a FoxO1/3/4$^{fl/fl}$ /

FoxO1/3/4$^{wt/wt}$ mouse model. FoxO1/3/4 KO was mediated via a MML-retrovirus encoding for Cre-recombinase (see 4.2.7).

2.1.1 Increase in proliferation and neurogenesis in FoxO1/3/4 deficient adult neural stem cells *in vitro*

The effects of FxoO1/3/4 KO on stem cell behavior were first studied *in vitro*. Therefore adult neural stem cells (aNSCs) were isolated from 8-week-old mice (P56) and cultured as neurospheres. The ability to form neurospheres, to proliferate and to differentiate into the neural lineages is considered characteristic of NSCs isolated from the adult brain (Reynolds et al., 1992; Reynolds & Weiss, 1996; Richards et al., 1992; Rietze et al., 2001; Wachs et al., 2003). The *in vitro* experiments were implemented according to the following scheme (Figure. 2.1). aNSCs were isolated from brains of 8 week-old FoxO1/3/4$^{fl/fl}$ mice. Cells were expanded and transduced with either a Cre-expressing retrovirus (CAG GFP/Cre) to induce the KO of FoxO1/3/4 or a GFP-expressing retrovirus (CAG GFP) as control. After further expansion cells were FACsorted for GFP expression to obtain genetically homogeneous populations with regard to FoxO recombination. All experiments were performed within the first 6 passages.

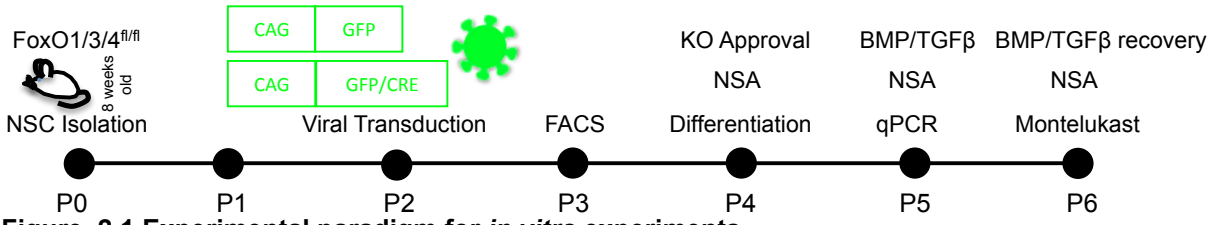

Figure. 2.1 Experimental paradigm for *in vitro* experiments.
aNSCs were isolated from SVZ of 8 week-old FoxO1/3/4$^{fl/fl}$ mice (P0). Cells were expanded, transduced with retroviruses at passage 2 (P2) and FACsorted at passage 3 (P3). Experiments were performed between passages 4 and 6.

Recombination of the conditional FoxO loci was controlled via immunocytochemistry and genotyping PCRs. To study the FoxO1/3/4 KO via immunocytochemistry, neurospheres were harvested, split into single cells and plated on PDL-Laminin-coated glass-coverslips. After 3 hours cells had attached to the glass-coverslips; at this time they were fixed with 4% PFA. Immunocytochemistry was performed with antibodies against GFP, FoxO1 and FoxO3 (Figure 2.2 A). Immunoflourescent staining showed strong reactivity for FoxO1 and FoxO3 in the control cells but not in

FoxO1/3/4 KO cells. Several antibodies were tested for immunocytochemistry of FoxO4; none was suitable for this application. Accordingly, additional genotyping PCRs were performed to validate the FoxO1/3/4 KO for all three loci. Cells were harvested at passage 4 (P4), DNA was isolated and PCRs for FoxO1, FoxO3 and FoxO4 were performed and analyzed on an agarose gel (Figure 2.2 B). The genotyping PCRs revealed PCR products at the sizes for the floxed alleles for FoxO1, FoxO3 and FoxO4 for the control cells (149 kb, 138 kb, 555 kb) and PCR products at the sizes for the knocked out alleles for FoxO1, FoxO3 and FoxO4 for the FoxO1/3/4 KO cells (190 kb, 186 kb, 471 kb). In sum, these results indicate that all FoxO alleles were efficiently ablated.

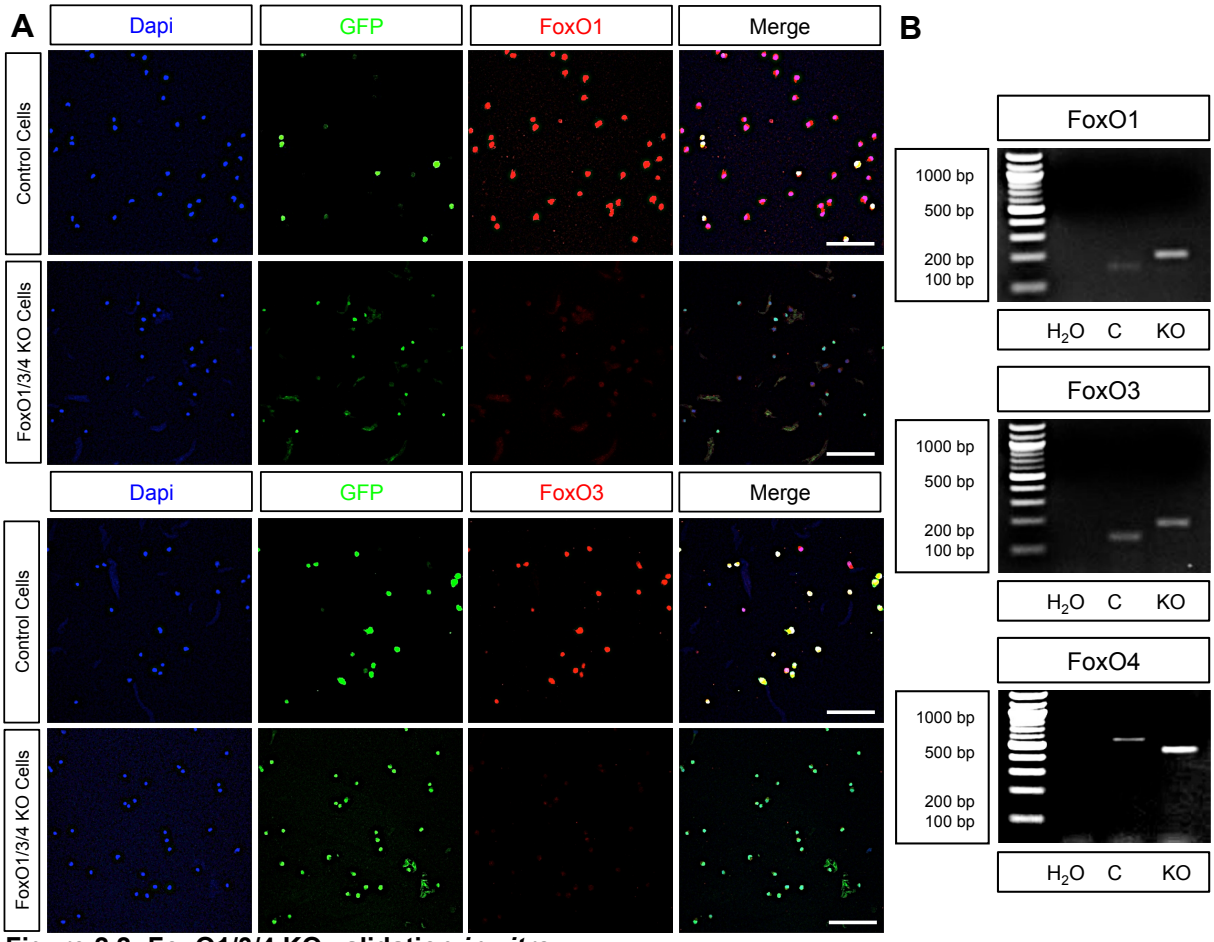

Figure 2.2: FoxO1/3/4 KO validation *in vitro*.
A Confocal images with a 20x objective of FoxO1/3/4 KO and control cells, stained with Dapi and antibodies against GFP, FoxO1 and FoxO3. The images of the control cells revealed a bright staining for FoxO1 and FoxO3, while the FoxO1/3/4 KO cells showed no staining for FoxO1 and FoxO3; n=4. Scale bar ≙ 100 µm. **B** Genotyping PCR products for FoxO1, FoxO3 and FoxO4 performed on DNA isolated from control cells (C) and FoxO1/3/4 KO cells (KO). The shifts in the product sizes from control cells to FoxO1/3/4 KO cells indicate that the KO induction via retrovirus worked; n=4.

To begin with, the proliferation potential of FoxO1/3/4 KO cells was analyzed using a single cell neurosphere assay (NSA). Control and FoxO1/3/4 KO neurospheres were split and seeded at a density of one cell per well onto 60-well-miniplates. Wells were

analyzed under a fluorescent microscope; wells that contained a single GFP-positive cell were marked. 7 days later, marked wells were again screened under a fluorescent microscope and the number of cells that formed neurospheres was determined. This experiment was replicated each three times at passages 4, 5 and 6 (P4, P5, P6; Figure 2.3 A). FoxO1/3/4 KO cells formed significantly more neurospheres as control cells (figure 2.8 F; control cells: 5,72 % - 8,2 %; FoxO1/3/4 KO cells: 20,52 % - 39,59 %; p-value=0,008). The number of formed neurospheres increased from passage 4 to passage 6 in FoxO1/3/4 KO cells compared to control cells, latter's proliferation potential stayed constant within the passages.

In a second experiment the differentiation potential of the FoxO1/3/4 KO cells was tested. Cells were grown as neurospheres and split into single cells. The dissociated cells were plated on PDL-Laminin-coated glass-coverslips under growth factor withdrawal to induce differentiation. After 4 or 8 days of differentiation, cells were fixed with 4% PFA and stained for either neuronal markers (DCX, Map2(a+b)) or a marker for astrocytes (GFAP; glial fibrillary acidic protein; Eng et al., 1971) (Figure 2.3 B - E). The microtubule-associated protein Doublecortin (DCX) is a marker for neuroblasts/immature neurons (Couillard-Despres et al., 2005) while Map2(a+b) (Microtubule-associated protein 2) is a marker for mature neurons (Chung et al., 1996). Significantly less FoxO1/3/4 KO cells (13,78±2,67 %) differentiated into $GFAP^+$ astrocytic cells compared to control cells (27,37±3,32 %) after 4 days of differentiation (Figure 2.3 A, E; p-value=0,0059) while significantly more cells differentiated into DCX^+ immature neurons compared to control cells (Figure 2.3 F; control cells: 25,10±10,91 %; FoxO1/3/4 KO cells: 46,70±9,62 %; p-value=0,0332). The amount of $Map2(a+b)^+$ cells was similar between control cells and FoxO1/3/4 KO cells after 4 days of differentiation (Figure 2.3 F; control cells: 21,48±7,72; FoxO173/4 KO cells: 24,45±1,83 %). After 8 days of differentiation a tendency of FoxO1/3/4 KO cells to generate less $GFAP^+$ (control cells: 45,84±8,26 %; FoxO1/3/4 KO cells: 28,27±9,85 %; p-value=0,2741) and more DCX^+ cells (control cells: 26,59±25,77 %; FoxO1/3/4 KO cells: 45,98±5,72 %; p-value=0,3099) was still present (Figure 2.3 G). The fraction of $Map2(a+b)^+$ mature neurons was now significantly (p-value=0,0033) higher in FoxO1/3/4 KO cells (35,93±1,73 %) compared to control cells (22,26±2,87 %). These results implicate, that neurogenesis is increased in FoxO1/3/4 KO cells *in vitro*.

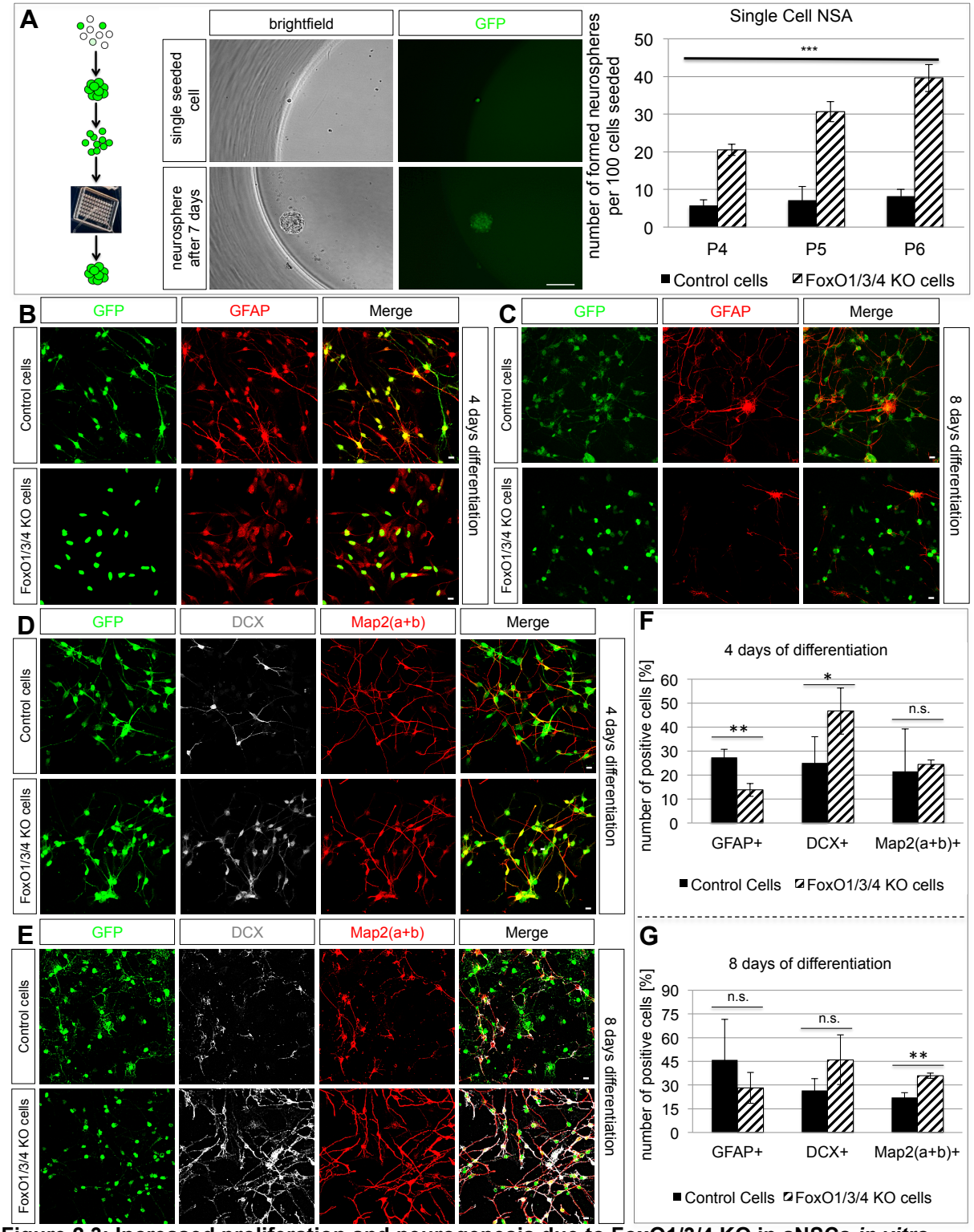

Figure 2.3: Increased proliferation and neurogenesis due to FoxO1/3/4 KO in aNSCs *in vitro*.
A, B, C and D Confocal images of control cells and FoxO1/3/4 KO cells after 4 days and 8 days of differentiation stained with antibodies against GFP, GFAP, DCX and Map2. Scale bar ≙ 10 µm. **E** Diagrams of the numbers of $GFAP^+$, DCX^+ and $Map2(a+b)^+$ cells after 4 days and 8 days of differentiation; n=3. Significantly less astrogenesis and more neurogenesis was observed after 4 days of differentiation. Increase in neurogenesis was still obvious after 8 days of differentiation. **F** Scheme of single cell neurosphere assay (NSA); cells were transduced with either GFP/Cre-expressing retrovirus or GFP retrovirus, FACsorted, dissociated and seeded as single cells in miniwells as one cell per well; number of formed neurospheres was analyzed 7 days later. Example picture of a single seeded cell and a formed neurosphere imaged by a fluorescent microscope; scale bar ≙ 10 µm. Diagram of numbers of formed neurospheres after 7 days; n=3. Proliferation was increased in Foxo1/3/4 KO cells *in vitro*.

2.1.2 Changed survival, proliferation and neurogenesis of FoxO1/3/4 KO adult neural stem cells *in vivo*

To address the question how FoxO1/3/4 affect in vivo adult hippocampal neurogenesis, the FoxO1/3/4 KO and the FoxO1/3/4 WT mouse model were studied. The principal experimental paradigm for the following experiments is schematically depicted in Figure 2.4. All mice were intraperitoneally (i.p.) injected with 1 mg Tamoxifen at P56 for five consecutive days twice a day every 12 hours, which should result in deletion of the conditional FoxO alleles in the FoxO134 KO mice from cells with Cre-recombinase activity. In both mouse lines, cells, in which Cre-recombinase was activated, should initiate the expression of the β-gal(Rosa26) reporter. Immediately after the Tamoxifen injections mice received daily injections of BrdU (10 g BrdU / kg bodyweight) for three consecutive days. One group of mice was sacrificed 3 hours after the last BrdU pulse and therefore 3 days after Tamoxifen treatment. Other time points were 28 days, 4 months or 8 months after Tamoxifen treatment (3 dpt, 28 dpt, 4mpt, 8mpt). Mice were sacrificed and brain tissue was prepared for immunohistochemistry (mice of the 4 months and 8 months timepoint were prepared by Amir Khan).

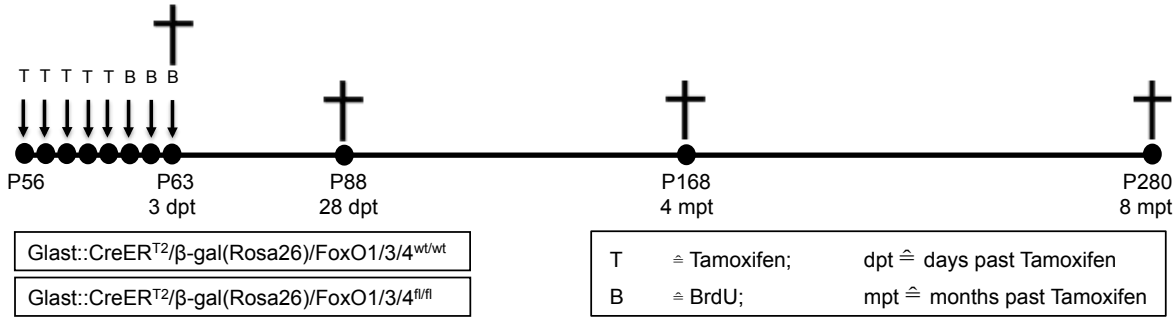

Figure 2.4: Experimental paradigm for FoxO1/3/4 KO analysis *in vivo*.
Glast::CreER^{T2}/β-gal(Rosa26)/FoxO1/3/4$^{fl/fl}$ and Glast::CreER^{T2}/β-gal(Rosa26)/FoxO1/3/4$^{wt/wt}$ mice were injected i.p. with 1 mg Tamoxifen for 5 consecutive days twice a day every 12 hours to induce FoxO1/3/4 KO. BrdU injections for 3 consecutive days once per day followed. Mice were sacrificed either directly 3 hours after the last BrdU pulse and therefore 3 days after Tamoxifen treatment or 28 days, 4 months or 8 months after Tamoxifen treatment (3 dpt, 28 dpt, 4mpt, 8 mpt).

2.1.2.1 Validation of the FoxO1/3/4 conditional KO mouse model

To control the KO induction via the Glast::CreER^{T2} system, immunohistochemistry with antibodies against FoxO3 and β-galactosidase was performed (Figure 2.5). At 28 dpt expression of FoxO3 was abolished or strongly reduced in β-galactosidase-

positive cells of the dentate gyrus of the FoxO1/3/4 KO mice. In contrast, β-galactosidase-positive cells in the FoxO1/3/4 WT mice were strongly immunoreactive for FoxO3. There are no antibodies available against FoxO1 and FoxO4, which are suitable for immunohistochemistry of adult mouse tissue sections. Therefore, it was not possible to determine their expression in Foxo1/3/4 KO. However, since the Glast::CreER^{T2} system efficiently induced the KO of FoxO3, it was assumed likely that the system also efficiently induced recombination of the conditional FoxO1 and FoxO4 loci.

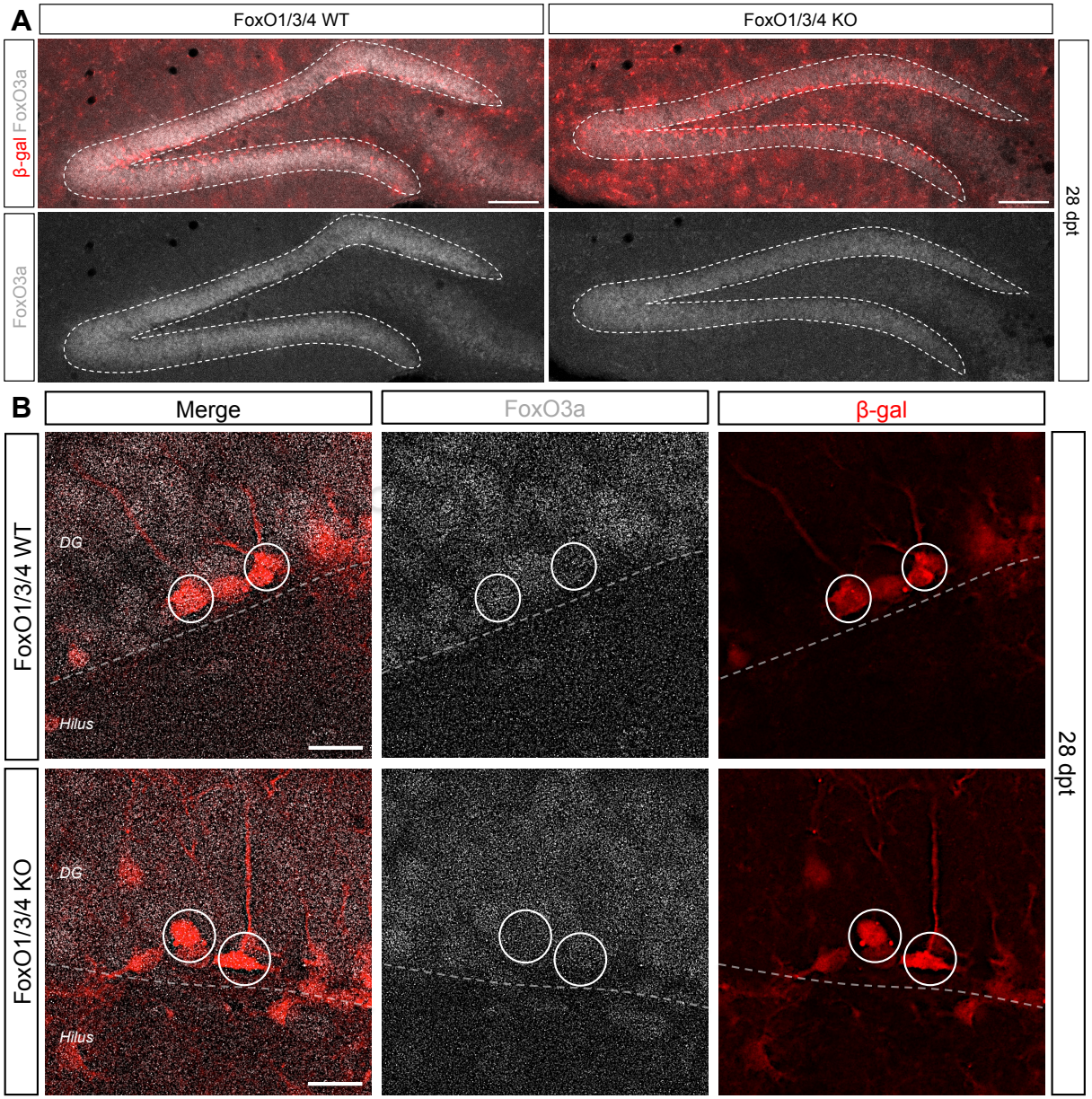

Figure 2.5: Validation of FoxO3 KO in the dentate gyrus at 28 dpt.
A Confocal images of the DG of FoxO WT and FoxO KO mice taken with a 10x objective. Scale bar ≙ 100 µm. **B** Higher magnification confocal images of the DG of FoxO WT and FoxO KO mice taken with a 40x objective. FoxO3 expression was deleted or at least reduced in β-gal-positive recombined FoxO1/3/4 KO cells in the dentate gyrus while the β-gal-positive cells in FoxO1/3/4 WT mice were still FoxO3 positive. Scale bar ≙ 10 µm.

2.1.2.2 Loss of β-galactosidase positive adult recombined cells over time in the dentate gyrus of FoxO1/3/4 KO animals

Paik et al. and Renault et al. showed that developmental deletion of FoxO1/3/4 as well as FoxO3 null mutation impair maintenance of the neural stem cell pool. To address the question how Foxo1/3/4 ablation specifically in the adult neural stem cell pool affects stem cell maintenance and neurogenesis, the β-galactosidase expression in the dentate gyrus of adult FoxO1/3/4 WT and KO mice 3 days, 28 days, 4 months and 8 months after KO induction (3 dpt, 28 dpt, 4 mpt, 8 mpt) was analyzed. Immunohistochemistry with Dapi and an antibody against β-galactosidase (β-gal) was performed and analyzed using confocal microscopy (Figure 2.6, numbers not count). More β-gal expressing cells were present in FoxO1/3/4 KO mice at 3 dpt. 28 days after the KO induction (28 dpt), β-gal$^+$ cell density was comparable between KO and control animals. 4 months after KO induction (4 mpt) a slight decrease in β-gal$^+$ cells was observed in FoxO1/3/4 KO animals, while 8 months after KO induction (8 mpt) an apparent loss of β-gal$^+$ cells was visible in FoxO1/3/4 KO animals compared to FoxO1/3/4 WT animals, suggesting that deletion of FoxO results in impairment of hippocampal neurogenesis.

Figure 2.6: Loss of β-gal$^+$ cells in FoxO1/3/4 KO animals over time.
Confocal tile scan with an 10x objective of the dentate gyrus of a FoxO1/3/4 WT and KO animal 3 days, 28 days, 4 months and 8 months after adult KO induction (3 dpt, 28 dpt, 4 mpt, 28 dpt) stained with Dapi and an antibody against β-galactosidase (β-gal). β-gal$^+$ cells were lost over time in the dentate gyrus of FoxO1/3/4 KO animals compared to FoxO1/3/4 WT animals. Scale bar ≙ 100 µm.

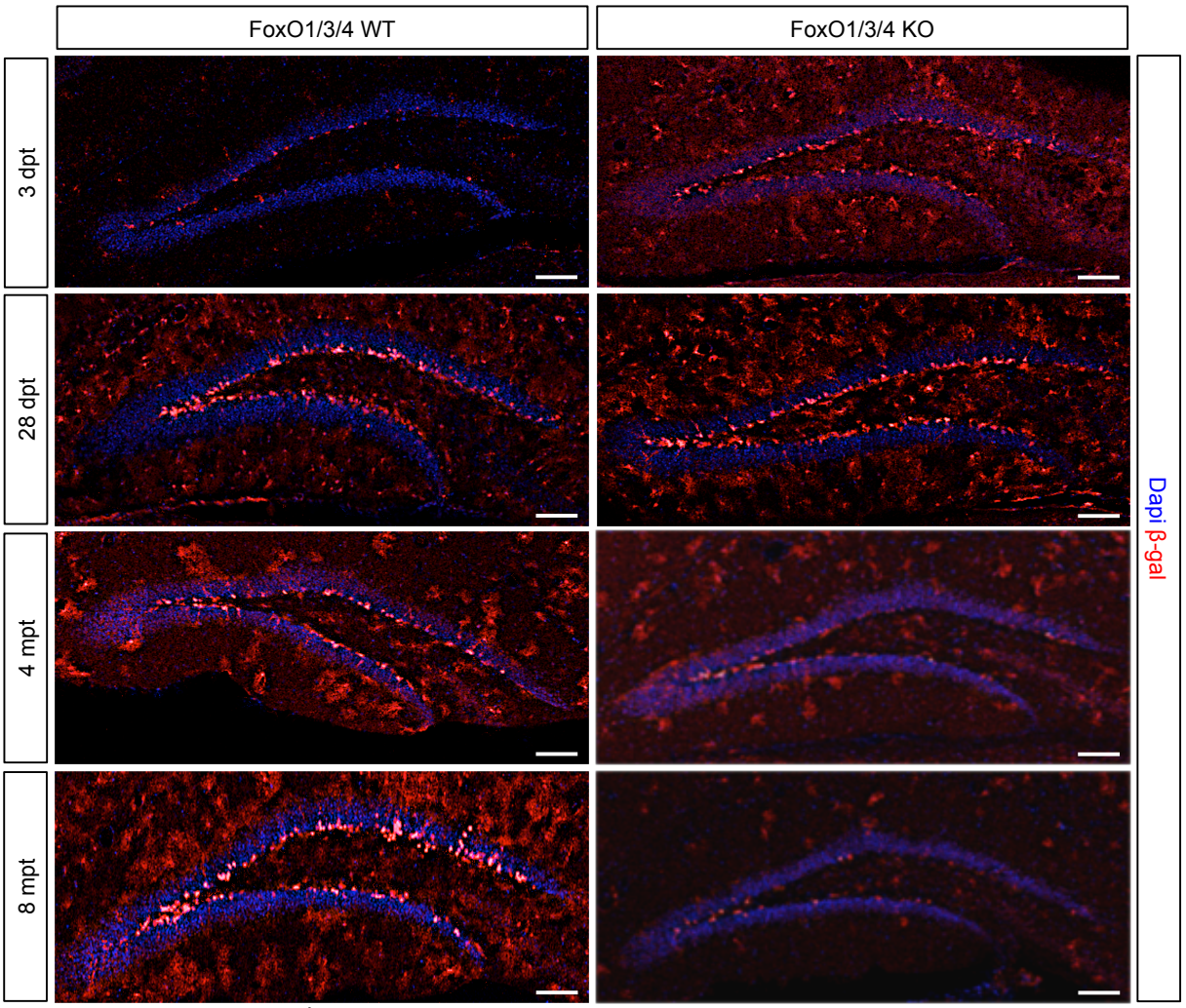

Figure 2.6: Loss of β-gal^{+} cells in FoxO1/3/4 KO animals over time.

2.1.2.3 Immediate increase in proliferation and neurogenesis in FoxO1/3/4 deficient aNSCs in the dentate gyrus *in vivo*

Next, the immediate effect of conditional removal of FoxO1/3/4 on precursor proliferation and neurogenesis in the dentate gyrus of the hippocampal formation was analyzed. To this end, KO of FoxO1/3/4 was induced by five days injection with Tamoxifen starting at P56 (Figure 2.4). Animals subsequently received daily BrdU injections for 3 consecutive days and were sacrificed 3 hours after the last BrdU injection. BrdU is a chemical analog of the nucleotide thymidine. Intraperitoneally injected BrdU is taken up by all cells, but is only stably integrated into newly synthesized DNA during S-phase of the cell cycle (Eidinoff et al., 1959). Consequently, BrdU permanently labels dividing cells and their progeny. Staining against β-galactosidase allowed visualization of recombined cells. Quantification of

BrdU was used to estimate the proliferation activity in the dentate gyrus. Doublecortin as a marker for neuroblasts and immature neurons was applied to determine the level of neurogenesis (Couillard-Despres et al., 2005). Confocal images were taken and the $BrdU^+$ cells in the dentate gyrus of at least three different animals were evaluated (Figure 2.7).

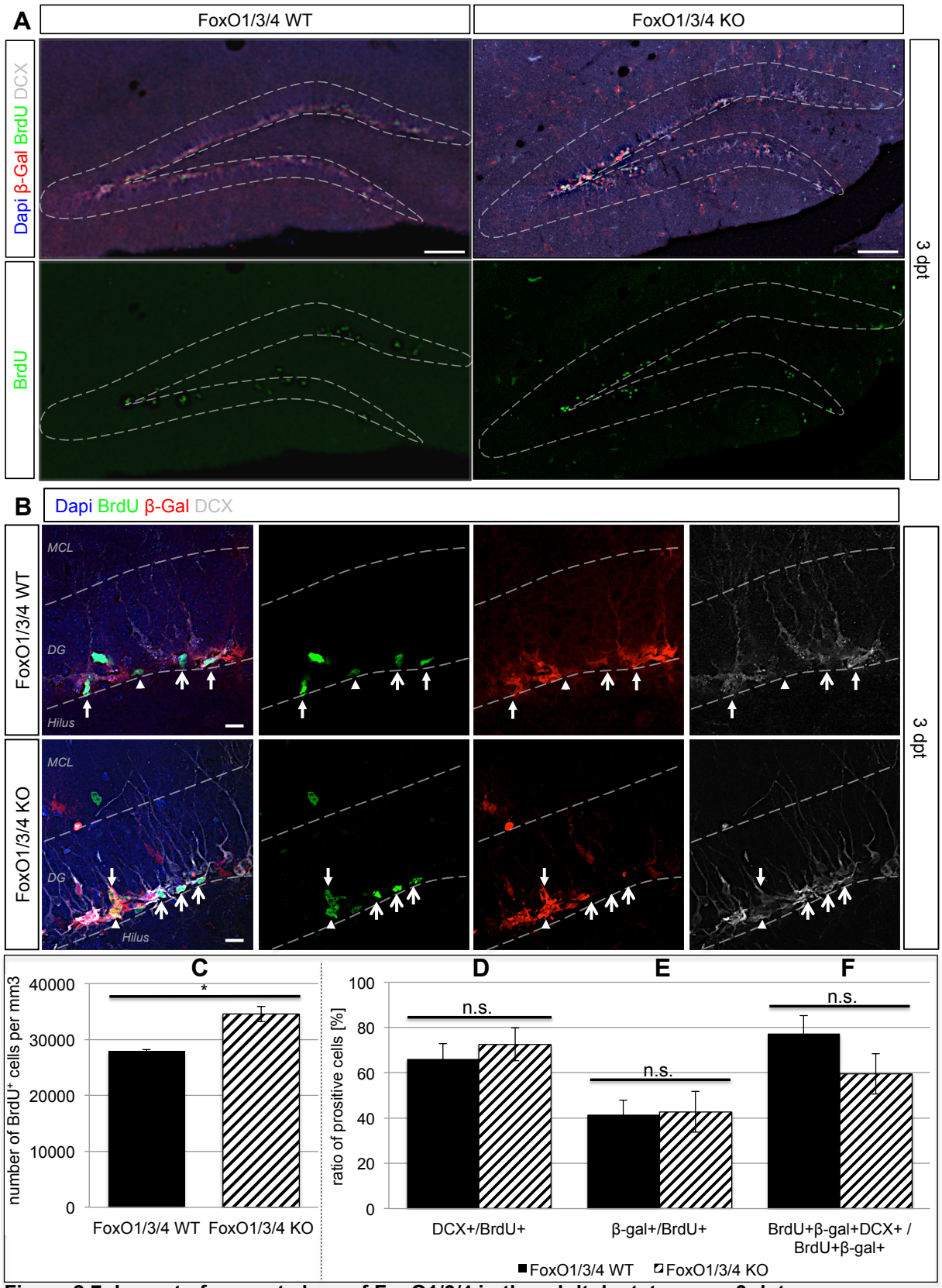

Figure 2.7: Impact of an acute loss of FoxO1/3/4 in the adult dentate gyrus 3 dpt.

Figure 2.7: Impact of an acute loss of FoxO1/3/4 in the adult dentate gyrus 3 dpt.
Confocal images of the dentate gyrus of a FoxO1/3/4 WT and a FoxO1/3/4 KO animal stained with Dapi and antibodies against BrdU, β-galactosidase and DCX. **A** Tile scans of the dentate gyrus imaged with a 10x objective. Scale bar ≙ 100 µm. **B** Section of the dentate gyrus imaged with a 63x oil objective. Triangular arrows label cells that were positive for BrdU and β-galactosidase. Large arrows point at cells positive for BrdU and DCX. Small arrows indicate cells, which were positive for BrdU, β-galactosidase and DCX. Scale bar ≙ 10 µm. **C** Diagram of the numbers of $BrdU^+$ cells per mm^3 of the dentate gyrus of FoxO1/3/4 WT versus FoxO1/3/4 KO animals 3 dpt; n=3. **D-F** Diagram of the ratios of DCX^+ to $BrdU^+$ cells, $β\text{-}gal^+$ to $BrdU^+$ cells and $BrdU^+β\text{-}gal^+DCX^+$ to $BrdU^+β\text{-}gal^+$ cells 3 dpt; n=3. Overall numbers of $BrdU^+$ cells were significantly increased in FoxO1/3/4 KO animals and the percentage of DCX^+ cells was slightly increased in the FoxO1/3/4 KO animals. Proliferation and neurogenesis were comparable between non-recombined and recombined cells in FoxO1/3/4 KO animals 3 dpt.

Overall proliferation and neurogenesis 3 dpt

First the number of $BrdU^+$ cells was determined. In the dentate gyrus of FoxO1/3/4 KO animals significant more $BrdU^+$ cells were found compared to FoxO1/3/4 WT animals (FoxO1/3/4 KO: 34581±1373 cells per mm^3; FoxO1/3/4 WT: 28007±187 cells per mm^3; p-value = 0,01299; Figure 2.7 A). To analyze the rate of neuronal differentiation, the fraction of DCX^+ cells among the $BrdU^+$ cells was quantified. WT animals and FoxO1/3/4 KO animals showed similar rate of neuronal differentiation: 66.12±6.66 % of the $BrdU^+$ cells in the FoxO1/3/4 WT animals and 72.53±7.21 % of the $BrdU^+$ cells in the FoxO1/374 KO animals were DCX^+ (p-value=0.3091; Figure 2.7 B, D). In summary, increased proliferation resulted in increased neuronal production in FoxO1/3/4 KO animals at 3dpt.

Proliferation and neurogenesis in the $β\text{-}gal^+$ cell compartment 3 dpt

To determine if recombined cells were responsible for the increase in $BrdU^+$ cells in the FoxO1/3/4 KO animals, the fraction of $β\text{-}gal^+$ cells among the $BrdU^+$ cells was assessed. Evaluating these numbers revealed that the percentage of $β\text{-}gal^+$ cells within the $BrdU^+$ cells was similar in FoxO1/3/4 WT and KO animals (FoxO1/3/4 WT: 41.55±6.43 %; FoxO1/3/4 KO: 42.69±9.01 %; Figure 2.7 B, E). Thus, the increase in $BrdU^+$ cells in the FoxO1/3/4 KO animals was caused by increased proliferation of recombined and non-recombined cells. Next the fate of the $β\text{-}gal^+$ cells was analyzed by determining the ratio of $BrdU^+β\text{-}gal^+DCX^+$ to $BrdU^+β\text{-}gal^+$ cells (Figure 2.7 F). 77.39±7.94 % of the $BrdU^+β\text{-}gal^+$ cells were DCX^+ in the FoxO1/3/4 WT animals, while 59.50±8.87 % were DCX^+ in the FoxO1/3/4 KO animals. This difference, however, was not significant (p-value=0,0605). In summary, these data indicate that the increase in $BrdU^+$ cells and in neurogenesis following FoxO1/3/4 ablation was caused by increased proliferation of both recombined and non-recombined cells.

2.1.2.4 Slightly ongoing increase in proliferation and neurogenesis 28 days after FoxO1/3/4 KO induction

Next, the long-term fate of newly generated cells was studied. Animals received daily injections of BrdU at the end of the Tamoxifen treatment and were sacrificed 28 days after Tamoxifen treatment (Figure 2.4). Immunohistochemistry was performed with antibodies against β-galactosidase, BrdU, Prox1 and Ki67. BrdU and DCX were used as markers for proliferation and neurogenesis as described in 2.1.2.3. Prox1 was applied as a marker for post mitotic granular neurons (Iwano et al., 2012; Lavado et al, 2010). Ki67 is expressed in all phases of the active cell cycle but not in G(0)-phase and thus can be used to distinguish dividing from resting cells (Kee et al., 2002; Scholzen & Gerdes, 2000). Confocal images were taken and the BrdU$^+$ cells in the dentate gyrus of at least three different animals were evaluated (Figure 2.8).

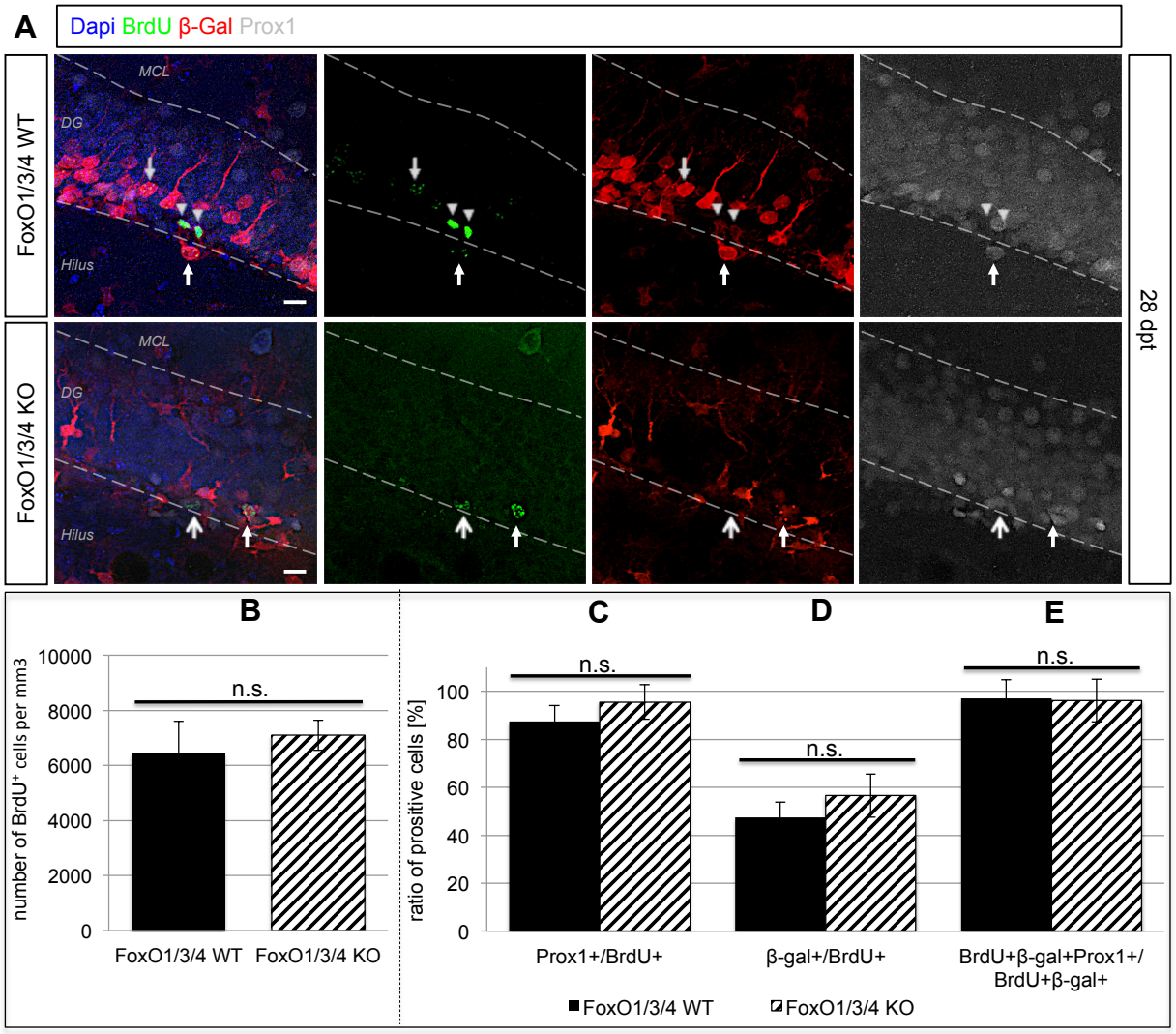

Figure 2.8: Effects of the loss of FoxO1/3/4 in the adult dentate gyrus 28 dpt.

Figure 2.8: Effects of the loss of FoxO1/3/4 in the adult dentate gyrus 28 dpt.
A Confocal images of the dentate gyrus of a FoxO WT and a FoxO KO animal stained with Dapi and antibodies against BrdU, β-galactosidase, and Prox1. Sections of the dentate gyrus were imaged with a 63x oil objective. Triangular arrows label cells that are positive for BrdU and β-galactosidase. Large arrows appoint to cells positive for BrdU and Prox1. Small arrows indicate cells, which were positive for BrdU, β-galactosidase and Prox1. Scale bar ≙ 10 µm. **B** Diagram of the numbers of $BrdU^+$ cells per mm^3 of the dentate gyrus of FoxO1/3/4 WT versus FoxO1/3/4 KO animals.; n=3. **C-D** Diagram of the ratio of $Prox1^+$ to $BrdU^+$ cells, $β\text{-}gal^+$ to $BrdU^+$ and $BrdU^+$ $β\text{-}gal^+Prox1^+$ to $BrdU^+β\text{-}gal^+$ cells in the dentate gyrus of FoxO1/3/4 WT versus FoxO1/3/4 KO animals 28 dpt; n=3. **D A** trend towards an increased number of $BrdU^+$ cells was observed in FoxO1/3/4 KO animals. The ratios of $Prox1^+$ to $BrdU^+$ cells and $β\text{-}gal^+$ to $BrdU^+$ were slightly, but not significantly raised in FoxO1/3/4 KO animals. The ratio of $BrdU^+$ $β\text{-}gal^+Prox1^+$ to $BrdU^+β\text{-}gal^+$ cells was similar in Foxo1/3/4 WT and KO animals. The observed increase in proliferation and neurogenesis in the FoxO1/3/4 KO animals was at least partially mediated by the $β\text{-}gal^+$ cell compartment.

First, the total number of $BrdU^+$ cells in the dentate gyrus of FoxO1/3/4 WT and KO animals was counted. 28 days after KO induction, there was a trend towards higher numbers of $BrdU^+$ cells in FoxO1/3/4 KO animals (7101±551 cells per mm^3) compared to FoxO1/3/4 WT animals (6447±1161 cells per mm^3, p-value=0,4460). The fraction of $Prox1^+$ to $BrdU^+$ cells was also slightly higher in the FoxO1/3/4 KO animals compared to the WT animals (FoxO1/3/4 WT: 87,40±4,08 %; FoxO1/3/4 KO: 95,55±2,06 %; p-value=0,0546). Thus, the increased proliferation, which was induced early after FoxO ablation resulted in a slight increase in the generation of new mature DG neurons at 28 dpt .

The fraction of $β\text{-}gal^+$ cells among the $BrdU^+$ cells at 28 dpt was comparable between FoxO1/3/4 WT and FoxO1/3/4 KO mice (47.39±5.21 % and 56.56±11.29 %, respectively; p-value=0,297). Moreover, the fraction of $β\text{-}gal^+$ cells among the $BrdU^+$ cells was largely comparable between the 3 dpt (FoxO1/3/4 WT: 41.55±6.43 %; FoxO1/3/4 KO: 42.69±9.01 %; Figure 2.7 B, E) and the 28 dpt time-point. These data indicate that FoxO KO did not have a major effect on the survival of newly generated cells. The fraction of $Prox1^+$ cells among the $BrdU^+β\text{-}gal^+$ cells was comparable in FoxO1/3/4 KO and WT animals (FoxO1/3/4 WT: 97,01±2,70 %; FoxO1/3/4 KO: 96,19±6,59 %). Moreover, in FoxO1/3/4 KO the fraction of Prox1+ cells among the BrdU+bgal+ cells (96,19±6,59 %) was similar to the fraction of Prox1+ cells among the BrdU+ cells (95,55±2,06 %). Thus, FoxO deletion did not affect neuronal cell fate of newly generated cells.

Finally, the levels of proliferation were examined at 28 dpt via analysis of Ki67+ cells. A significant increase in Ki67-positive ($ki67^+$) and $β\text{-}gal^+$ double positive cells was determined in the FoxO KO (4668,04±773,96 cells per mm^3) versus Foxo1/3/4 WT

(1914,07±1109,14 cells per mm^3) animals (p-value=0,0292) while the total numbers of $Ki67^+$ cells were similar per mm^3 of the dentate gyrus (FoxO1/3/4 WT: 6199,28±850,92; FoxO1/3/4 KO: 6042,43±788,33) (Figure 2.9). These data indicate that loss of FoxO1/3/4 resulted in a cell autonomous increase in proliferation at 28 dpt.

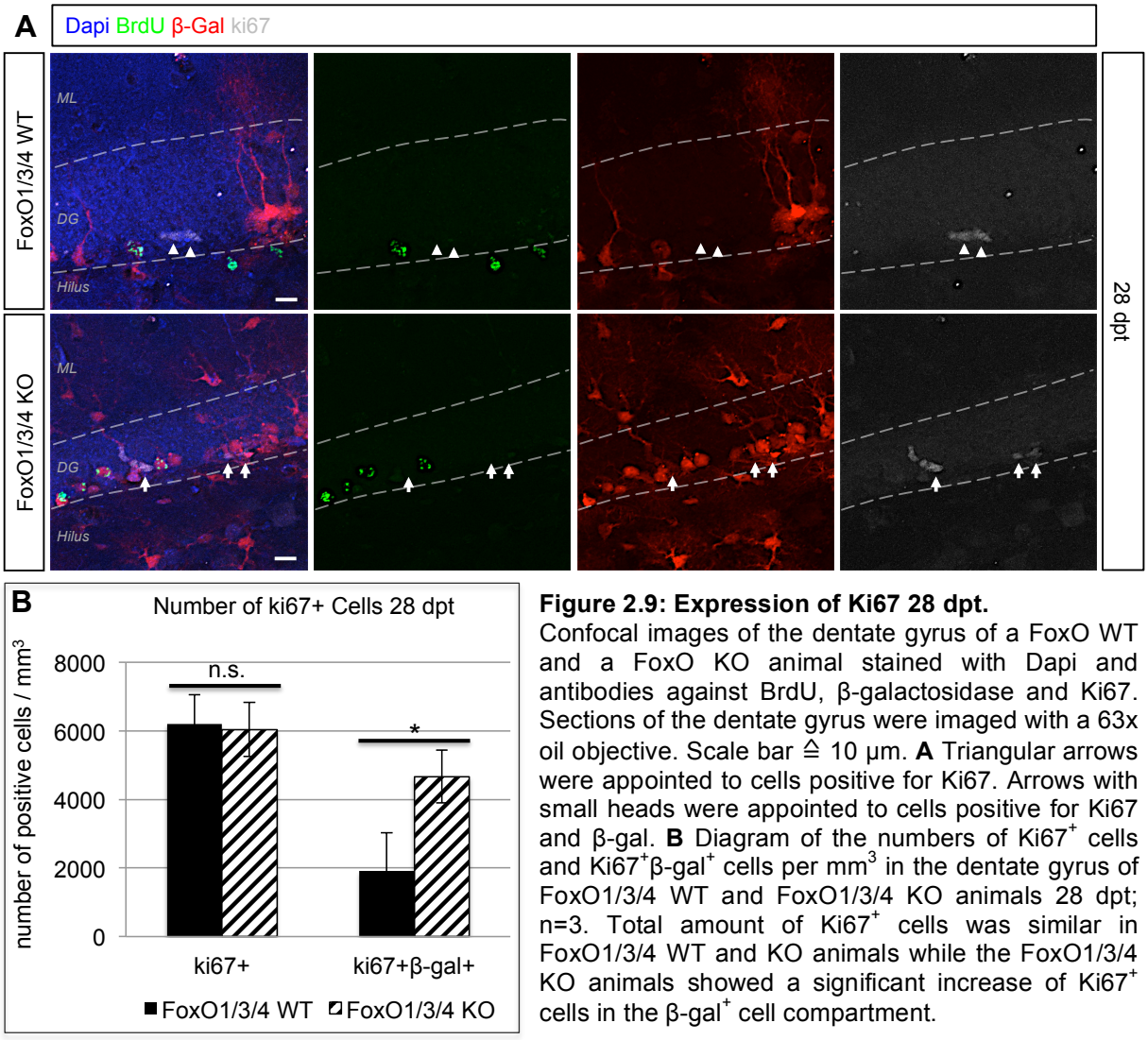

Figure 2.9: Expression of Ki67 28 dpt.
Confocal images of the dentate gyrus of a FoxO WT and a FoxO KO animal stained with Dapi and antibodies against BrdU, β-galactosidase and Ki67. Sections of the dentate gyrus were imaged with a 63x oil objective. Scale bar ≙ 10 µm. **A** Triangular arrows were appointed to cells positive for Ki67. Arrows with small heads were appointed to cells positive for Ki67 and β-gal. **B** Diagram of the numbers of $Ki67^+$ cells and $Ki67^+β\text{-}gal^+$ cells per mm^3 in the dentate gyrus of FoxO1/3/4 WT and FoxO1/3/4 KO animals 28 dpt; n=3. Total amount of $Ki67^+$ cells was similar in FoxO1/3/4 WT and KO animals while the FoxO1/3/4 KO animals showed a significant increase of $Ki67^+$ cells in the $β\text{-}gal^+$ cell compartment.

Additional unpublished data from Dr. Amir Khan (HMGU, now DKFZ) revealed decreased proliferation and neurogenesis in aged FoxO1/3/4 KO mice (8 mpt). In summary, these findings demonstrate that deletion of FoxO1/3/4 lead to an initial burst in proliferative activity and increased neurogenesis followed by loss of proliferative activity and neurogenesis. Overall, these data strongly suggest a function for FoxO transcription factors in the modulation of stem cell proliferation and the control of stem cell maintenance.

2.1.3 Smad pathways as possible signaling pathways controlling FoxOs

2.1.3.1 Active Smad signaling in FoxO1/3/4 deficient cells *in vivo*

The *in vitro* and *in vivo* phenotype of FoxO1/3/4 KO showed intriguing discrepancies. The hyperproliferation phenotype and the distinct increase in neurogenesis detected *in vitro* were only temporarily observed *in vivo*. Moreover, the proliferation phenotype was very mild. A reason for the discrepancies may be that the in vivo adult neurogenic niche provides specific extracellular cues like the cytokines BMP, FGF or TGFβ, which are known to control stem cell quiescence and self-renewal (Battista et al., 2006; Jin et al., 2003; Mira et al. 2010, Kandasamy et al., 2010). Those could have partially over-written the impact of loss of FoxO1/3/4 in aNSCs *in vivo* and their activity was not considered in the *in vitro* model. BMP and TGFβ induced Smad-signaling are critical for stem cell quiescence in various tissues (David et al., 2008; Ewan et al., 2005; Kandasamy et al., 2010; Kandyba et al., 2013; Mira et al., 2010). A KO of BMPR-Ia (bone morphogenic protein receptor one a) for example leads to a burst in proliferation and subsequent loss of the neural stem cell pool in the adult mouse dentate gyrus (Mira et al., 2010). There are indications that the inhibitory effects of Smads on proliferation in neural cells are dependent on intact FoxO signaling (Seoane et al., 2004). BMP binding to their receptors leads to a signaling cascade that culminates in the phosphorylation of Smad1, Smad5 and Smad8 (pSmad1, pSmad5, pSmad8); similarly TGFβ induced signaling results in the phosphorylation of Smad2 and Smad3 (pSmad2, pSmad3); the phosphorylation of Smad transcription factors leads to a translocation to the nucleus and transcription is activated (Flanders et al., 2001; Luukko et al., 2001; Miyazono et al., 2010). Hence, immunohistochemistry against pSmads can be used to investigate Smad signaling activity. To analyze, if Smad signaling is still active in FoxO1/3/4 deficient cells *in vivo*, immunohistochemistry on slices of FoxO1/3/4 KO animals and WT animals 28 days and 8 months after Tamoxifen treatment was performed with antibodies against pSmad1/5/8 and pSmad2 (Figure 2.10). At 28 dpt, pSmad1/5/8 as well as pSmad2 were expressed in the β-gal$^+$ recombined cells both in FoxO1/3/4 WT and FoxO1/3/4 KO cells in the dentate gyrus. The immunoreactivity for both pSmads was reduced in the whole dentate gyrus of old FoxO1/3/4 WT and KO mice (8 mpt). The recombined β-gal$^+$ cells were still positive for pSmad1/5/8 and pSmad2 in the older mice, although as week as the other granular cells in the dentate gyrus. One difference

was noticed. The immunoreactivity of pSmad2 was much lower in the dentate gyrus of FoxO1/3/4 KO mice 8 mpt compared to FoxO1/3/4 WT mice 8 mpt.

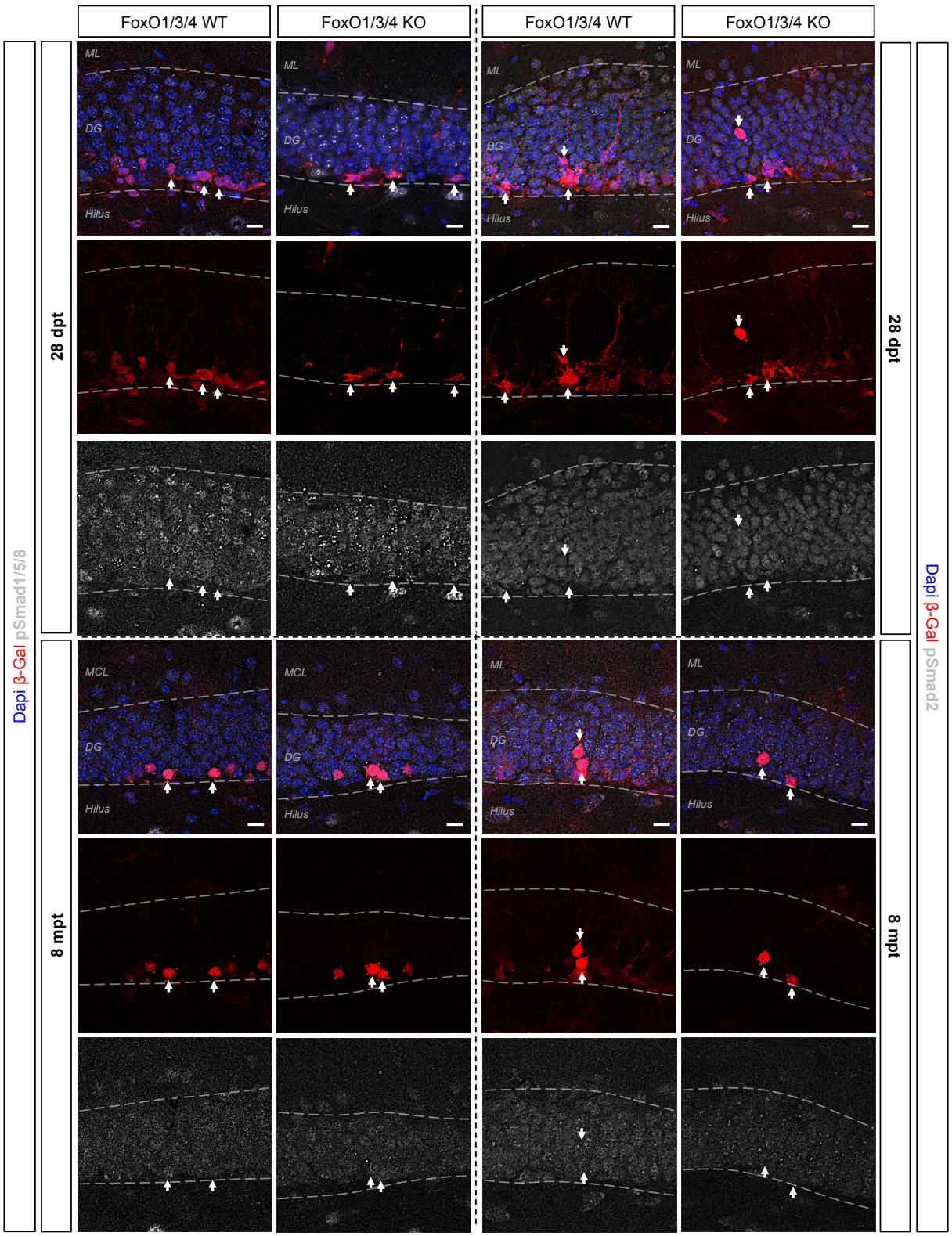

Figure 2.10 Active pSmad signaling in FoxO1/3/4 WT and KO mice 28 dpt and 8 mpt.
Confocal images with a 63x oil objective of the dentate gyrus of FoxO1/3/4 WT and KO animals 28 dpt and 8 mpt stained with Dapi and antibodies against β-gal and pSmad1/5/8 or pSmad2. Smad signaling was detected as active in recombined β-gal$^+$ cells in WT and FoxO1/3/4 KO animals 28 dpt. Smad signaling was reduced in older mice (8 mpt) in all groups. pSmad2 expression seemed to be even more reduced in FoxO1/3/4 KO animals compared to FoxO1/3/4 WT animals. Scale bar≙10 µm.

The detection of active Smad signaling in adult mice might be an explanation for the mild impact of loss of FoxOs in adult mice, which got finally stronger in aged mice due to reduced Smad signaling.

2.1.3.2 Smad signaling is able to control FoxO1/3/4 KO cells *in vitro*

Next, it was tested if FoxO1/3/4 KO cells were capable to respond to BMPs or TGFβ and whether the hyperproliferative phenotype could be explained by the insensitivity of FoxO-deficient cells to these cytokines. FoxO1/3/4 KO and wildtype cells were seeded as single cells in a 96-well-plate at a density of 200 cells per well in 200 µl medium with growth factors. Cells were treated with either 10 ng/ml recombinant BMP4 or 20 ng/ml TGFβ. Control groups were kept in proliferation conditions. 7 days after seeding, the number and size of neurospheres were analyzed (Figure 2.11 A, C, D, E). Consistent with previous results (2.1.1) FoxO1/3/4 KO cells showed a significant increase in number of formed neurospheres compared to control cells under control conditions. Both, BMP4 and TGFβ treatment, decreased number of formed neurospheres significantly. BMP4 treatment was more potent and slowed down neurosphere formation even to less than 10% in both FoxO1/3/4 KO and wildtype cells. The diameters of formed neurospheres were significantly decreased through BMP4 treatment in case of the control cells; in FoxO1/3/4 KO cells there was a clear tendency to a decrease in neurosphere diameters. In a second experiment it was analyzed if the cells could recover from BMP4 and TGFβ treatment and resume proliferation. Cells were cultured at a density of 50000 cells per 5 ml medium with growth factors in 25cm^2 flasks and treated with either 10 ng/ml BMP4 or 20 ng/ml TGFβ; the control group was kept in proliferation medium. Neurospheres were harvested after 7 days, were dissociated into single cells, and seeded again in 96-well-plates at a density of 200 cells per well in 200 µl of proliferation medium without BMP4 or TGFβ. A fourth group was added, where cells, which were previously treated with BMP4, were additionally exposed to the BMP antagonist Noggin (100 ng/ml) to promote recovery (Yanagita, 2005; Bonaguidi et al., 2008). 7 days later number and diameter of formed neurospheres were again quantified (Figure 2.11 B, C, D, E). Control cells and FoxO1/3/4 KO cells both recovered from BMP4 and TGFβ treatment, both in number of formed neurospheres and diameter of formed

neurospheres significantly; except in the case of the recovery of TGFβ treatment of the control cells. Here only a tendency for a recovery from TGFβ treatment was observed in the number of formed neurospheres. The recovery of the FoxO1/3/4 KO cells was even more efficient as of the control cells both for number and diameter of formed neurospheres (Table 2.1). Thus, neural stem cells are responsive to cytokines of the TGFβ-superfamily *in vitro* in the absence of expression of FoxO proteins. Consequently the discrepancies *in vitro* and *in vivo* might be affiliated to persisting activity of TGFβ and BMPs *in vivo* leading to the observed mild changes in proliferation *in vivo*.

Figure 2.11: BMP4 and TGFβ treatment of adult FoxO1/3/4 KO NSCs *in vitro.*
A, B Both numbers and diameters of formed neurospheres were reduced due to BMP4 or TGFβ treatment in control and FoxO1/3/4 KO cells. All groups recovered from BMP4 or TGFβ treatment. **C** Example pictures (fluorescence microscope) of formed neurospheres of control and FoxO1/3/4 KO cells under BMP4/TGFβ treatment and after recovery of both. Scale bar ≙ 100 µm. **D** Summary of numbers and diameters of formed neurospheres of control and FoxO1/3/4 KO cells after BMP4/TGFβ treatment and after recovery of both; n=3. **E** Summary of p-values calculated via Student's t-test for numbers and diameters of formed neurospheres of control and FoxO1/3/4 KO cells after BMP4/ TGFβ treatment and after recovery of both.

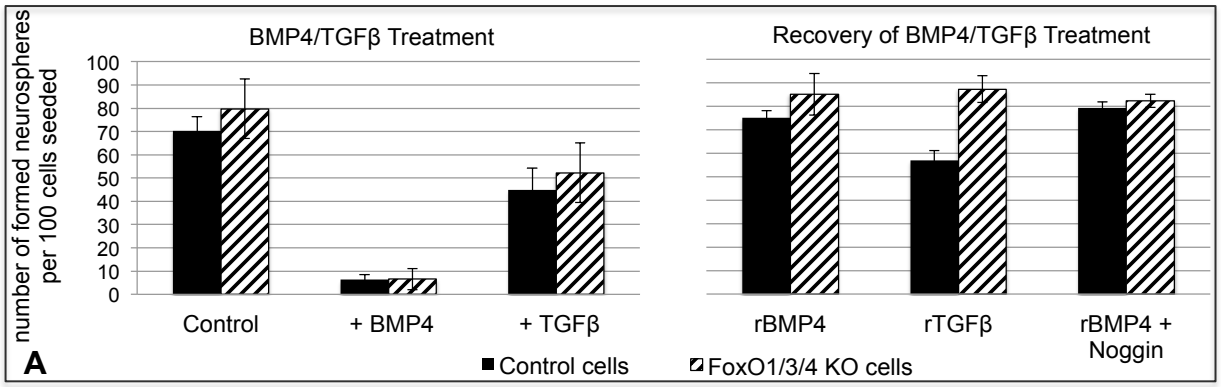

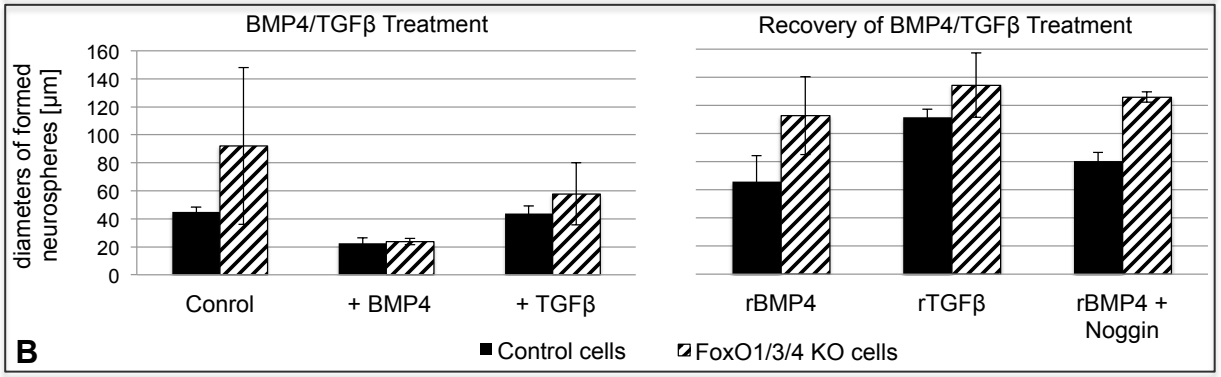

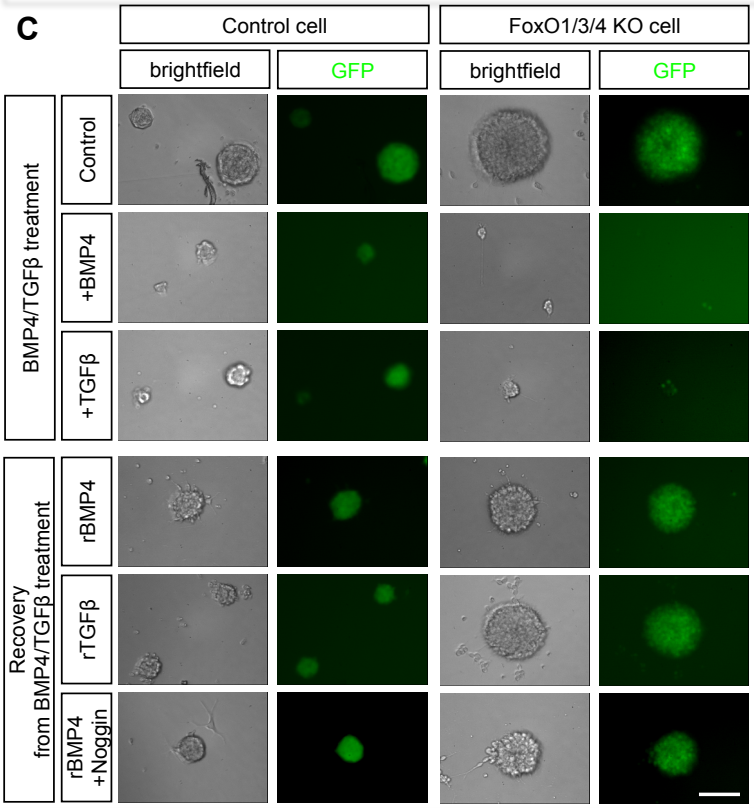

D

neurosphere numbers / 100 cells seeded	Control Cells	FoxO1/3/4 KO Cells
Control	70,23±6,23	79,77±12,74
+BMP4	6,28±2,10	6,53±4,53
+TGFβ	44,78±9,56	52,30±12,81
rBMP4	75,06±3,13	85,10±8,86
rTGFβ	56,93±4,30	87,35±5,69
rBMP4 +Noggin	79,28±2,51	82,33±2,78
neurosphere diameters (µm)	Control Cells	FoxO1/3/4 KO Cells
Control	44,93±3,56	92,01±56,11
+BMP4	22,57±4,01	23,79±2,28
+TGFβ	43,82±5,27	57,84±22,29
rBMP4	65,81±18,24	112,65±27,68
rTGFβ	111,54±5,72	134,22±22,76
rBMP4 +Noggin	80.50±5,93	125,75±3,65

E

p-value *neurosphere number*	Control	Control + rBMP4	Control + rTGFβ	Control + rBMP4/Noggin	FoxO1/3/4 KO + BMP4	FoxO1/3/4 KO + TGFβ
Control + BMP4	0,0014	0,00002	-	0,0192	-	-
Control + TGFβ	0,0239	-	0,1458	-	-	-
FoxO1/3/4 KO	0,0043	-	-	-	0,0052	0,0480
FoxO1/3/4 KO + rBMP4	-	-	-	-	0,0009	-
FoxO1/3/4 KO + rTGFβ	-	-	-	-	-	0,0269
FoxO1/3/4 KO + rBMP4/Noggin	-	-	-	-	0,0498	-
p-value *neurosphere diameter*						
Control + BMP4	0,0013	0,0487	-	0,0001	-	-
Control + TGFβ	0,7958	-	0,0014	-	-	-
FoxO1/3/4 KO	0,2831	-	-	-	0,1373	0,1969
FoxO1/3/4 KO + rBMP4	-	-	-	-	0,0301	-
FoxO1/3/4 KO + rTGFβ	-	-	-	-	-	0,00001
FoxO1/3/4 KO + rBMP4/Noggin	-	-	-	-	0,0142	-

Figure 2.11: BMP4 and TGFβ treatment of adult FoxO1/3/4 KO NSCs *in vitro*.

2.1.1.4 Possible downstream targets of FoxO1/3/4 transcription factors

Notch signaling

Recent studies have identified a number of pathways, which bias tissue stem cell self-renewal, proliferation and differentiation like PI3K-AKT, PTEN and Notch (Ehm et al., 2010; Groszer et al., 2001; Imayoshi et al., 2010; Paling et al., 2004; Yilmaz et al., 2006). To gain insight into the molecular mechanisms by which the FoxO1/3/4 transcription factors may regulate adult neural stem cells a set of potential target genes and signaling pathways were analyzed.

FoxO and Notch were shown to cooperate to regulate progenitor cell maintenance and differentiation in muscle cells (Kitamura et al., 2007). Quantitative RT-PCR (qPCR) was performed for Notch signaling target genes Hes1, Hes5 (hairy enhancer of split), NFIA (nuclear factor I A), NFIX (nuclear factor I X) and ASCL1 (achaete scute complex homolog 1). The Hes genes are repressor-type basic helix-loop-helix (bHLH) genes, which play an important role in nervous system development (Bertrand et al., 2002, Kageyama et al., 2007). Hes proteins of the Hes1/5/7 family repress proneural gene expression and thereby inhibit neuronal differentiation (Jarriault et al., 1995; Jarriault et al., 1998; Kageyama et al., 1997). NFIA and NFIX are members of the transcription factor family nuclear factor one (NFI), which have been shown to be critical regulators of the embryonic hippocampus (Heng et al., 2012; Piper et al., 2010). NFIA regulates, for example, gliogenesis of the embryonic spinal cord, is responsible for proper cortical glia development, and represses the Notch effector Hes1 (Deneen et al., 2006; Piper et al., 2010; Shu et al., 2003; Subramanian et a., 2012). NFIX deficiency leads to abnormal morphologies in the adult dentate gyrus, defects in hippocampal dependent learning and memory and was recently shown to be critical for neural stem cell quiescence (Harris et al., 2013; Martynoga et al., 2013). ASCL1, also known as Mash1 (mammalian achaete scute homolog-1) in mammals, is a proneuronal gene and belongs to the activator-type bHLH transcription factors. ASCL1 for example not only induces neuronal-specific gene expression but also inhibits glia-specific gene expression (Nieto et al., 2001; Tomita et al., 2000). RNA was isolated from neurospheres and transcribed into cDNA. qPCR was performed to analyze the expression via the $\Delta\Delta C_t$-method (Figure 2.12). The mRNA expression of Hes1 was significantly increased (fold change=1,64±0,12; p-value=0,0099), while the expression of Hes5 was drastically

decreased in FoxO1/3/4 KO cells (fold change=0,11±0,05; p-value=0,0425). NFIA and NFIX mRNA expression were both significantly decreased by 50% in FoxO1/3/4 KO cells (NFIA: fold change=0,39±0,11; p-value=0,0057; NFIX: fold change=0,55±0,14; p-value=0,0487). ASCL1 mRNA expression is slightly increased but not significantly in FoxO1/3/4 KO cells (fold change=1,27±0,19; p-value=0,14).

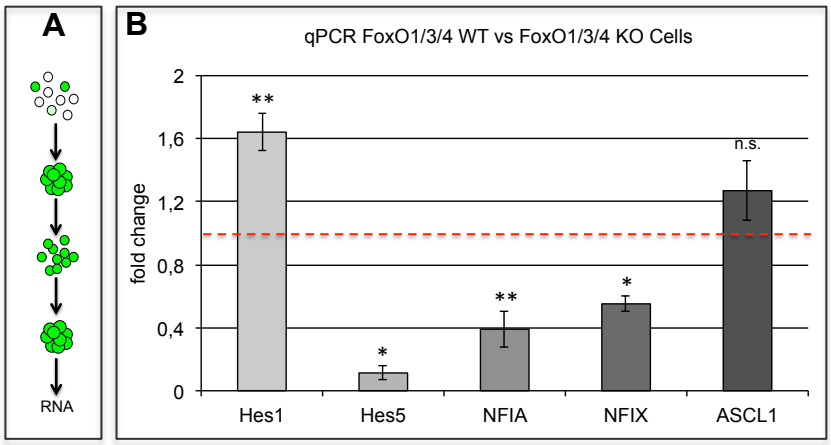

Figure 2.12: qPCR of potential FoxO1/3/4 target genes.
A Experimental paradigm for qPCR. FoxO1/3/4$^{fl/fl}$ neural stem cells were cultivated as neurospheres, transduced with either a GFP/Cre-expressing retrovirus to induce FoxO1/3/4 KO or with a GFP-expressing retrovirus as control. Neurospheres were split into single cells and FACsorted. RNA was isolated from FoxO1/3/4 KO cells and control cells. **B** Diagram of qPCR data depicted as fold changes in mRNA expression calculated via $\Delta\Delta C_t$-method; n=3. Hes1 mRNA expression is significantly increased in FoxO1/3/4 KO cells while Hes5, NFIA and NFIX mRNA expression are decreased.

In summary, the expression of genes for stem cell quiescence like Hes5 and NFIX was decreased in FoxO1/3/4 KO cells *in vitro*, as well as genes, which promote glial differentiation (NFIA, NFIX), while a tendency to an increase in the expression of a proneuronal gene could be observed (ASCL1).

GPR17 signaling

Two recent studies implied the possibility that GPR17 signaling might be regulated via FoxO signaling and that the high proliferative phenotype observed in this study *in vitro* in FoxO1/3/4 KO cells is caused subsequently by changes in GPR17 signaling due to the loss of FoxO1/3/4 (Huber et al., 2011, Ren et al., 2012). Ren et al. showed in ChIP experiments that FoxO1 binds to the GPR17 promoter; in addition, they showed in *in vitro* experiments with Neuro2A cells an increase in GPR17 receptor expression due to enriched FoxO1. They further revealed that an *in vivo* KO of FoxO1 in AgRP (Agouti Related Peptide) neurons (hypothalamic neurons; critical for initiating food intake) results in a reduction of GPR17 expression. Huber et al. showed that inhibition of GPR17 signaling by the GPR17 antagonist Montelukast stimulates proliferation in adult hippocampal rat neural progenitor cells. These

observations raised the hypothesis that GPR17 might be a direct target of FoxO transcription factors in adult neural stem cells and that the elevated proliferation level in FoxO1/3/4 KO cells is caused by a FoxO mediated reduction in GPR17 signaling. To validate this hypothesis expression of the GPR17 receptor was analyzed in vivo. Immunohistochemical analysis revealed that GPR17 receptor expression was reduced in β-gal$^+$ recombined cells of FoxO1/3/4 KO animals compared to FoxO1/3/4 WT animals (figure 2.13 A), which is consistent with the report that GPR17 is a direct target of FoxO transcription factors.

To study whether FoxO KO resulted in altered GPR17-dependent proliferation, the behavior of cultured FoxO KO cells under Montelukast treatment was analyzed. First, a bulk assay was performed. 50000 cells were seeded in a 25 cm^2 culture flask in 5 ml medium under proliferative conditions (with growth factors) and with or without Montelukast. 7 days later, neurospheres were harvested and dissociated into single cells. Total numbers of cells were counted and normalized to untreated control cells (Figure B'). Total cell number of FoxO1/3/4 KO cells was significantly increased compared to control cells (p-value=0,0012). Montelukast treatment doubled total cell number in case of control cells, but not significantly (p-value=0,3301), while total cell number of FoxO1/3/4 KO cells was not changed under Montelukast treatment.

To analyze proliferation in more detail, neurosphere assays were performed. Cells were seeded into the wells of a 96-well-plate at a density of 200 cells per 200 µl of medium. Cells were cultured in the presence and absence of Montelukast. After 7 days numbers and diameters of formed neurospheres were determined (Figure 2.13 B''). FoxO1/3/4 KO cells formed more neurospheres under control conditions (control cells: 62,33±1,85%; FoxO1/3/4 KO cells: 77,35±0,61 %; p-value=0,0371). Montelukast treatment increased neurosphere formation significantly in WT cells but not in FoxO1/3/4 KO cells. The diameters of formed neurospheres were similar under all conditions and cell types (Figure 2.13 B''').

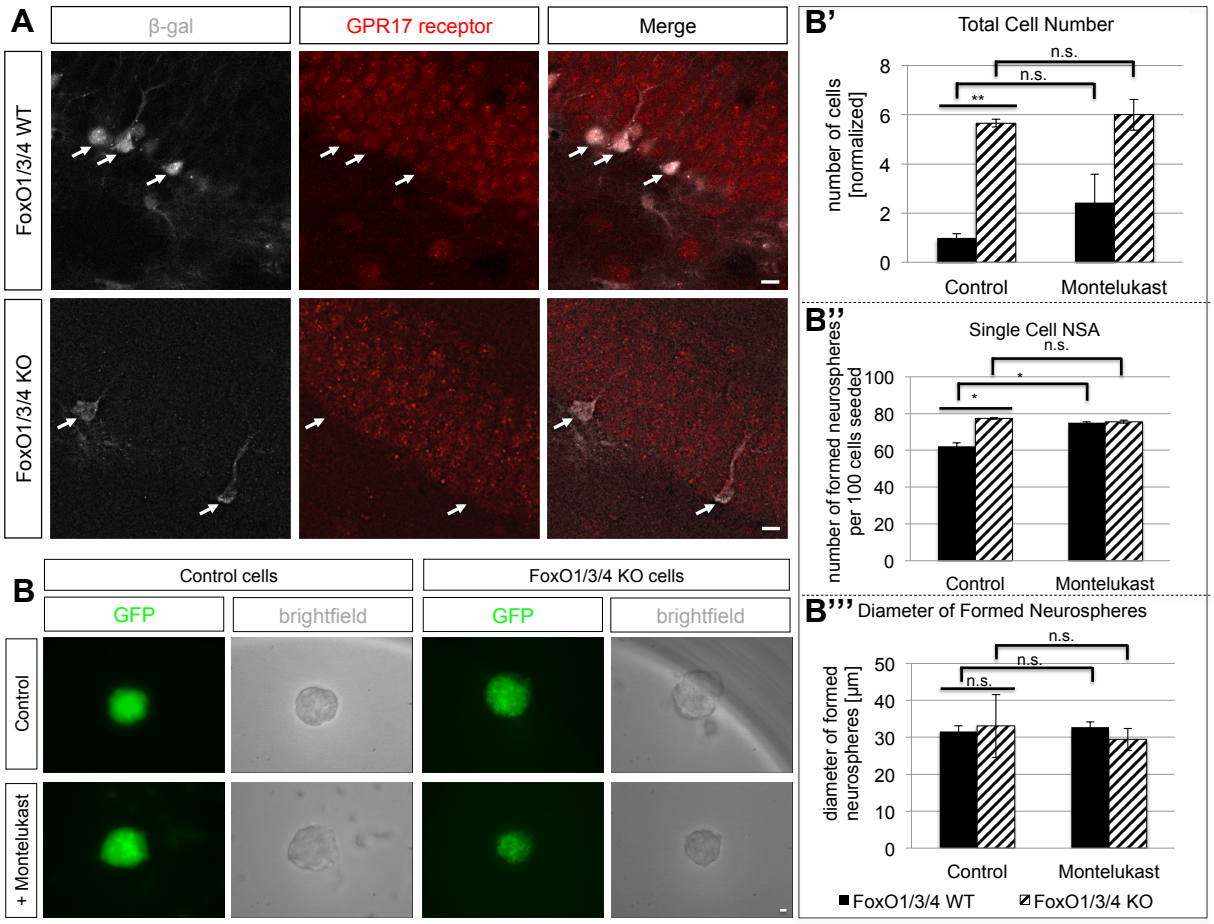

Figure 2.13: GPR17 signaling is altered in FoxO1/3/4 KO cells.
A Confocal pictures of the adult dentate gyrus of FoxO1/3/4 WT and KO animals 28 days after KO induction (28 dpt) imaged with a 40x objective and stained with antibodies against β-gal and GPR17 receptor. Expression of the GPR17 receptor is reduced in β-gal$^+$ recombined cell in FoxO1/3/4 KO animals compared to β-gal$^+$ cells in FoxO1/3/4 WT animals. Scale bar ≙ 10 µm. **B** Example pictures of formed control and FoxO1/3/4 KO neurospheres under control condition and Montelukast treatment imaged with a fluorescent microscope. **B'** Diagram of total cell number of control and FoxO1/3/4 KO cells with or w/o Montelukast, normalized to control cells under control condition. Total cell number of control cells was increased due to Montelukast treatment, while total cell number of FoxO1/3/4 KO cells didn't change; n=2. **B''** Diagram of 96-well-plate neurosphere assays with or w/o Montelukast. Proliferation of control cells was significantly increased with Montelukast treatment in 96-well-plate neurosphere assay. Montelukast couldn't further increase proliferation of the FoxO1/3/4 KO cells; n=2. **B'''** Diagram of diameters of formed neurospheres with or w/o Montelukast. Average diameters of formed neurospheres were similar under all conditions in both cell types; n=2.

In summary, both Notch targets and GPR17 signaling might be downstream of FoxO transcription factors and therefore effectors of FoxO signaling, responsible for the observed phenotype of the FoxO1/3/4 KO.

2.1.5 Impaired dendritic, synaptic and mitochondrial morphology of FoxO1/3/4 deprived cells *in vivo*

FoxO transcription factors have not been analyzed regarding a potential function in neuronal growth and maturation of adult-born dentate granule neurons. To address this question the morphology of adult-born dentate granule neurons was studied in the context of FoxO1/3/4 KO. Retroviral injections into the dentate gyrus of adult FoxO1/3/4$^{wt/wt}$ and FoxO1/3/4$^{fl/fl}$ mice were performed to target single cells and induce the KO of FoxO1/3/4 (Tashiro et al., 2006). Retroviral particles transduce only dividing cells and target reliably fast proliferating precursor cells in the adult dentate gyrus. The FoxO1/3/4 KO was achieved by stereotactic injections of a retrovirus in both hemispheres. The retrovirus (CAG-GFP-IRES-Cre) encoded bicistronically for a Cre-recombinase and the green fluorescence protein (GFP) to label the cells. This retrovirus was co-injected with a retrovirus coding for a mitochondrially-targeted dsRED (mito-dsRed) (CAG-IRES-mito-dsRed). This strategy not only induced the KO auf FoxO1/3/4, but also allowed detailed analysis of dendrite morphology, spine formation and mitochondrial distribution or shape in double transduced cells. FoxO1/3/4$^{wt/wt}$ animals injected with the same combination of retroviruses were used as controls. The experimental paradigm is schematically depicted in Figure 2.14. Injections of retroviruses into the dentate gyrus were performed at P56. Mice were sacrificed 21 or 42 days after retroviral injection (21 dpi, 42 dpi; dpi ≙ days post injection).

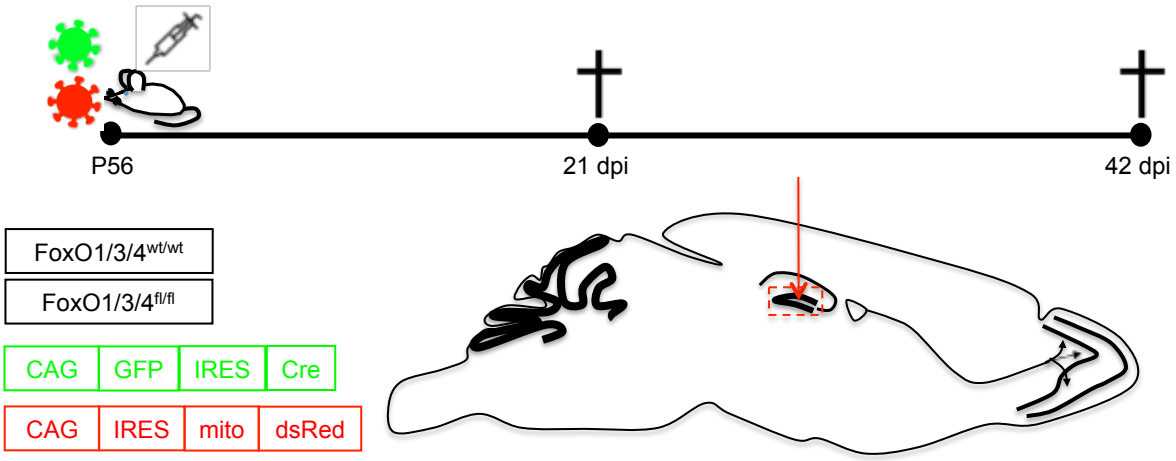

Figure 2.14: Scheme of experimental paradigm for morphology analysis of FoxO1/3/4 KO cells. Double injections of a Cre-expressing retrovirus (CAG-GFP-IRES-Cre) and a mito-dsRed expressing retrovirus (CAG-IRES-mito-dsRed) into the dentate gyrus of FoxO1/3/4$^{fl/fl}$ and FoxO1/3/4$^{wt/wt}$ animals to analyze the effect of the triple conditional KO of FoxO1/3/4 on morphology of adult born granule neurons. Mice were analyzed either after 21 days post injection (21 dpi) or 42 days post injection (42 dpi).

2.1.5.1 Morphology changes in 21-day-old newborn neurons deficient for FoxO1/3/4 in the adult dentate gyrus

The first time point to be analyzed was 21 days post injection (21 dpi). The GFP expression of the CAG-GFP-IRES-Cre retrovirus was used to identify the transduced cells.

First, the maturation level of the 21-day-old new neurons was analyzed via DCX expression. Immunohistochemistry was performed with antibodies against GFP and DCX (Figure 2.15 D). The amount of GFP^+ FoxO1/3/4 KO cells, which were still DCX positive, was significantly higher than in the GFP^+ cells of FoxO1/3/4 WT animals (FoxO1/3/4 WT cells: 65,2±15,74 %; FoxO1/3/4 KO cells: 82,0±3,46 %; p-value=0,026) (Figure 2.15 E), indicating that maturation of FoxO 1/3/4 deficient neurons was protracted or stalled.

To estimate the size of the dendritic tree, a maximal dendrite extension analysis was performed (Krzisch et al., 2013). Fully mature dentate granule cells extend dendrites up to the hippocampal fissure. The distance soma to hippocampal fissure was defined as the distance from the position of the cell soma in the dentate gyrus orthogonally to the hippocampal fissure of the hippocampal formation. The size of the cells at 21 dpi, the length of the cells from cell soma to the tip of its longest dendrite (maximum extension) was measured and put into relation to the distance soma to hippocampal fissure. (Figure 2.15 A, B). At least 50 cells per animal were analyzed via confocal images. The calculated ratio was depicted as cumulative numbers of cells in percentage (Figure 2.15 C). The cumulative plot of the maximum dendritic extension index of FoxO1/3/4 KO cells was shifted to the left indicating that FoxO deletion resulted in a dendritic growth defect (Two-Way-Anova: p-value =0,00000018).

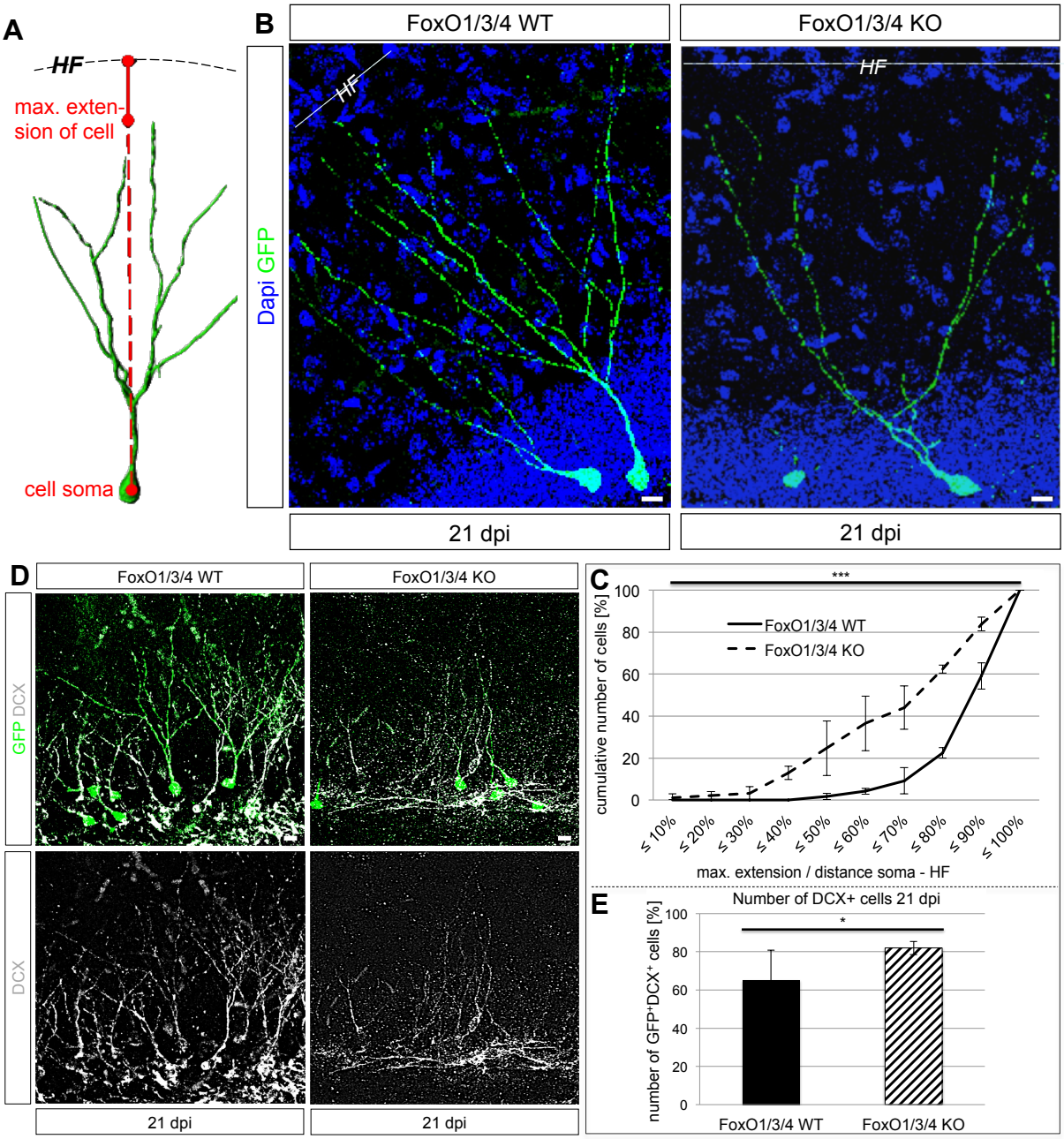

Figure 2.15: FoxO1/3/4 KO cells were more immature than FoxO1/3/4 WT cells 21 dpi.
A Schematic illustration of the ratio maximum extension of cell relative to distance soma to hippocampal fissure. **B** Example pictures of a FoxO1/3/4 WT and a FoxO1/3/4 KO cell (both retroviral transduced with CAG-GFP-IRES-Cre due to stereotactic injections into the dentate gyrus) taken with a 40x objective of a confocal microscope. Scale bar ≙ 10 µm. **C** Diagram of cumulative representation of relative dendritic extension. FoxO1/3/4 KO cells were determined as significantly shorter than FoxO1/3/4 WT cells, indicated by the shift to the left of the data line of the FoxO1/3/4 KO cells relative to the data line of the FoxO1/3/4 WT cells; n=3. **D** Confocal images taken with a 40x objective of the dentate gyrus of a FoxO1/3/4$^{wt/wt}$ and a FoxO1/3/4$^{fl/fl}$ animal. GFP-labeling indicated cells transduced with a CAG-GFP-IRES-Cre retrovirus due to stereotactic injections. Co-expression with DCX was analyzed. **D** Diagram of numbers of DCX^{+}/GFP^{+} cells in FoxO1/3/4$^{wt/wt}$ and FoxO1/3/4$^{fl/fl}$ animals. Significantly more FoxO1/3/4 KO cells still express the immature marker DCX compared to FoxO1/3/5 WT cells; n=3.

Next, the morphology of FoxO1/3/4 KO cells 21 dpi more in detail. Confocal images were taken and double-transduced (GFP^+ and mito-$dsRed^+$) cells were analyzed regarding total dendritic length, branch points, Sholl intersections, number of mitochondria and volume of mitochondria (Figure 2.16). Consistent with the results of the maximum dendritic extension analysis the total dendritic length of the FoxO1/3/4 KO cells (936,91±175,28 µm) was significantly (p-value=0,0377) reduced vs. FoxO1/3/4 WT cells (1225,76±78,18 µm) (Figure 2.16 D) (Figure 2.15 C). In addition, the primary dendrite, which is defined as the dendrite that originates from the cell soma and ends at the first branch point of the cell, was significantly shorter in the FoxO1/3/4 KO cells (FoxO1/3/4 WT cells: 24,39±13,11 µm; FoxO1/3/4 KO cells: 7,51±5,33 µm; p-value=0,0012) (Figure 2.16 E). KO cells frequently did not have a single primary dendrite but two dendrites, which originated from the cell soma. The KO of FoxO1/3/4 did not affect the number of branch points (FoxO1/3/4 WT cells: 9,93±2,43; FoxO1/3/4 KO cells: 10,2±2,95) (Figure 2.16 F). The Sholl analysis, which depicted the numbers of intersections relative to distance of the cell soma, reflected the changed morphology of the FoxO1/3/4 KO cells (Figure 2.16 G). Due to the shortened primary dendrite the first branch point was very near to the cell soma and this lead to a shift of the curve in the Sholl analysis to the left for the FoxO1/3/4 KO cells (p-value(Two-Way-Anova)=0,00001).

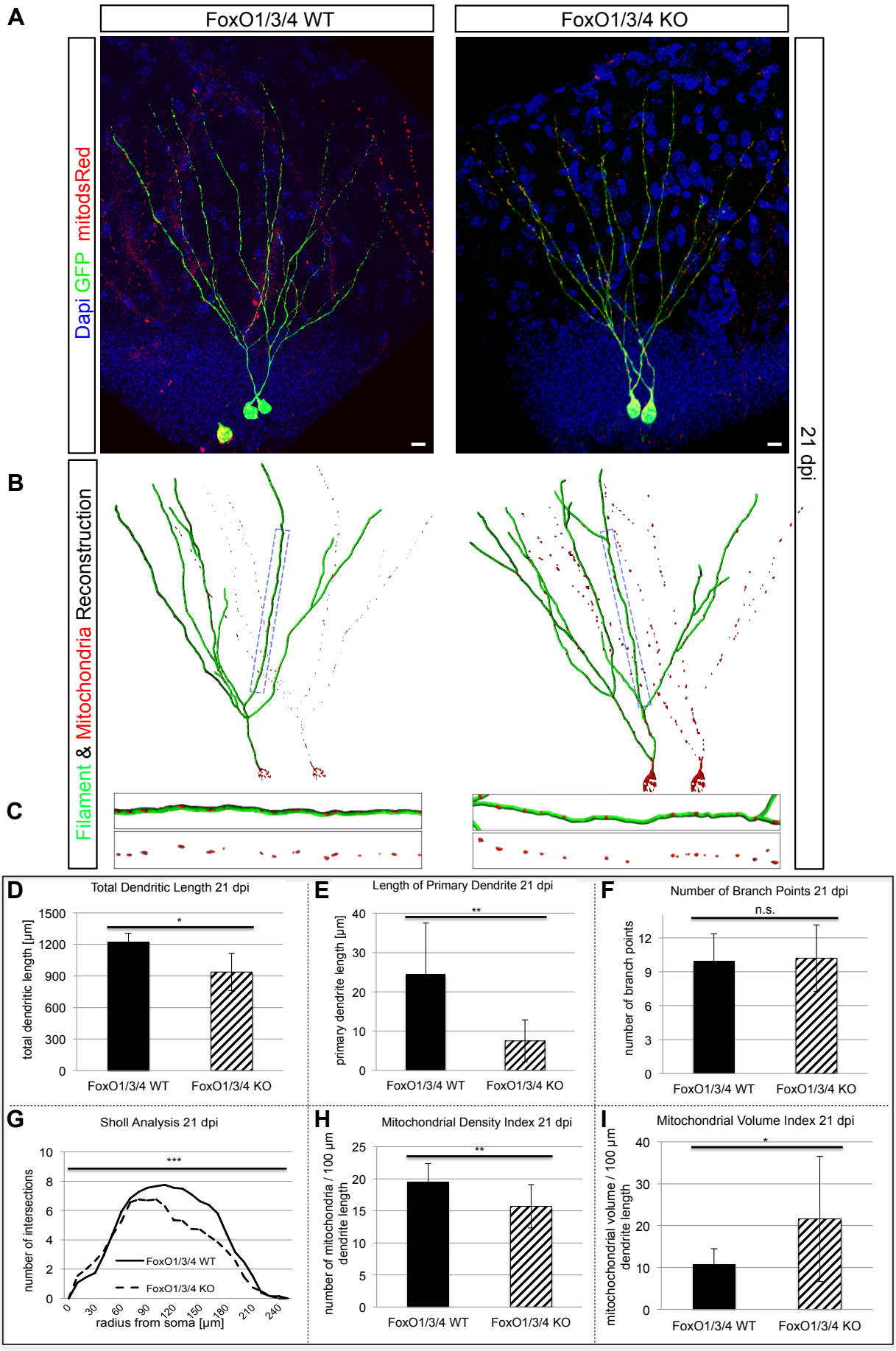

Figure 2.16: Morphological changes in FoxO1/3/4 KO cells 21 dpi.

Figure 2.16: Morphological changes in FoxO1/3/4 KO cells 21 dpi.
A Illustration of morphological analysis of CAG-GFP-IRES-Cre and CAG-IRES-mito-dsRed double-transduced newborn dentate gyrus neurons of FoxO1/3/4$^{wt/wt}$ (FoxO1/3/4 WT) and FoxO1/3/4$^{fl/fl}$ (FoxO1/3/4 KO) mice 21 dpi. Confocal images, taken with a 63x oil objective; scale bar ≙ 10 µm. **B** Illustration of morphological reconstruction of respectively one of the double transduced cells depicted in A with the software Imaris. In green is the reconstructed filament and in red the reconstructed mitochondria depicted. **C** Blow-ups of respectively one dendrite and the corresponding mitochondria. **D – I** Diagrams of morphology analysis regarding total dendritic length (D), length of primary dendrite (E), number of branch points (F), Sholl analysis (G), number of mitochondria (H) and mitochondrial volume (I) 21 dpi; n=3. FoxO1/3/4 KO cells were significantly shorter and had with significance a shortened or doubled primary dendrite. The FoxO1/3/4 KO did not affect number of branch points. The number of mitochondria per dendrite length (termed as mitochondrial density index) was significantly reduced whereas the mitochondrial volume per dendrite length (termed as mitochondrial volume index) was significantly increased in the FoxO1/3/5 KO cells compared to the WT cells.

Due to the double transduction with GFP and mito-dsRed mitochondrial morphology in 21-day-old newborn neurons could be analyzed. The soma of the cells was excluded from the analysis since the density of the mitochondria is very high in the soma and could not be reliably quantified. The number of mitochondria was counted and put into relation to the total dendritic length of each cell to exclude differences due to varying cell length. This ratio was defined as mitochondrial density index. The mitochondrial volume was also calculated and related to the total dendritic length of each cell. This ratio was defined as mitochondrial volume index. The analysis revealed a significant decrease in mitochondrial density in the FoxO1/3/4 KO cells (15,71±3,38 mitochondria per 100 µm dendrite length) compared to the FoxO1/3/4 WT cells (19,54±2,85 mitochondria per 100 µm dendrite length) (p-value=0,0095). In contrast the mitochondrial volume of the FoxO1/3/4 KO cells (21,61±14,95 µm^3 per 100 µm dendrite length) was significantly increased twofold compared to FoxO1/3/4 WT cells (10,81±3,66 µm^3 per 100 µm dendrite length) (p-value=0,0396).
In summary, 21-day-old FoxO1/3/4 KO cells revealed to be more immature and shorter compared to 21-day-old FoxO1/3/4 WT cells. Furthermore the FoxO1/3/4 KO cells showed a changed primary dendrite outgrowth and had less mitochondria; however, mitochondria in FoxO1/3/4 KO neurons were substantially bigger.

2.1.3.2 Morphology changes in 42-day-old newborn neurons deficient for FoxO1/3/4 in the adult dentate gyrus

The second time point to be analyzed was 42 dpi. Under physiological circumstances, 42-day-old cells are mature and integrated into the existing circuitry

(Jagasia et al., 2009). Again CAG-GFP-IRES-Cre and CAG-IRES-mito-dsRed double transduced cells were analyzed in the dentate gyrus of FoxO1/3/4$^{wt/wt}$ and FoxO1/3/4$^{fl/fl}$ mice (Figure 2.17 A, B, C). The same parameters as for the 21-day-old cells were investigated – total dendritic length, primary dendrite length, branch points, Sholl intersections, mitochondrial density and mitochondrial volume density (Figure 2.17 D, E, F, G, H, I). Interestingly, total dendritic length between FoxO1/3/4 KO cells and WT cells was comparable. (FoxO1/3/4 WT cells: 1222,29±151,06 µm; FoxO1/3/4 KO cells: 1245,97±38,92 µm). However, the primary dendrite of the FoxO1/3/4 KO cells was still significantly reduced or absent (FoxO1/3/4 WT cells: 21,43±14,17 µm; FoxO1/3/4 KO cells: 10,94±7,55 µm; p-value=0,0162). Numbers of branch points were comparable in FoxO1/3/4 KO and WT cells (FoxO1/3/4 WT: 8,00±1,51; FoxO1/3/4 KO: 8,17±1,83). The Sholl analysis depicted small but significant changes in the morphological buildup due to the shortened/doubled primary dendrite, which were indicated by the shift to the left of the data point line of the FoxO1/3/4 KO cells in Figure 2.17 G (p-value(Two-Way-Anova)=0,0033). In contrast to the 21 dpi timepoint, the mitochondrial density was now comparable between FoxO1/3/4 WT cells (29,20±2,76 mitochondria per 100 µm dendrite length) and FoxO1/3/4 KO cells (29,95±2,95 mitochondria per 100 µm dendrite length). The mitochondrial density increased twice as much compared to 21 dpi in both groups. The mitochondrial volume density was still significantly elevated in the FoxO1/3/4 KO cells (33,30±17,76 per 100 µm dendrite length) vs. FoxO1/3/4 WT cells (22,44±8,00 µm^3 per 100 µm dendrite length) (p-value=0,0454).

Figure 2.17: Morphological changes in FoxO1/3/4 KO cells 42 dpi.
A Illustration of morphological analysis of CAG-GFP-IRES-Cre and CAG-IRES-mito-dsRed double-transduced newborn dentate gyrus neurons of FoxO1/3/4$^{wt/wt}$ (FoxO1/3/4 WT) and FoxO1/3/4$^{fl/fl}$ (FoxO1/3/4 KO) mice 42 dpi. Confocal images, taken with a 63x oil objective; scale bar ≙ 10 µm. **B** Illustration of morphological reconstruction of respectively one double transduced cells depicted in A with the software Imaris. In green is the reconstructed filament and in red the reconstructed mitochondria depicted. **C** Blow-ups of respectively one dendrite and the corresponding mitochondria. **D – I** Diagrams of morphology analysis regarding total dendritic length (D), length of primary dendrite (E), number of branch points (F), Sholl analysis (G), number of mitochondria (H) and mitochondrial volume (I) 21 dpi; n=3. FoxO1/3/4 KO cells showed a significantly shortened or doubled primary dendrite. Total dendritic length, numbers of branch points and mitochondrial density was similar in FoxO1/3/4 KO and WT cells. The mitochondrial volume per dendrite length (termed as mitochondrial volume index) was significantly increased in the FoxO1/3/4 KO cells vs. WT cells.

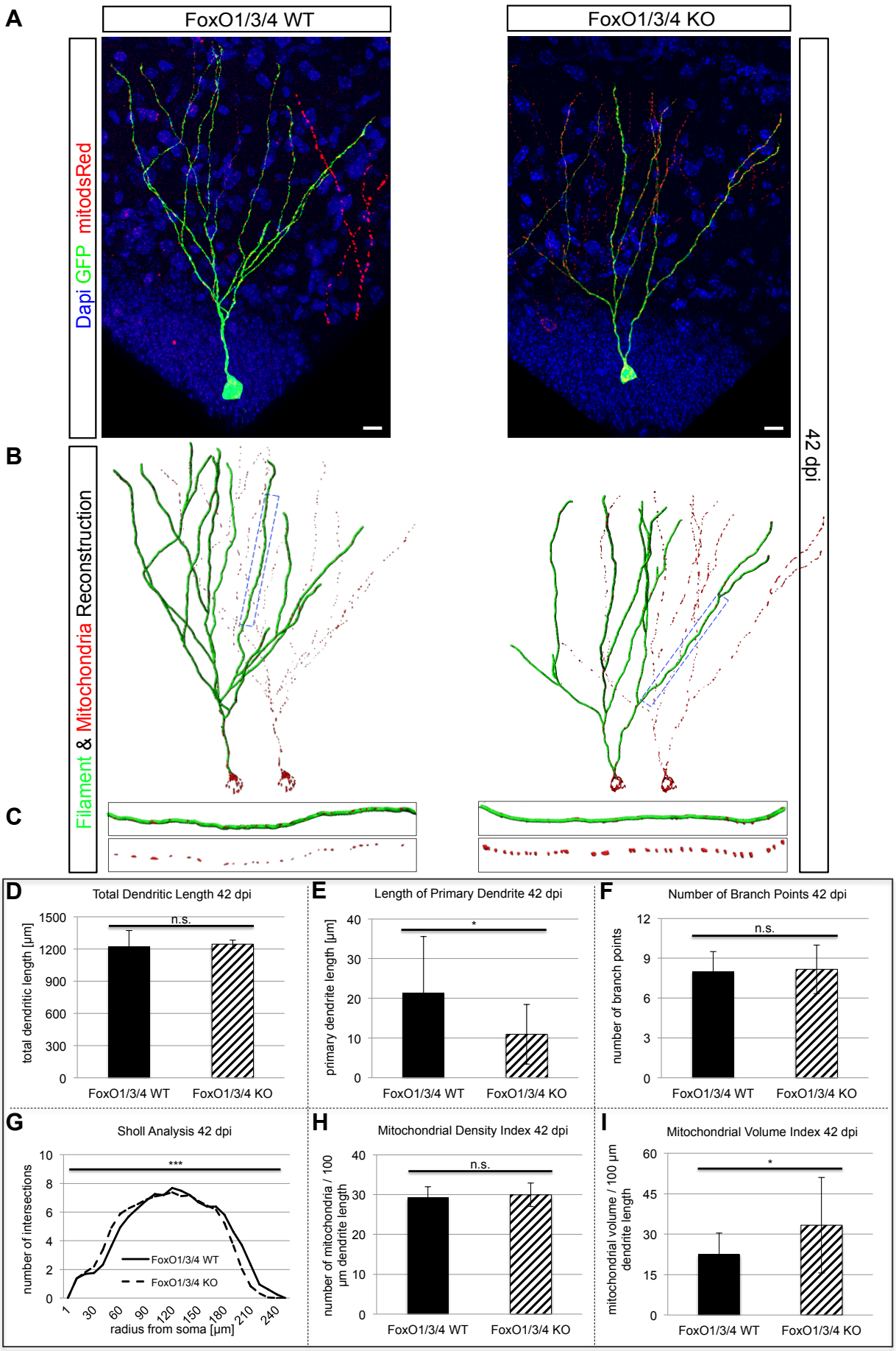

Figure 2.17: Morphological changes in FoxO1/3/4 KO cells 42 dpi.

In summary FoxO1/3/4 KO cells continued to show changes in the morphology of the primary dendrite. Total dendritic length and number of branch points, however, were comparable to wildtype cells, indicating that FoxO KO cells had partially caught up with their wildtype counterparts. Differences in mitochondria compartment were still visible with mitochondria of the FoxO1/3/4 KO cells being bigger compared to mitochondria in WT cells.

Finally, the synaptic integration of 42 dpi neurons was studied on the morphological level. Dendritic spines are the morphological correlate of the excitatory glutamatergic postsynaptic compartment. Here, spine density and the density of mushroom spines in the apical dendrites of the newborn GFP^+ cells were evaluated (Figure 2.18). The analysis revealed significantly enhanced spinegenesis in the FoxO1/3/4 KO cells. The apical dendrites of the FoxO1/3/4 KO cells showed 20 % more spines than FoxO1/3/4 WT cells (FoxO1/3/4 WT cells: 16,65±1,44 spines per 100 µm dendrite length; FoxO1/3/4 KO cells: 20,14±1,36 spines per 100 µm dendrite length; p-value=0,0379). The amount of mushroom spines, which are morphological correlate of mature spines, was unchanged in FoxO1/3/4 KO cells (3,16±0,29 mushroom spines per 100 µm dendrite length) compared to WT cells (3,17±0,18 mushroom spines per 100 µm dendrite length).

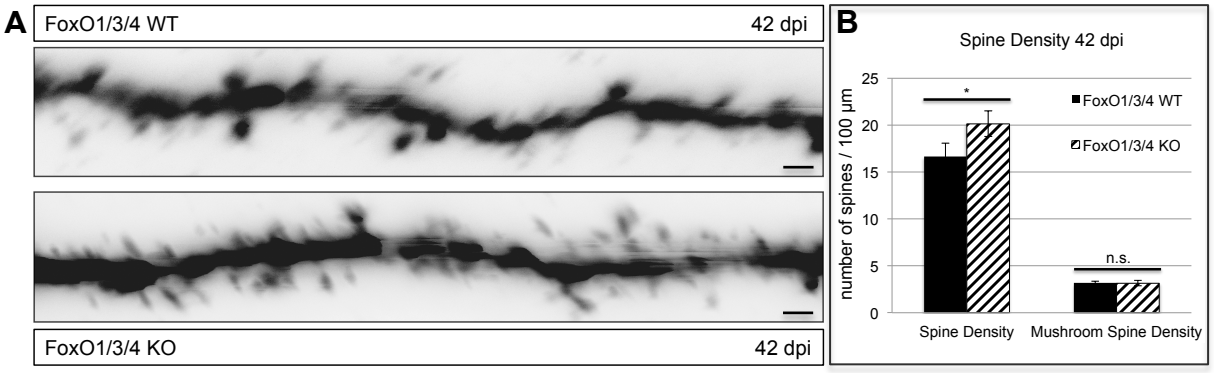

Figure 2.18: Enhanced spinegenesis in FoxO1/3/4 KO cells 42 dpi.
A Confocal images taken with a 63x oil objective and a 5x zoom of a apical dendrite of a FoxO1/3/4 WT cell and a FoxO1/3/4 KO cell 42 dpi. Scale bar ≙ 1 µm. **B** Diagram of total numbers of spines and numbers of mushroom spines 42 dpi; n=3. FoxO1/3/4 KO cells had 20 % more spines than FoxO1/3/4 WT cells. Numbers of mushroom spines were the same in both groups.

2.2 Transcription factor FoxG1 in adult neurogenesis

The transcription factor FoxG1 is known to play an important role in embryonic neurogenesis (Tai & Lai, 1992; Xuan et al., 1995; Hanashima et al., 2002; Hanashima et al., 2004; Seoane et al., 2004). In humans several mutations, duplications and deletions in the FoxG1 gene were reported, which result in a congenital variant of Rett syndrome of different severity (Ariani et al., 2008; Bahi-Buisson et al., 2010; Brunetti-Pierri et al., 2011; Kumakura et al., 2013; Le Guen et al., 2011; Mencarelli et al. 2013; Takagi et al., 2013). Thus, regulated FoxG1 dosage and activity is crucial for proper brain development. Shen et al. showed that FoxG1 haploinsufficiency leads to impaired neurogenesis in the postnatal hippocampus. The majority of early postnatally generated neurons in the FoxG1 deficient dentate gyrus do not survive, and precursor proliferation and differentiation of adult born granule cells is affected (Shen et al., 2006). A conditional mouse mutant, in which FoxG1 was perinatally and early postnatally removed from the hippocampal primordium and its derivatives showed malformation of the postnatal dentate gyrus; FoxG1 deletion appeared to particularly impact on subgranular zone formation (Tian et al., 2012). The subgranular zone was lost and the secondary radial glial scaffold was disrupted, which lead to impaired migration of granule cells. The role of FoxG1 for adult neurogenesis has not been systematically evaluated before; considering the severe phenotypes caused by the mutations and duplications of the FoxG1 gene in humans, the focus was set on evaluating a gain of function regarding the FoxG1 gene.

2.2.1 FoxG1 expression in the adult dentate gyrus

FoxG1 mRNA was reported to be expressed in the adult neurogenic niches (Shen et al., 2006). Immunohistochemical stainings in the hippocampus with an antibody against FoxG1 revealed expression of FoxG1 in the dentate gyrus and the CA regions (Tian et a., 2012). Immunohistochemistry using a commercially available antibody against FoxG1 confirmed the expression of FoxG1 in the dentate gyrus and the CA1, CA2 and CA3 regions of adult mice (Figure 2.19). In the dentate gyrus, FoxG1 expression was found to be stronger in cells occupying the lower layers of the dentate gyrus.

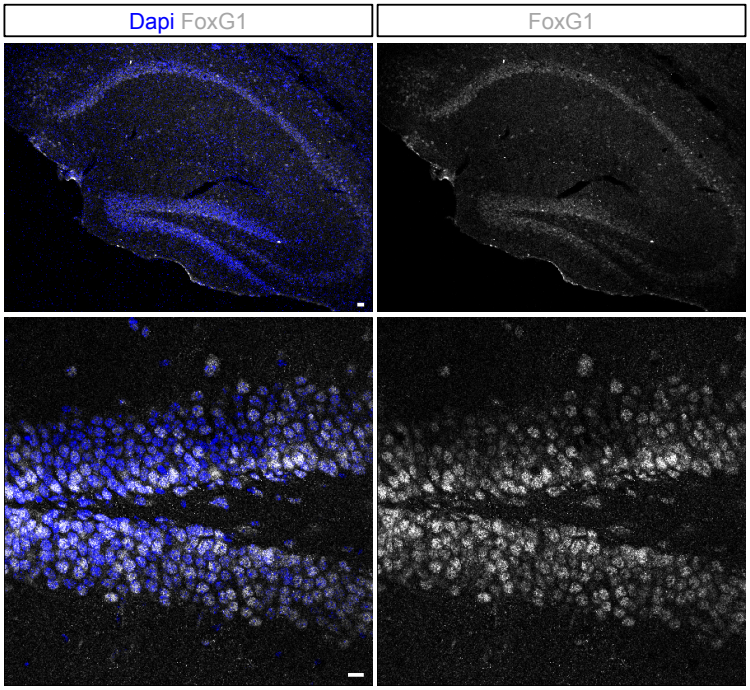

Figure 2.19: FoxG1 is expressed in the adult dentate gyrus.
Confocal images taken with a 10x or a 40x objective of the dentate gyrus of a wild type mouse (C57/Bl6). Scale bar ≙ 10 µm. FoxG1 is expressed in the dentate gyrus and CA1, CA2 and CA3 regions of the hippocampal formation.

Stage specific markers were used to define the expression pattern of FoxG1 in the adult dentate gyrus of 2-month-old C57/Bl6J mice. Antibodies against Sox2, GFAP, TBR2, DCX and Map2(a+b) were used. Cells positive for Sox2 and GFAP with a radial glia like morphology are considered the stem cells in the adult hippocampal neurogenic lineage (Seri et al., 2001). Co-localization analysis with FoxG1 revealed that 96,41±2,94 % of the $Sox2^+GFAP^+$ cells were weakly positive for FoxG1 (Figure 2.20 A, D). TBR2 is a marker for transit amplifying progenitor cells (Hodge et al., 2008). Only 48,73±5,63 % of the $TBR2^+$ cells was weakly positive for FoxG1 (Figure 2.20 B, D). Almost all DCX^+ immature neurons expressed FoxG1 (97,52±2,83 %) (Figure 2.20 C, D). The expression level of FoxG1 was higher in this cell population compared to the neural stem cells and transit amplifying progenitors (Figure 2.20 A, B, C). Map2(a+b) is a marker for mature neurons. There is almost no overlap between the DCX^+ and $Map2(a+b)^+$ cell populations (Figure 2.20 C). 43,74±11,81 % of the $Map2(a+b)^+$ cells were $FoxG1^+$ (Figure 2.20 C, D). FoxG1 expression was low or absent in the $Map2(a+b)^+$ cells (Figure 2.20 C). In summary, immunofluorescent analysis showed that FoxG1 was expressed from adult neural stem cells to immature neurons, albeit the expression level is varying between the stages.

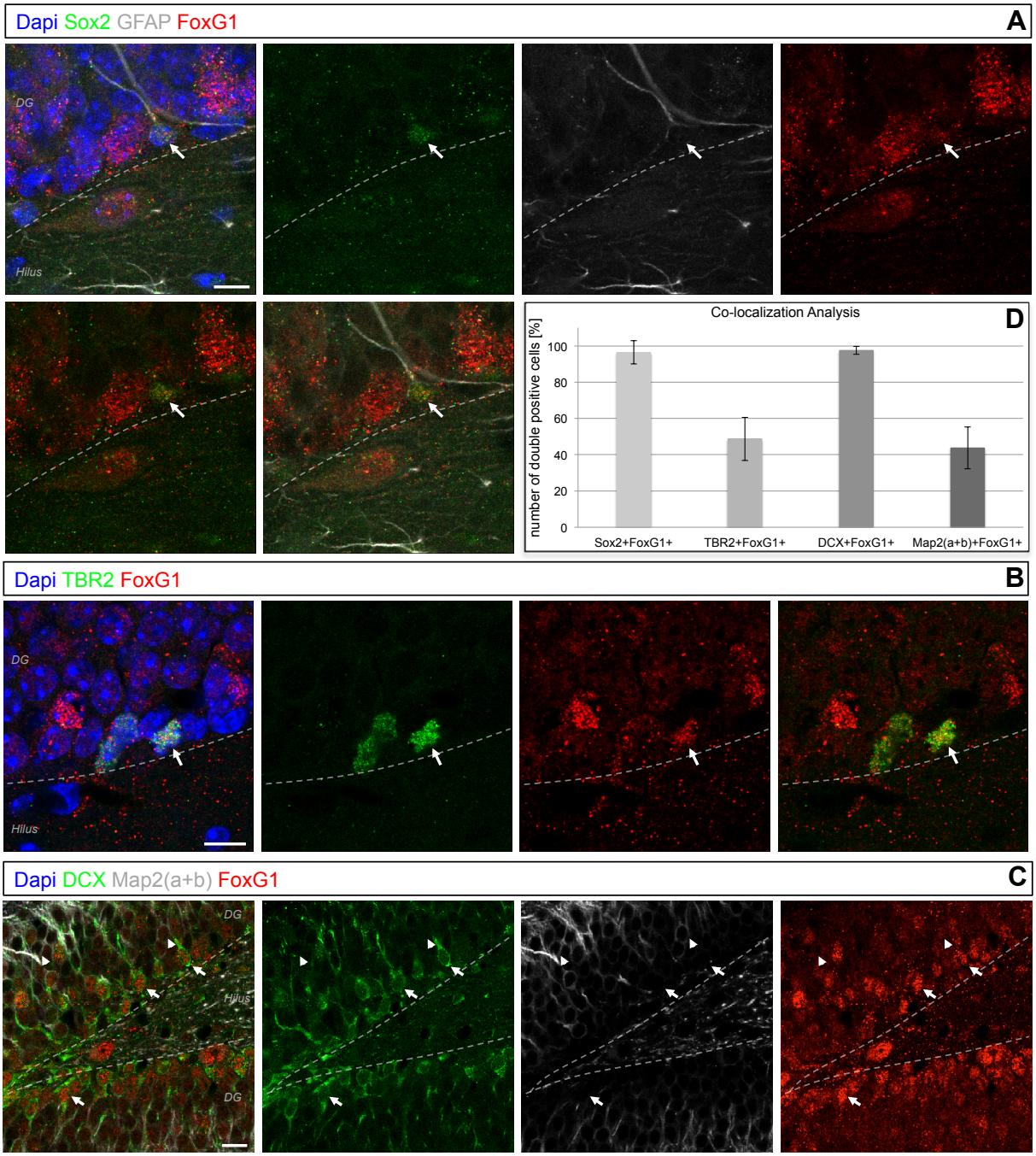

Figure 2.20: Co-localization analysis of FoxG1 with stage specific markers.
A, B, C Confocal images with a 63x oil or 40x objective of immunohistochemistry performed on brain slices of 8-week-old C57/Bl6J mice. Antibodies against Sox2, GFAP, TBR2, DCX, Map2(a+b) and FoxG1 were used. Scale bar ≙ 10 µm. **D** Diagram of the numbers of the co-localization analysis; n=3. Nearly all of the $Sox2^{+}GFAP^{+}$ adult neural stem cells and DCX^{+} immature neurons were positive for FoxG1 while only around 50 % of the $TBR2^{+}$ transit amplifying progenitors and $Map2(a+b)^{+}$ mature neurons were $FoxG1^{+}$.

To further define the expression pattern of FoxG1 in dentate gyrus neuronal development, FoxG1 expression was studied in retrovirally birthdated adult-generated neurons. A CAG-GFP retrovirus was stereotactical injected into the dentate gyrus of 8-week-old adult C57/Bl6J mice. The mice were sacrificed 3, 7, 14,

21, 28 or 42 days post injection (dpi) (injections were performed by Mr. Fabian Gruhn) (Figure 2.21 A). Around 90 % of all 3-day-old to 28-day-old cells expressed FoxG1 (for example 89,38±2,24% of the 14-day-old GFP$^+$ cells expressed FoxG1), while only 52,08±1,94 % of the 42-day-old cells were positive for FoxG1 (Figure 2.21 B).

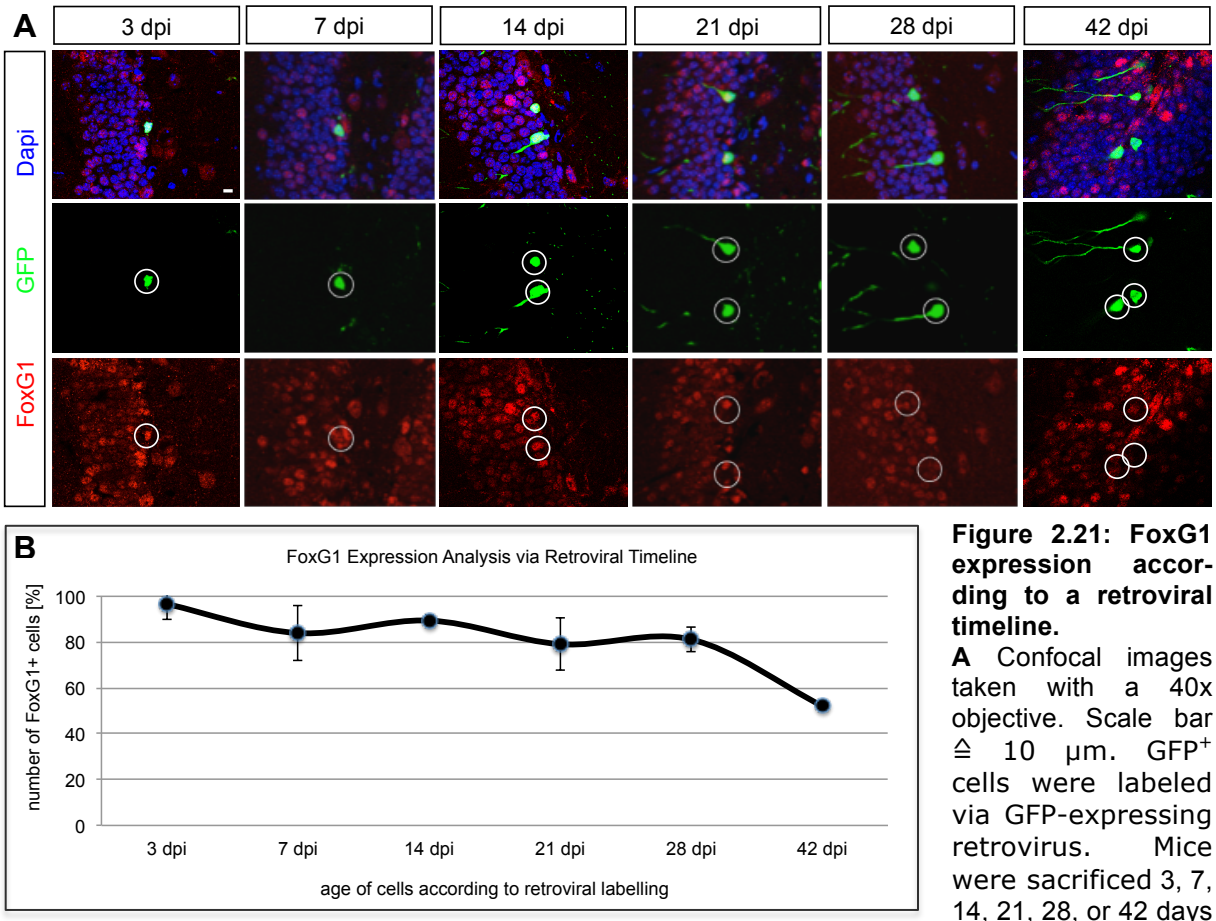

Figure 2.21: FoxG1 expression according to a retroviral timeline.
A Confocal images taken with a 40x objective. Scale bar ≙ 10 µm. GFP$^+$ cells were labeled via GFP-expressing retrovirus. Mice were sacrificed 3, 7, 14, 21, 28, or 42 days post injection (dpi). Co-localization with FoxG1 was analyzed. **B** Diagram of numbers of FoxG1$^+$ cells according to the age of the labeled GFP$^+$ cells; n=3. Most cells were positive for FoxG1 from 3 to 28 dpi. Numbers got halved till 42 dpi.

Summarized, FoxG1 signaling is present in stem cells, peaks in immature neurons and is down-regulated in mature neurons.

2.2.2 Impaired survival, changes in differentiation and aberrant morphology of newborn cells in the adult dentate gyrus due to over-expression of an endogenous or a dominant-active mutant form of FoxG1 *in vivo*

Some of the severe phenotypes in humans associated with mutations in the FoxG1 gene were traced back to either duplications or gain-of-function mutations of the

FoxG1 gene. Here, the impact of increased FoxG1 on development of adult dentate gyrus neurons was investigated. To this end, the WT form of FoxG1 or a constitutively active mutant form of FoxG1 was over-expressed using a retroviral approach. The constitutively active FoxG1 mutant corresponded to a point mutant that was found in a Rett syndrome patient (Le Guen et al., 2010). This point mutation affects the nuclear localization signal of FoxG1. As a consequence FoxG1 is permanently located in the nucleus and cannot be shuttled out of the nucleus, resulting in constitutively active FoxG1 signaling. The constructions of the two retroviruses were described in 4.2.6. The retrovirus with the endogenous form of FoxG1 was termed CAG-FoxG1-IRES-GFP and the retrovirus with the point mutation of FoxG1 was termed CAG-mutFoxG1-IRES-GFP. The retroviral-transduced cells were identified by the GFP expression of the bicistronic vector constructs. The experimental paradigm is depicted in Figure 2.22. C57/Bl6 mice had 7 days free access to running wheels, to enhance neurogenesis and the amount of cells that could be labeled by the retroviruses. Mice were stereotactical injected with retrovirus at the age of 8 weeks.

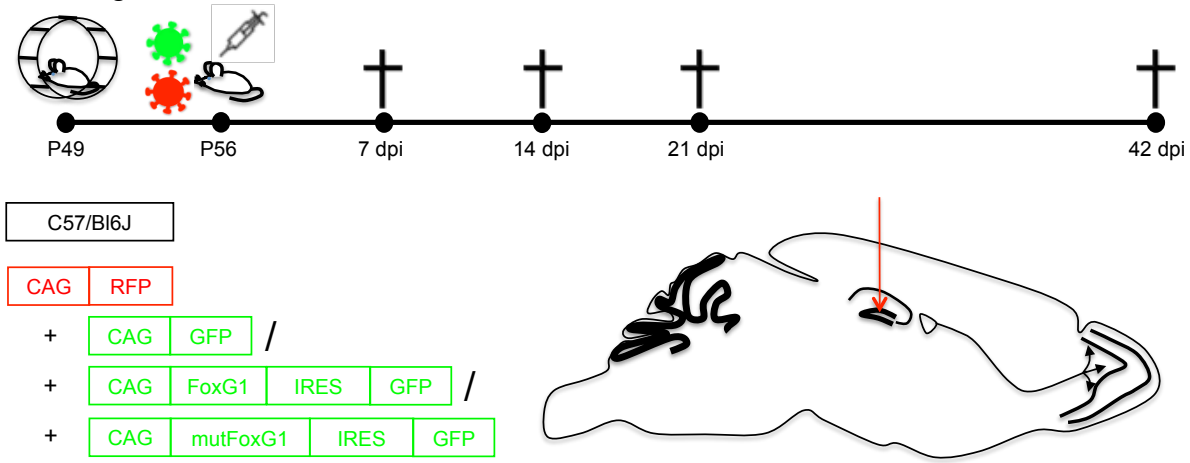

Figure 2.22: Experimental paradigm for the FoxG1 gain of function analysis.
C57/Bl6 got free access to running wheels for 7 days followed by stereotactical injections into the dentate gyrus at P56. Double injections of either CAG-RFP and CAG-GFP (control group) or CAG-RFP and CAG-FoxG1-IRES-GFP or CAG-mutFoxG1-IRES-GFP were performed. Mice were sacrificed 7, 14, 21 or 42 days post injections (dpi).

Double injections with an RFP-expressing retrovirus (CAG-RFP) were performed to control the injection efficiency and to allow for survival analysis. The control group was injected with CAG-RFP and CAG-GFP retroviruses. The second group was injected with CAG-RFP and CAG-FoxG1-IRES-GFP retroviruses; the third group was injected with CAG-RFP and CAG-mutFoxG1-IRES-GFP retroviruses. Mice were sacrificed 7, 14, 21 or 42 dpi.

At first the expression of the CAG-FoxG1-IRES-GFP and CAG-mutFoxG1-IRES-GFP retroviruses was tested. Retrovirus-transduced cells expressing GFP (termed below as FoxG1-GFP$^+$ and mutFoxG1-GFP$^+$) almost always showed a much stronger nuclear signal for FoxG1 compared to the surrounding dentate granule cells (Figure 2.23 A, B), indicating, that the CAG-FoxG1-IRES-GFP and CAG-mutFoxG1-IRES-GFP retroviruses increased FoxG1 expression.

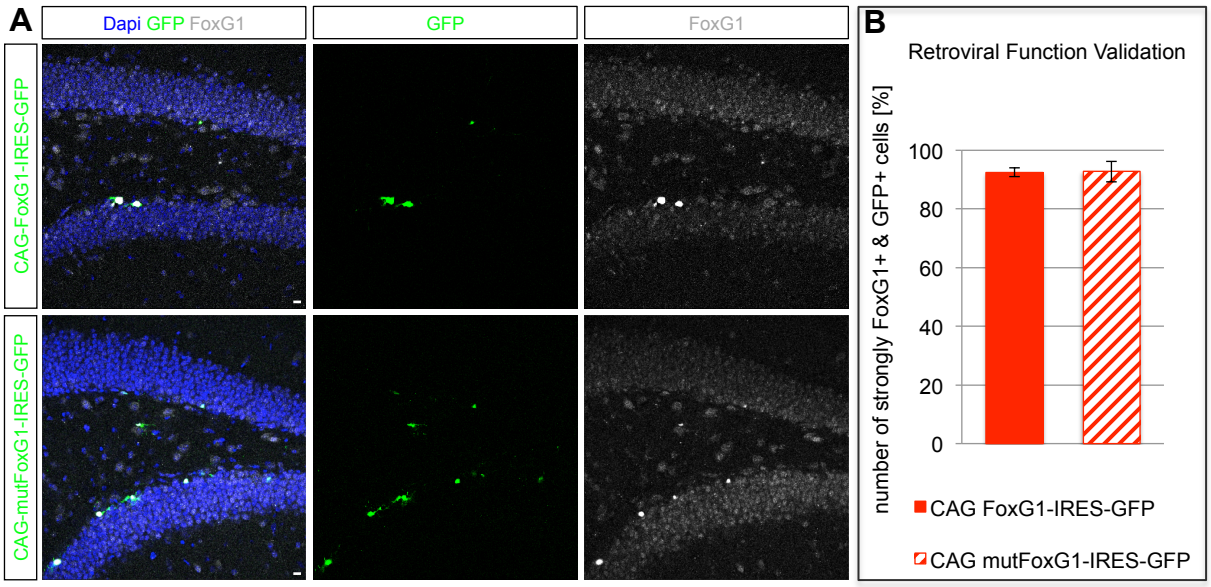

Figure 2.23: Validation of the retroviruses for the FoxG1 gain of function analysis *in vivo*.
A Confocal images taken with a 40x objective of the dentate gyrus of C57/Bl6 mice, which were retrovirally injected with either CAG-FoxG1-IRES-GFP or CAG-mutFoxG1-IRES-GFP retrovirus. Scale bar ≙ 10 µm. **B** Diagram of the numbers of GFP$^+$ cells that were strongly FoxG1$^+$. An antibody against FoxG1 detected a much stronger FoxG1 expression in 92,4±1,49 % and 92,69±3,52 % of the transduced GFP$^+$ cells compared to the surrounding granule neurons; n=3.

2.2.2.1 Decreased survival due to FoxG1 gain of function

Next the survival of the GFP$^+$ cells compared to the RFP$^+$ cells was analyzed. Immunohistochemistry with antibodies against RFP and GFP were performed in slices of at least 3 animals of each group for each time point. Confocal pictures were taken and the numbers of RFP$^+$ and GFP$^+$ cells per animal were counted. The numbers of GFP$^+$ cells were put into ratio to the RFP$^+$ cells (GFP$^+$/RFP$^+$) (Figure 2.24). Normalization to the first time point was performed for each group. The ratio of GFP$^+$ to RFP$^+$ cells should stay stable over time if all cells show comparable survival rates.

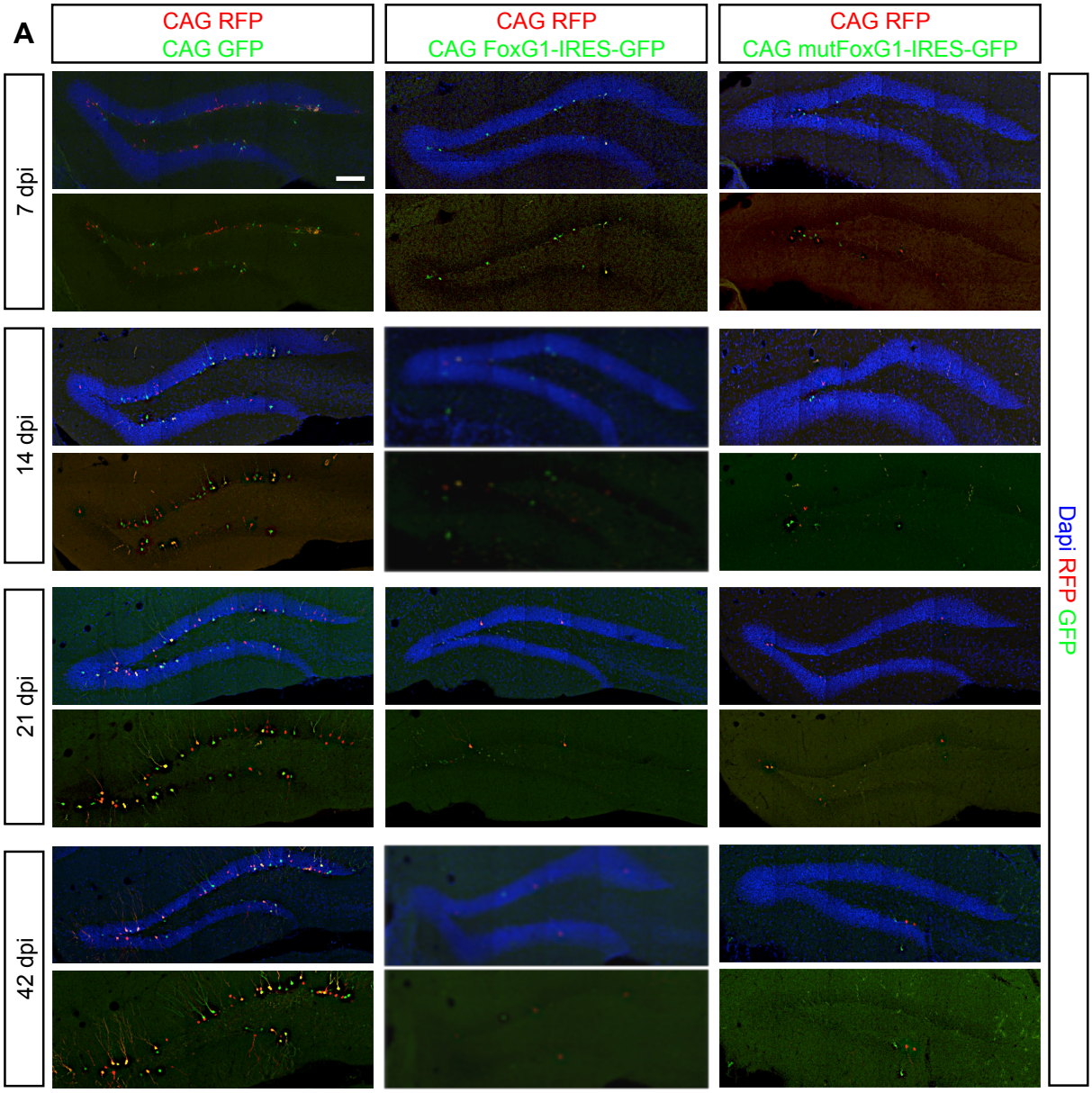

Figure 2.24 Decreased survival of FoxG1 and mutFoxG1 over-expressing cells in the adult dentate gyrus. A Tile scans of retroviral injections of CAG-GFP and CAG-RFP, CAG-FoxG1-IRES-GFP and CAG-RFP and CAG-mutFoxG1-IRES-GFP and CAG-RFP into the dentate gyrus of adult C57/Bl6 mice 7, 14, 21 and 42 dpi. Scale bar ≙ 100 µm. **B** Diagram of ratio of GFP^+ to RFP^+ (GFP^+/RFP^+) cells. FoxG1-GFP^+ and mutFoxG1$^+$ cells survive worse compared to RFP^+ and GFP^+ control cells; n=3.

In case of the control group (CAG-GFP, CAG-RFP) the survival of the GFP^+ cells was slightly impaired compared to the survival of the RFP^+ cells (Figure 2.24 B). The ratio oscillated between 100±15,4 % (7 dpi) and 64,7±7,5 % (42 dpi). However, the

differences were not significant. FoxG1 over-expression decreased the survival as illustrated by the decrease in ratio of the FoxG1-GFP$^+$ cells to the RFP$^+$ cells over time from 100±38,6 % (7 dpi) to 29,2±12,3 % (42 dpi). The FoxG1-GFP$^+$ cells showed significant impairment in survival over time compared to the corresponding GFP$^+$ cells in the control animals (p-value(Two-Way-Anova)=0,0015). The same was observed in the mice injected with the over-expression construct of the mutated form of FoxG1. The ratio of the mutFoxG1-GFP$^+$ to RFP$^+$ cells decreased from 100±11,3 % (7 dpi) to 19,8±7,9 % (42 dpi) (p-value(Two-Way-Anova)=0,0005). In summary, gain of function of FoxG1 in adult born granule neurons leads to a survival defect of the cells.

2.2.2.2 FoxG1 overexpression reduces neurogenesis and increases oligodendrogenesis

Next the fate of the surviving FoxG1 cells was investigated. The time points 14 dpi and 21 dpi were used for the analysis. The 42 dpi time point could not be used since so many FoxG1-GFP$^+$ and mutFoxG1-GFP$^+$ cells already died. At least 100 GFP$^+$ cells per animal per group were analyzed and the numbers of GFP$^+$DCX$^+$ cells (Figure 2.25 A, A', B, B'), GFP$^+$Prox1$^+$ cells (Figure 2.25 C, C') and GFP$^+$Sox10$^+$ cells (Figure 2.25 D, D') determined. 89,71±0,55 % of the GFP$^+$ cells in the control group were DCX$^+$ at 14 dpi. In contrast, only 53,88±26,64 % of the FoxG1-GFP$^+$ cells and 60,00±24,02 % of the mutFoxG1-GFP$^+$ cells were DCX$^+$ (p-value(FoxG1)=0,12; p-value(mutFoxG1)=0,11). At 21 dpi the amount of DCX$^+$ cells in the GFP$^+$ control group dropped to 64,04±12,78 %. The DCX$^+$ cells within the FoxG1-GFP$^+$ and mutFoxG1-GFP$^+$ cells decreased further to 25,91±13,08 % (p-value(FoxG1)=0,0181) and 24,77±1,86 % (p-value(mutFoxG1)=0,0121), respectively. At 14 dpi 99,34±0,57 % of the GFP$^+$ cells in the control group were Prox1$^+$. Only 57,14±8,3 % of the FoxG1-GFP$^+$ cells and 55,10±6,69 % of the mutFoxG1-GFP$^+$ cells were Prox1$^+$. The difference between control group and mutFoxG1 group was significant (p-value=0,0072). Interestingly enough, a tendency to an increase in Sox10$^+$ cells within the FoxG1-GFP$^+$ and mutFoxG1-GFP$^+$ cells was observed. Only 2,3±2,99 % of the GFP$^+$ control cells was Sox10$^+$ while 24,37±22,2 % and 30,41±2,97 % of the FoxG1-GFP$^+$ cells and mutFoxG1-GFP$^+$ cells were positive for Sox10. Overall these data suggest that less of the still surviving cells differentiated into neurons and more into oligodendrocyte precursors.

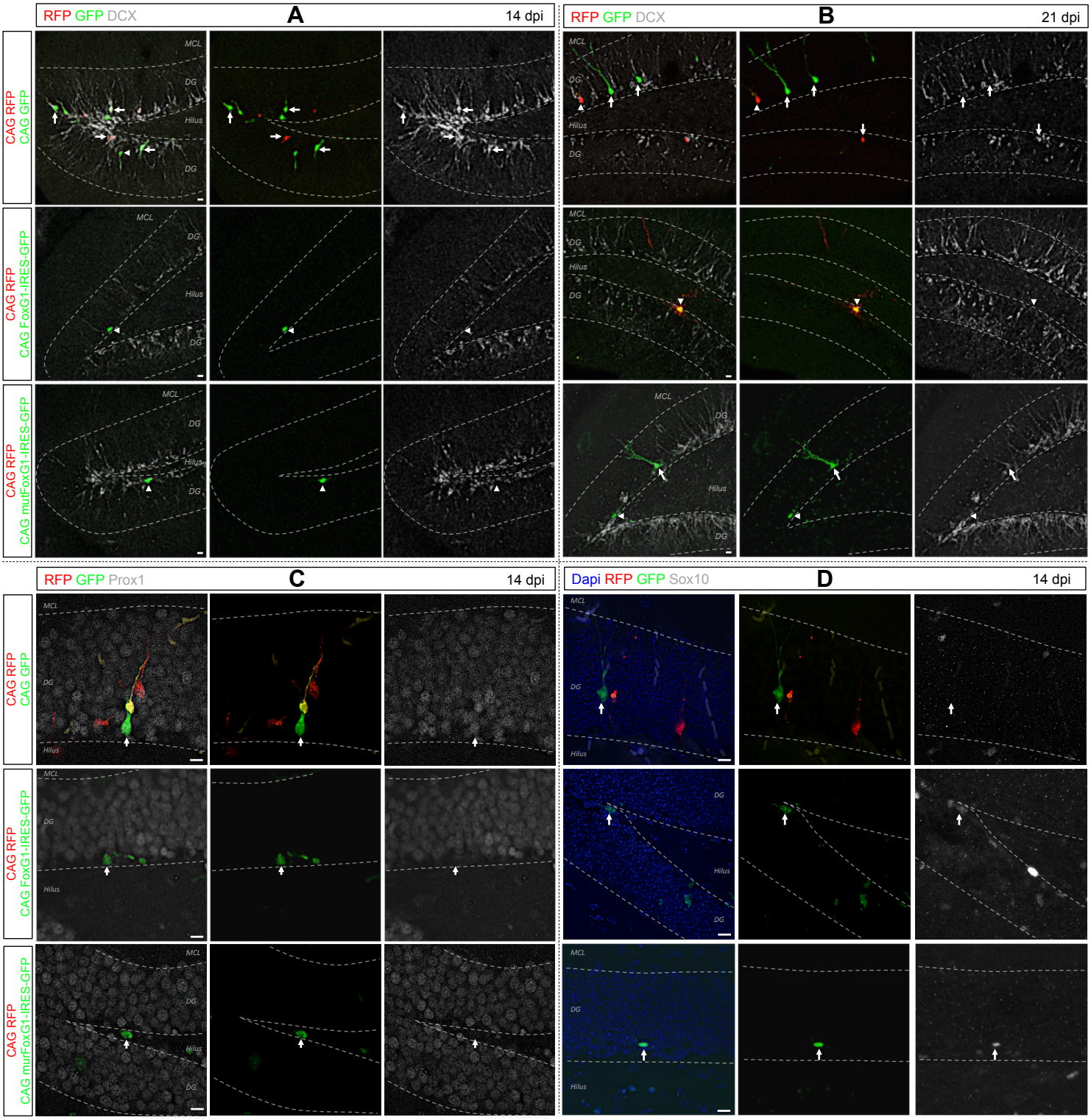

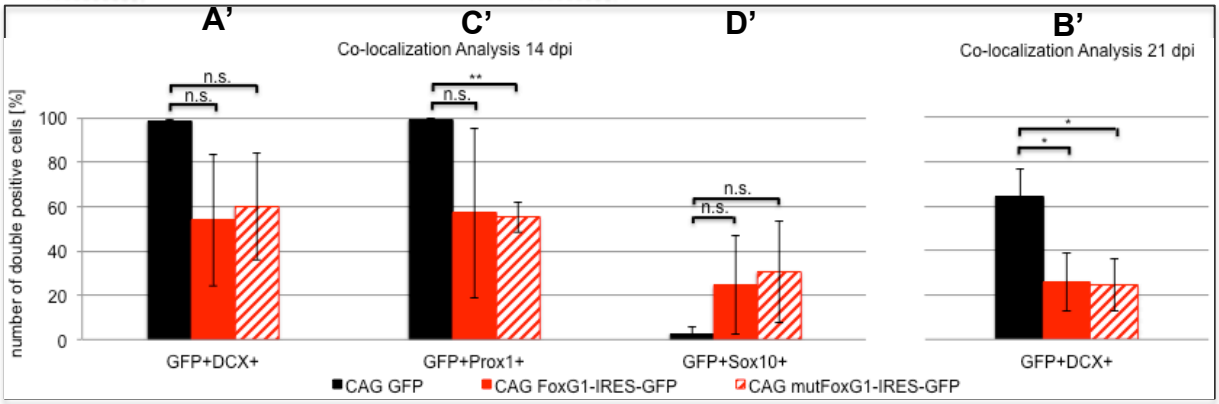

Figure 2.25: Changed differentiation of FoxG1 and mutFoxG1 over-expressing cells.

Figure 2.25: Changed differentiation of FoxG1 and mutFoxG1 over-expressing cells.
A - D Confocal images of retroviral injections of CAG-GFP and CAG-RFP, CAG-FoxG1-IRES-GFP and CAG-RFP and CAG-mutFoxG1-IRES-GFP and CAG-RFP into the dentate gyrus of adult mice 14 and 21 dpi. Scale bar ≙ 10 µm. Immunohistochemistry with neuronal markers for DCX and Prox1 revealed decreased neuronal differentiation in FoxG1-GFP$^+$ and mutFoxG1-GFP$^+$ cells compared to GFP$^+$ cells in the control group (**A', B', C'**). Instead more of the FoxG1-GFP$^+$ and mutFoxG1-GFP$^+$ cells differentiated into oligodendrocyte precursor cells indicated by Sox10 expression (**D'**).

2.2.2.3 FoxG1 over-activity results in aberrant morphology

FoxG1 over-expressing and mutFoxG1 over-expressing cells showed massive morphology defects (Figure 2.26 A). While the control cells started to differentiate into neurons with an apical process and developed a mature dendritic tree between 14 dpi to 42 dpi, around 80 % of the FoxG1-GFP$^+$ cells and of the mutFoxG1$^+$ cells showed an aberrant and highly variable morphology (Figure 2.26). For example 78,07±3,38 % of the FoxG1-GFP$^+$ cells were morphological impaired 14 dpi (Figure 2,26 A). Cells showed a high degree of morphological aberration: some were short or had no dendrites, some developed a dendritic tree towards the hilus, and some cells appeared to be caught in a neuroblast stage. Examples were depicted in Figure 2.16 B. Supporting the assumption the morphological impairment was caused by the gain of function of FoxG1 is the observation that directly next to the FoxG1-GFP$^+$ and mutFoxG1-GFP$^+$ cells RFP-only$^+$ cells developed a normal neuronal morphology (indicated in Figure 2.26 by triangular arrows).

The performed gain of function analysis lead to the assumption that proper timed FoxG1 expression is critical for survival and maturation of adult born granule cells in the dentate gyrus

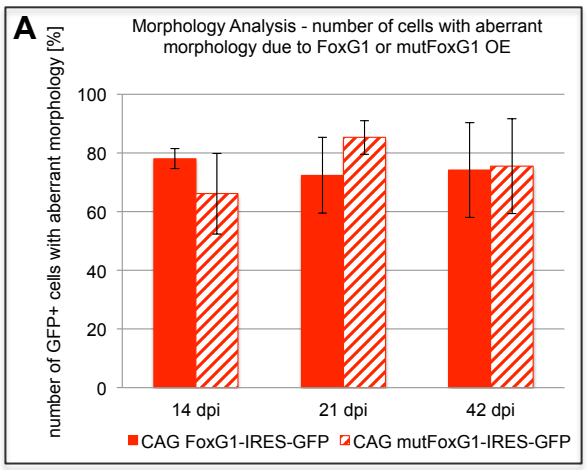

Figure 2.26: Aberrant morphology of FoxG1 and mutFoxG1 over-expressing cells in the adult dentate gyrus.
A Diagram of numbers of FoxG1-GFP$^+$ and mutFoxG1-GFP$^+$ with impaired morphology 14, 21 and 42 dpi. A majority of cells were morphologically impaired due to the FoxG1 gain of function in the adult dentate gyrus. **B** Example pictures of morphologically normal developed GFP$^+$ and RFP$^+$ control cells compared to morphologically impaired FoxG1-GFP$^+$ and mutFoxG1$^+$ cells 14, 21 and 42 dpi. Cells with aberrant morphology were depicted by arrows and regular developed RFP-only$^+$ cells by triangular arrows. Confocal images taken with a 40x oil objective. Scale bar ≙ 10 µm.

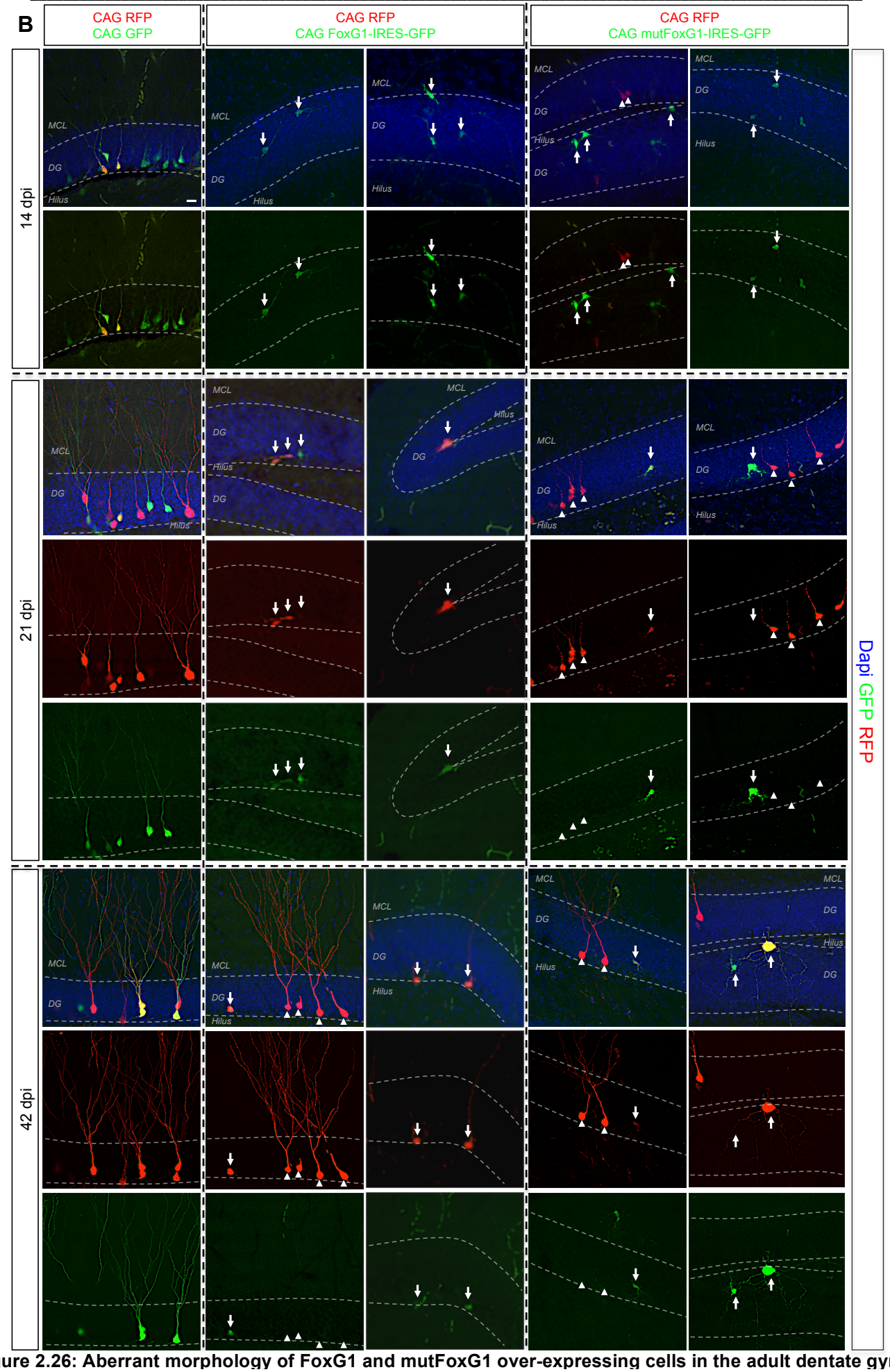

Figure 2.26: Aberrant morphology of FoxG1 and mutFoxG1 over-expressing cells in the adult dentate gyrus.

2.2.3 No phenotypic changes in newborn cells in the adult SVZ after over-expression of an endogenous or a dominant-active mutated form of FoxG1 *in vivo*

The role of FoxG1 in the second adult neurogenic niche – the SVZ – has not been evaluated in detail. From in situ hybridizations expression of FoxG1 was expected in the SVZ and RMS of adult mice (Shen et al., 2006). Therefore also an impact of FoxG1 on SVZ neurogenesis was anticipated. Immunohistochemistry for FoxG1 was performed and SVZ and RMS analyzed via confocal microscopy (Figure 2.29). In contrast to the known transcriptional expression of FoxG1 in SVZ and RMS from the in situ hybridization data, there were only few cells in the SVZ positive for FoxG1 protein, while cells in the RMS were completely devoid of FoxG1 protein. Importantly, FoxG1 expression in the corresponding dentate gyrus on the same sagittal mouse brain slice was clearly visible, demonstrating that the lack of FoxG1 immunoreactivity was not the result of a technical problem with the immunofluorescent staining procedure.

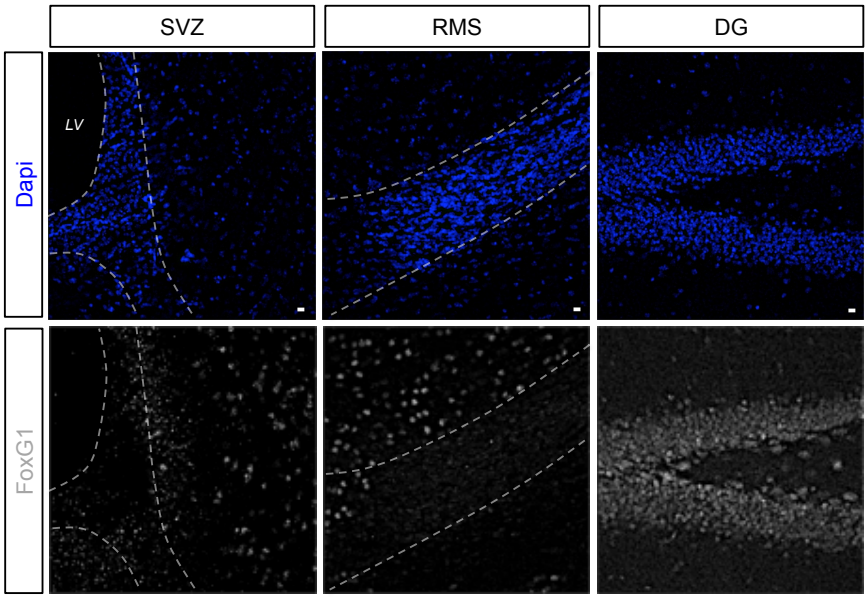

Figure 2.27: FoxG1 is not expressed in SVZ and RMS of adult mice. Confocal images of the SVZ, RMS and corresponding dentate gyrus of an adult mouse 10 days after stereotactical injection with a CAG-RFP retrovirus taken with a 40x objective. Scale bar ≙ 10 µm. Antibody staining for FoxG1 revealed virtually no expression in cells from SVZ and RMS, while cells in the striatum and the dentate gyrus were positive for FoxG1.

Since the phenotype in the gain of function analysis in the adult dentate gyrus was so severe, gain-of-functions experiments were performed for the adult SVZ. Again stereotactic injections of the FoxG1 over-expression and the mutFoxG1 over-expression retroviral constructs (CAG-FoxG1-IRES-GFO, CAG-mutFoxG1-IRES-GFP) together with a RFP expressing retroviral construct (CAG-RFP) were

performed (see experimental paradigm in Figure 2.27). A control group of animals were injected with the CAG-GFP and CAG-RFP retroviruses. The injections were applied this time into the RMS of both hemispheres in C57/Bl6 mice at P56. The mice were sacrificed 10 days later for analysis

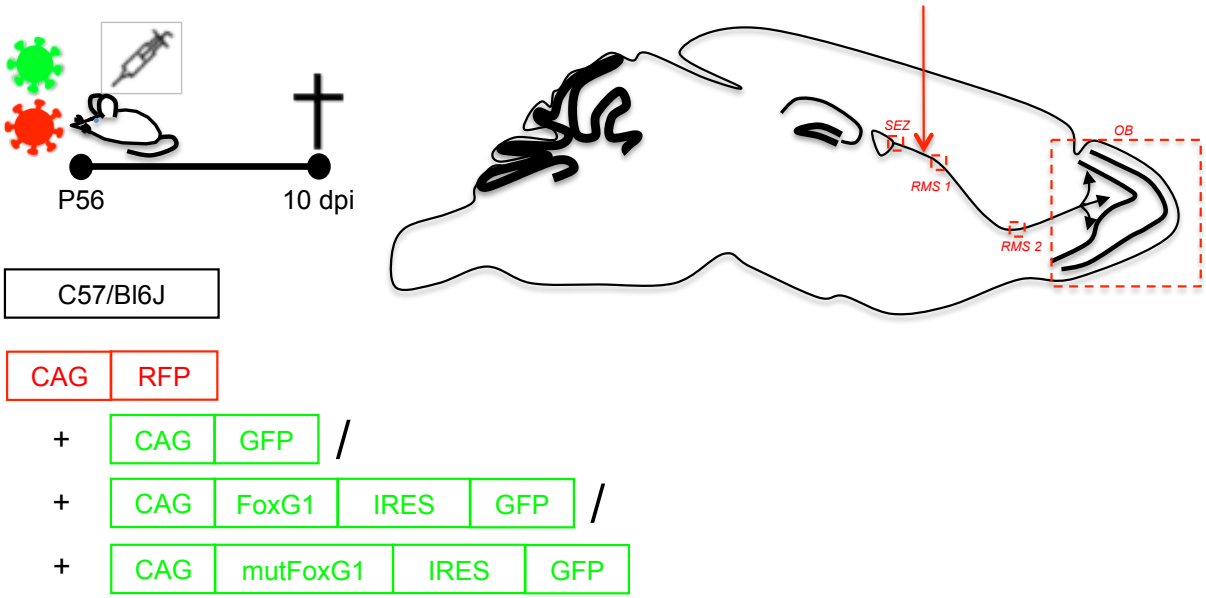

Figure 2.28: Experimental paradigm for the gain of function analysis of FoxG1 in the RMS. C57/Bl6 mice were stereotactical injected into the RMS with either the FoxG1 over-expression retroviral construct (CAG-FoxG1-IRES-GFP) or the mutFoxG1-over-expression retroviral construct (CAG-mutFoxG1-IRES-GFP) each together with an RFP-expressing control retrovirus (CAG-RFP) as internal control. A control group of animals was injected with GFP expressing retrovirus (CAG-GFP) and RFP expressing retrovirus. The animals were sacrificed 10 days post injections (10 dpi). The SVZ, two positions within the RMS (RMS 1 and RMS 2) and the olfactory bulb (OB) were analyzed.

Brains were cut into 50 µm thick sections and immunohistochemistry with antibodies against GFP, RFP and FoxG1 was performed on slices of at least 3 different animals for each of the 3 groups. Confocal pictures were taken and analyzed regarding migration and survival of the transduced cells. Surprisingly both the FoxG1-GFP$^+$ cells and the mut-FoxG1$^+$ cells migrated properly through the rostral migratory stream (RMS) to the olfactory bulb (OB) (Figure 2.27). No differences to the RFP$^+$ internal control cells or the GFP$^+$ cells in the control group could be detected. The survival of the cells seemed to be as well unaffected by the gain of function of FoxG1, as there were high numbers of FoxG1 over-expressing neurons present (cells not count).

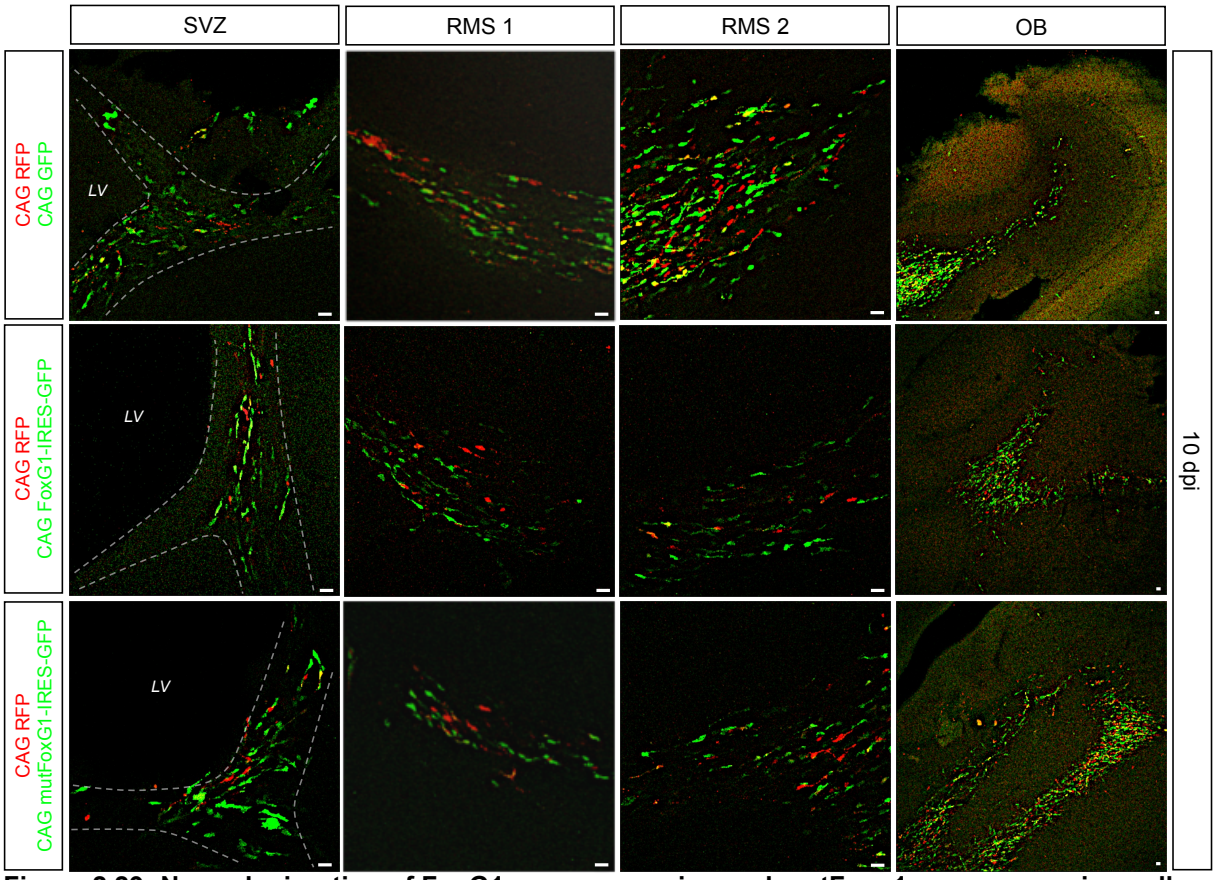

Figure 2.29: Normal migration of FoxG1 over-expressing and mutFoxg1 over-expressing cells from SVZ over RMS to the OB in adult mice.
Confocal pictures of the SVZ, RMS 1, RMS 2 and OB of C57/Bl6 mice 10 days post stereotactical injections into the RMS of CAG-RFP and CAG-GFP resp. CAG-FoxG1-IRES-GFP resp. CAG-mutFoxG1-IRES-GFP retroviruses. Images were taken with a 40x or 20x objective. Scale bar ≙ 10 µm. FoxG1-GFP$^+$ and mutFoxG1-GFP$^+$ cells migrated properly from the SVZ over the RMS to the OB. No migration of survival defects could be determined.

Newly generated cells of the SVZ neural stem cells differentiate into neuroblasts and migrate through the RMS to the OB. One of the markers expressed by neuroblasts is DCX. DCX expression was analyzed in the FoxG1 over-expressing and mutFoxG1-overexpressing cells compared to the RFP$^+$ and GFP$^+$ cells of the control animals in the RMS (Figure 2.28). Contrary to the data gathered in the dentate gyrus the FoxG1-GFP$^+$ and mutFoxG1-GFP$^+$ cells showed normal DCX expression (cells not count). No differences were found between the groups.

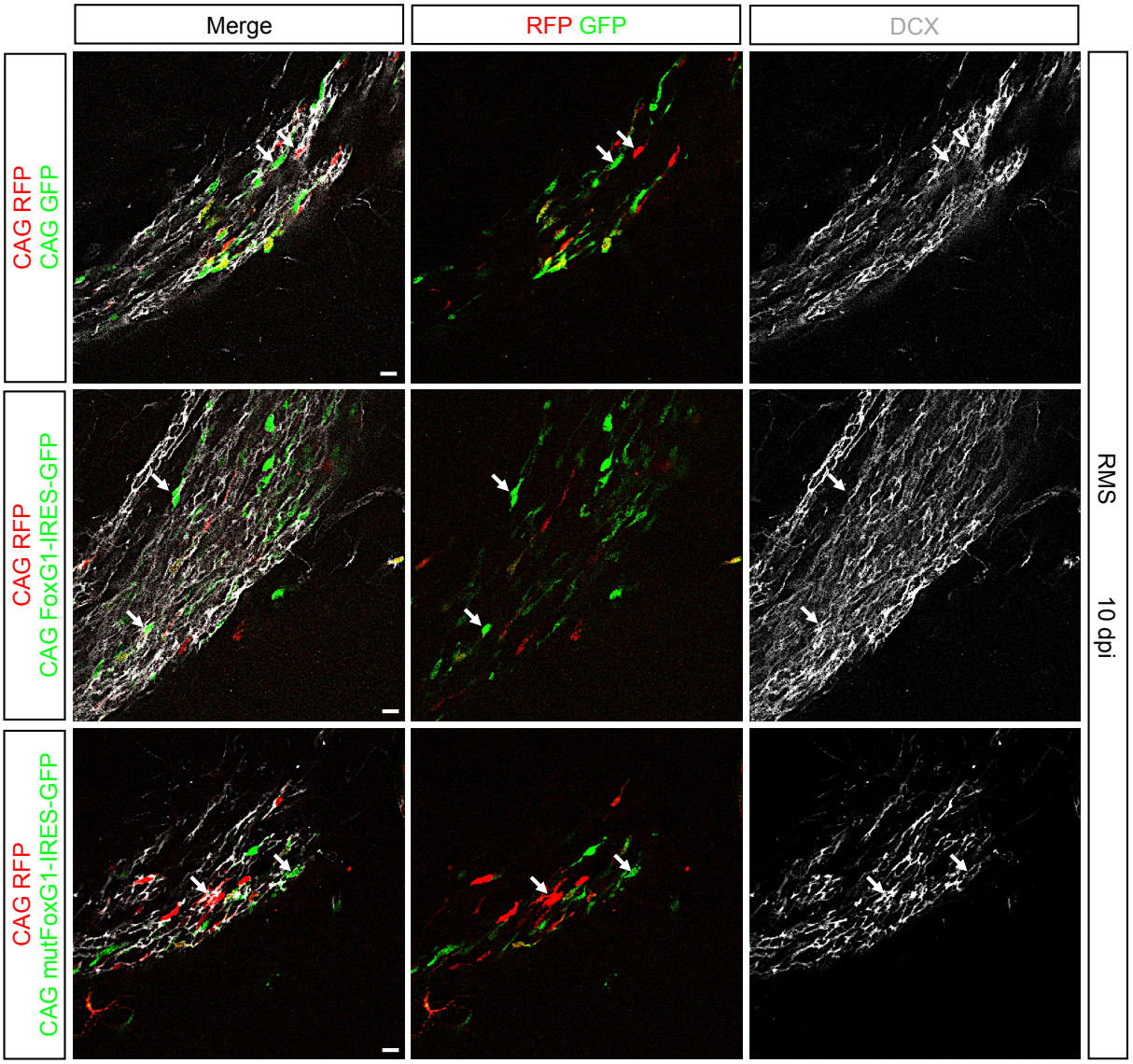

Figure 2.30: Normal DCX expression in FoxG1 and mutFoxg1 over-expressing cells in the RMS of adult mice 10 dpi.
Confocal images of the RMS of C57/Bl6 mice 10 days post stereotactical injections into the RMS of CAG-RFP and CAG-GFP resp. CAG-FoxG1-IRES-GFP resp. CAG-mutFoxG1-IRES-GFP retroviruses. Images were taken with a 40x or 20x objective. Scale bar ≙ 10 µm. Immunohistochemistry with antibodies against GFP, RFP and DCX was revealed normal DCX expression of Foxg1-GFP$^+$ and mutFoxG1$^+$ cells compared to RFP$^+$ and GFP$^+$ control cells.

In summary, a gain of function regarding the transcription factor FoxG1 revealed no impact on survival, migration behavior or differentiation in adult born cells of the SVZ. This finding was in stark contrast to the effects of FoxG1 overexpression on the adult hippocampal neurogenic niche, indicating that the two neurogenic niches had different sensitivity to increased FoxG1 activity.

3 Discussion

3.1 FoxO transcription factors in stem cell maintenance and neurogenesis in the adult brain

In the first part of this thesis the role of FoxO1, FoxO3 and FoxO4 in adult neurogenesis was investigated. These transcription factors were evaluated in a triple conditional KO regarding their part in stem cell maintenance, proliferation and neuronal differentiation in hippocampal neurogenesis of adult mice.
Analysis of FoxO conditional knockout mice from adulthood to aging showed a transient increase in the amount of recombined cells directly after the KO induction, followed by a gradual depletion of FoxO-deficient cells from the neurogenic lineage. BrdU pulse labeling studies revealed that FoxO-deletion transiently enhanced proliferation but in the long-run resulted in decreased proliferative activity. These observations demonstrate that FoxOs play an important function in long-term maintenance of adult hippocampal neurogenesis through control of the proliferative capacity in the adult hippocampal neurogenic niche. A function for FoxOs in the control of adult neural stem cells was previously suggested based on the findings that embryonic/developmental FoxO deletion affected neurogenesis in the adult subventricular zone and dentate gyrus (Paik et al., 2009; Renault et al., 2009). The phenotype of the present adult neural stem cell specific FoxO KO mice provides for the first time unequivocal proof for a key function of FoxO transcription factors in the control of proliferation and maintenance of neural stem cells in the adult hippocampal neurogenic niche.

Potential mechanisms conferring FoxOs function in stem cell proliferation and maintenance

Adult neural stem cells are predominantly in a quiescent state. There is evidence that precise control of quiescence is crucial for long-term maintenance of a functional stem cell pool (Ables et al., 2010; Mira et al., 2010; Gao et al., 2011), as quiescence appears on one hand to prevent excessive proliferation and depletion and on the other hand to protect stem cells from accumulating oxidative damage associated with high proliferative and metabolic activity. The present finding that excessive proliferation of adult neural stem cells following FoxO deletion results in stem cell

depletion provides further support for the importance of quiescence for long-term maintenance of the stem cell population.

FoxOs may control stem cell maintenance by directly controlling proliferation and protection of stem cells from oxidative damage. In order to give rise to new neurons quiescent stem cells need to enter into cell cycle and to progress through G1 (gap phase 1), S (DNA synthesis), G2 (gap phase 2) and M (mitosis) phase. The transition from one phase to the next is under stringent control by a complex set of regulatory proteins (reviewed by Sherr et al., 1996 and Sherr & Roberts, 1999). A key function in cell cycle regulation is ascribed to the PI3K-Akt pathway, which operates upstream of FoxOs and negatively controls their transcriptional activity. PI3K-Akt pathway activity is critical for the recruitment of quiescent stem cells into proliferation. Groszer and colleagues, for example, showed that loss of the negative PI3K-Akt-pathway regulator PTEN results in significantly enhanced proliferation of neural stem/progenitor cells (Groszer et al., 2001). Similarly, Bonaguidi and colleagues demonstrated that stem cell specific deletion of PTEN was sufficient to induce the proliferation of stem cells in the adult dentate gyrus (Bonaguidi et al., 2011).

FoxO transcription factors are negatively regulated by the PI3K-Akt-pathway. Intriguingly, one of the first functions discovered for FoxOs was their ability to regulate G1 to S phase transition via transcriptional regulation of $p27^{kip1}$ (Dijkers et al., 2000a; Medema et al., 2000). FoxOs positively regulate the transcriptional expression of $p27^{kip1}$, which blocks cell cycle progression at G1 phase. Hence, the loss of FoxO transcription factors might have led to an insufficient expression of $p27^{kip1}$ and in further consequence to a decreased block of the G1/S phase transition. Notably, lack of $p27^{kip1}$ was found to result in a selective increase of transit-amplifying progenitors in SVZ adult neurogenesis, illustrating the importance of $p27^{kip1}$ in proliferation in adult neurogenic niches (Doetsch et al., 2002).

FoxOs were also shown to induce cell cycle arrest via down regulation of Cyclin D1 and D2 independently from $p27^{kip1}$ (Schmidt et al., 2002). Expression of FoxOs leads to reduced protein expression of Cyclin D1 and D2 and is associated with an impaired capacity of CDK4 (cyclin-dependent-kinase 4) to phosphorylate and inactivate the S phase repressor pRb (retinoblastoma protein). Progression from G1 to S phase is among others regulated by the combined actions of the G1 cyclin/CDK complexes (Ekkholm & Reed, 2000; Sherr & Roberts, 1999). Thus, lack of FoxOs may have resulted in the de-repression of Cyclin D1 and D2 expression, increased

CDK4 inactivation of the S phase repressor pRb and consequently promotion of cell cycle progression. These regulatory mechanisms might have contributed to the observed increase in proliferation directly after loss of FoxOs in the adult dentate gyrus.

Le Belle and colleagues showed that endogenous ROS levels are high in proliferative neural stem cells (Le Belle et al., 2011). ROS are oxygen free radicals that are highly reactive towards proteins, lipids and DNA. UV light, ionizing radiation but also normal aerobic cell metabolism, like growth factor induced activation of enzyme complexes such as NADH oxidase, cause the formation of ROS (reviewed by Finkel & Holbrook, 2000). In case of excessive damage due to ROS or ineffective detoxification, cell death (apoptosis) is triggered. FoxOs are activated in response to oxidative stress caused by reactive oxygen species (ROS) (Brunet et al., 2004; Furukawa-Hibi et al., 2002). FoxOs protect cells from cell death by up-regulating genes involved in ROS detoxification like SOD2 (superoxide dismutase 2) or CAT (catalase)) and genes involved in cell cycle arrest (Gadd45) (Brunet et al., 2004; Furukawa-Hibi et al., 2002). The activation of FoxOs in response to oxidative stress was shown among others to be mediated by deacetylation through SIRT1 (sirtuin 1) or by activation via JNK (Jun-N-terminal kinase), which lead to the translocation of FoxOs to the nucleus (Essers et al., 2004; Salminen et al., 2013; Sunters et al., 2006). As a consequence FoxO target genes are expressed, which induce cell cycle arrest and resistance to oxidative stress. It is therefore tempting to speculate that tight control of ROS levels through FoxOs significantly contributes to mediating stem cell self-renewal and stem cell maintenance and that loss of FoxOs may have led to an insufficient initiation of detoxification and quiescence; cell cycle progressed and apoptosis was finally initiated, which contributed to the observed loss of FoxO deficient cells over time. This is in line with previous data from Tothova and colleagues in hemapoetic stem cell homeostasis (Tothova et al. 2007). They revealed increased ROS levels, increased cycling and apoptosis due to the loss of FoxOs.

An interesting observation was, that the FoxO-deficient cells alone were not responsible for the direct increase in proliferation but that potentially non-recombined stem cells and their progeny contributed to the transient hyperproliferation phenotype. This observation suggests that the FoxO deficient cells may initiate a signaling cascade, which led to the proliferation of cells in the surrounding. Malmersjö and colleagues showed that embryonic stem cell-derived neural

progenitors form networks exhibiting synchronous calcium ion (CA^{2+}) activity, which stimulate cell proliferation (Malmersjö et al., 2013). Inhibition of this network activity suppressed proliferation. Loss of FoxO and the resulting increase in proliferation might change the calcium signaling activity of the recombined cells so that the proliferation of other non-recombined cells, which are part of the network, is also increased.

Potential target genes and signaling pathways mediating FoxOs function in stem cell proliferation and maintenance

This study unraveled new candidate downstream targets of FoxOs in aNSCs. It was found that members of the bHLH (basic-helix-loop-helix) family of transcription factors such as Hes1, Hes5 and ASCL1 were differentially expressed in FoxO deficient cells. In general, bHLH transcription factors fulfill numerous functions through embryonic and adult neurogenesis, including transcriptional regulation of neural fate commitment, subtype specification, migration and axon guidance (reviewed by Bertrand et al., 2002 and Guillemot et al, 2007). Genome-wide analysis revealed further that the bHLH gene family is required for adult neurogenesis and neuronal regeneration (Cowles et al., 2013). The Hes (hairy enhancer of split) transcription factors belong to the repressor type bHLH transcription factors. They are important downstream targets of Notch signaling, a signaling pathway critical for maintaining stem cell quiescence in the early postnatal and adult brain. Loss of Notch signaling transiently increases cell proliferation and neurogenesis, but it leads finally to loss of the neural stem cell pool (Ables et al., 2010; Breunig et al., 2007; Ehm et al., 2010; Imayoshi et al., 2010). Hes genes repress pro-neural genes like ASCL1 and inhibit neuronal differentiation (Chen et al., 1997). Overexpression of Hes genes in mouse embryos was shown to inhibit neurogenesis and maintain neural stem cells (Ohtsuka et al., 2001). Here it was found that the loss of FoxOs in adult neural stem cells *in vitro* led to a major decrease in the expression of Hes5 and, surprisingly, a strong increase in the expression of Hes1, while ASCL1 was slightly increased. Webb and colleagues showed that FoxO3 inhibits ASCL1-dependent neurogenesis and thereby contributes to preserve the neural stem cell pool (Webb et al., 2013). These findings raise the possibility that proliferation and increased neurogenesis were at least in part the consequence of decreased expression of Hes5, which resulted in impaired stem cell quiescence, and in increased expression of the pro-

neural bHLH factor ASCL1, which promoted differentiation of precursors and thereby exhausted the proliferation capacity of the hippocampal niche too early. The elevated levels of Hes1 may reflect the possibility that Hes1 is not a direct target of FoxOs and that Hes1 was up-regulated by FoxO-deficient cells in an effort to compensate for the reduced Hes5 expression.

Two members of another group of transcription factors were also differentially expressed in FoxO deficient neural stem cells. NFIA (nuclear factor I A) and NFIX (nuclear factor I X) were strongly down-regulated *in vitro*. NFIA was previously found to be required for the onset of gliogenesis by driving the transcription of glia specific genes like Glast and GFAP in the cortex and the hippocampus (Barry et al., 2008; Deneen et al., 2006; Piper et al., 2010). It was further shown that induction of the Notch pathway results in the activation of NFIA expression and that NFIA promotes gliogenesis by repressing the Notch effector gene Hes1 (Piper et al., 2010). Additionally, NFIA KO mice show elevated Hes1 expression in the telencephalon during embryogenesis (Shu et al., 2003) and the promoter region of the Hes1 gene contains a cluster of conserved NFI binding sites (Piper et al., 2010). NFIX was recently reported to control the quiescent state of NSCs (Martynoga et al., 2013). Martynoga and colleagues performed RNA-sequencing of neural stem cells in culture, which were forced into quiescence by exposure to BMP4. They showed that quiescence was associated with a high increase in NFIX expression, while NFIA and the other two NFI family members (NFIB, NFI) were down regulated, suggesting a role of NFIX to initiate or maintain the quiescent state. The down regulation *in vitro* of NFIX due to the loss of FoxOs might have contributed to the loss of quiescence and increase in proliferation and neurogenesis. In summary, it is very interesting that several of the differentially expressed genes in FoxO ablated stem cells are bona fide Notch target genes. This raises the promising possibility that the observed stem cell phenotype following FoxO deletion is caused by a modulation of the Notch signaling pathway. This assumption is supported by data from Kitamura and colleagues, which showed that FoxO and Notch pathways interact biochemically and functionally to control differentiation in muscle cells (Kitamura et al., 2007).

The present study also provided first evidence that the hyperproliferative phenotype may be the consequence of dysregulated GPR17-dependent signaling. GPR17 was recently suggested as a direct transcriptional target of FoxO1 (Ren et al., 2012). GPR17 is a leukotriene receptor, whose expression has been reported in neural

progenitor cells and neural stem cells (Huber et al., 2011). Huber and colleagues showed that inhibition of GPR17 signaling via the competitive receptor inhibitor Montelukast increased neural progenitor proliferation *in vitro*, indicating that GPR17-dependent signaling negatively regulates NSC proliferation. Intriguingly, Montelukast treatment did not increase proliferation of FoxO-deficient neural stem cells, raising the possibility that FoxO deletion altered GPR17-dependent signaling. Analysis of the recombined FoxO-deficient cells *in vivo* indeed revealed that loss of FoxO strongly reduced the expression of the GPR17 receptor in the hippocampal neurogenic niche. Collectively, these observations suggest that the loss of FoxOs led to a decrease in GPR17 receptor expression, which in turn resulted in decreased inhibition of proliferation, loss of quiescence and increase in proliferation and neurogenesis *in vitro* and *in vivo*.

Potential signaling pathways compensating the loss of FoxO phenotype

Cultured FoxO-deficient adult neural stem cells showed intriguing differences in behavior compared to their *in vivo* counterparts. Similar to the behavior of FoxO-deficient NSCs *in vivo*, ablation of FoxOs led to an increase in proliferation and neurogenesis in cultured NSCs. The observed depletion of FoxO-deficient cells over time, however, and the decrease in stem cell activity in aged FoxO-deficient mice was not seen *in vitro*. Instead, hyperproliferation persisted *in vitro* over several passages and did not decrease at any point of the observation period. These observations raised the possibility that the *in vivo* neurogenic niche provided signals restricted the hyperproliferative phenotype of FoxO-deficient cells.

Two members of the TGFβ-superfamily were shown to be critical for the regulation of stem cell quiescence and neurogenesis throughout lifetime. TGFβ signaling was shown to be associated with stem cell quiescence in the hippocampal niche in adult mice (Kandasamy et al., 2010). Previous data indicate that TGFβ signaling is able to reduce stem cell proliferation (Buckwalter et al., 2006; Kandasamy et al., 2010, Wachs et al., 2006). In addition, it was shown in aged mice that increased TGFβ expression strongly inhibits hippocampal neurogenesis (Buckwalter et al., 2006). Furthermore, a previous study showed complex formation of FoxOs and Smad proteins, which were activated by TGFβ signaling, to cooperatively induce the cell cycle inhibitor $p21^{Cip1}$ to reduce proliferation of neuroepithelial and glioblastoma cells. The ability of FoxOs to directly interact with the TGFβ pathway to control proliferation

raises the possibility that FoxOs and TGFβ signaling depend on each other to precisely control neural stem cell homeostasis (Seoane et al., 2004). With this, loss of FoxOs may have led to a reduced ability of TGFβ signaling to block cell cycle and maintain quiescence. Mira and colleagues revealed that BMPs (bone morphogenic proteins) are potent regulators balancing NSC quiescence and proliferation to prevent loss of the stem cell activity (Mira et al., 2010). They showed that BMP receptors are active in quiescent neural stem cells but not in non-quiescent neural precursors in the adult hippocampus. Loss of BMP signaling transiently increases proliferation but later leads to a reduced number of precursors. Hence, BMP and TGFβ signaling appear to be important keepers of stem cell quiescence. Most strikingly, cultured FoxO-deficient neural stem cells were still amenable to the anti-proliferative effects of BMP/TGFβ signaling. Moreover, the FoxO deficient cells showed active BMP and TGFβ signaling both in the young adult and the aged hippocampal niche *in vivo*. These observations raised the possibility that the observed mild proliferation phenotype in FoxO-deficient cells in the adult dentate gyrus, which is contrary to the strong increase in proliferation and neurogenesis *in vitro*, might be due to the activity of BMP/TGFβ signaling *in vivo.* BMP/TGFβ signaling might restrict the proliferation of FoxO-deficient neural stem cells *in vivo*.

3.2 FoxO transcription factors and their role in morphological maturation of newborn cells in the adult dentate gyrus

Intrinsic mechanisms and extrinsic cues regulate the maturation and synaptic integration of newborn neurons in the dentate gyrus (Ming & Song, 2011). The newborn cells start to extend dendritic processes two to five days after cell birth. Within the first two to three weeks extensive dendritic and axonal growth takes place; the development of first spines can be detected approximately 16 days after neuronal birth and the new neurons receive glutamatergic inputs from axosomatic, axodendritic and axospinous synapses (Toni et al., 2007; Zhao et al., 2006). The full maturation of dendrites and spines of the newborn cells takes approximately six weeks (Ge et al., 2008; Marín-Burgin et al., 2012; Schmidt-Hieber et al., 2004). Retroviral labeling of newborn cells allowed the analysis of the morphological maturation of FoxO-deficient cells in the adult hippocampus. FoxO KO cells showed

delayed maturation. 21 days after their birth total dendritic length of FoxO KO cells was reduced and they showed prolonged expression of DCX - a marker for immature neurons, which is down regulated during neuronal maturation (Brown et al. 2003). At 42 days FoxO-deficient cells were comparable to control cells with regard to their total dendritic length and dendritic complexity. A majority of the FoxO-deficient cells, however, displayed a peculiar dendritic phenotype and bore an extremely shortened primary dendrite; in some cases they lacked the typical single primary dendrite and instead extended two dendrites from the soma. Thus, FoxO knockout resulted in delayed maturation and aberrant dendritic patterning.

Huynh and colleagues showed that FoxO1 forms a complex with SnoN1 and directly binds to the DCX promoter to repress DCX. The repression of DCX mediates the ability of SnoN1 to the regulate branching in primary neurons and migration of granule neurons of the cerebellar cortex of postnatal rats (Huynh et al., 2011). DCX has been implicated as a critical player in neuronal morphology and inhibition of DCX function stimulates branching of processes in neurons (Kappeler et al., 2006). Due to the loss of FoxOs, maturing neurons may fail to properly repress DCX expression, which might explain the observed prolonged DCX expression in newborn FoxO-deficient cells; impaired dendritic growth may also be a consequence of dysregulated DCX expression as DCX was found to repress dendrite branching (Kappeler et al., 2006). FoxOs were further reported to orchestrate neuronal polarity in hippocampal and cortical granule neurons via the downstream target Pak1 (p21-activated kinase 1) and they are required for axon outgrowth in primary cerebellar granule neurons during development (Christensen et al., 2011; de la Torre-Ubieta et al., 2010). Localized Pak1 expression in a single neurite was shown to be critical to define the future axon in primary hippocampal neurons (Jacobs et al., 2007). Similar regulatory mechanisms might be responsible for the observed crucial reduction in the primary dendrite resp. the duplicated primary dendrite, if Pak1 expression has a related function in defining the primary dendrite as it has in defining the future axon. Further analysis is necessary to determine the underlying mechanisms and also if there are any functional impairments of newborn neurons due to the morphological alterations and to the delayed maturation sequence.

3.3 FoxO deficiency affects the mitochondrial compartment in newborn neurons- hints towards a new mechanism underlying FoxO dependent neuronal development

Mitochondria are multifunctional organelles: next to being the main site for the generation of the energy-yielding molecule ATP (adenosine triphosphate), they are important for Ca^{2+} buffering, β-oxidation of lipid acids, and for the regulation of apoptosis (reviewed by McBride et al., 2006). Mitochondria are emerging players in the control of neuronal development, where they have been found to control dendritogenesis, axonogenesis, and synaptogenesis (reviewed by Cheng et al., 2010).

Interestingly, the present study revealed alterations in the mitochondrial compartment of FoxO-deficient neurons. Specifically, it was found that the number of mitochondria was decreased in young FoxO-deficient newborn neurons. Moreover, it was found that mitochondria were enlarged in both immature and mature FoxO deficient adult-born neurons. While the decreased number of mitochondria in immature neurons may reflect the maturation delay (Steib, 2013), the fact that mitochondria were enlarged in immature and mature FoxO-deficient neurons indicates potential defects in mitochondrial homeostasis.

Mitochondria change their shape constantly by fusion and fission, which is correlated with their bioenergetics function (reviewed by Chan, 2006 and Mannella, 2008). The morphologies of mitochondria range from small roundish elements to larger interconnected networks. E.g. before cells enter S phase of cell cycle, which is a highly energy costing process, mitochondria become hyperfused and increase their ATP production (Mitra et al., 2009). Therefore morphological changes of mitochondria may imply defects in mitochondrial function. To date no function in fusion and fission was revealed for FoxO transcription factors except that FoxO3 KO mice showed enhanced mitochondrial fission in cardiomyocytes (Wang et al., 2012a). It is therefore unlikely that the enlarged mitochondria in the FoxO-deficient cells, which would rather argue for enhanced fusion, are caused by a direct transcriptional effect of FoxOs on the fusion and fission dynamics.

Mitochondrial size is influenced not only by mitochondrial fusion and fission processes but is also dictated by the integrity of the mitochondrion. Enlargement of mitochondria has been observed in post-mitotic neurons of the ageing brain. Such

mitochondrial enlargement is hypothesized to be the consequence of accumulation of ROS during the lifetime of the cell or defects in mitochondrial fission (Vanneste & van den Bosch de Aguilar, 1981). As FoxO deficient cells were shown to have elevated ROS levels (Paik et al., 2009), mitochondrial enlargement in FoxO-deficient newborn neurons may reflect premature mitochondrial damage via elevated ROS.

The presence of enlarged mitochondria may also point at defects in the autophagy pathway, as it has been suggested that large mitochondria are less efficiently removed via autophagy than small ones (Brunk & Terman, 2002). Autophagy is an evolutionary conserved process, during which cytoplasmic material and organelles including mitochondria are segregated into autophagosomes, which in turn are degraded within autolysosomes. The continuous elimination of dysfunctional proteins and damaged organelles via autophagy is necessary to prevent the accumulation of abnormal proteins, which can disturb cellular function. Moreover, autophagy serves to provide nutrients and cellular building blocks under metabolic stress (Levine et al., 2008). Defects in autophagy affect the intracellular communication and contribute to neurodegeneration (Komatsu et al., 2006). More recently, autophagy has also been linked to stem cell function: thus, impairing autophagy via ablation of the pro-autophagic gene FIP200 results in a progressive loss of the neural stem cells in the postnatal brain (Wang et al., 2013). Moreover, there is circumstantial evidence that autophagy is essential for neuronal morphogenesis and synaptogenesis (Komatsu et al., 2007; Liu & Shio, 2008).

Intriguingly, recent studies implied FoxOs as mediators of autophagy (Mammucari et al., 2007; Zhao et al., 2007a). FoxO3 was found to be both necessary and sufficient to induce autophagy in skeletal muscle fibers by inducing autophagy-related genes like LC3 and the Bcl2-related autophagy regulator.

Overall, these observations suggest that the enlargement of mitochondria may be related to FoxO-deficiency induced mitochondrial damage and FoxO-deficiency induced impairment in autophagy of damaged mitochondria. Given the emerging key function of mitochondrial function to neuronal morphogenesis and synaptogenesis, the present results raise the intriguing hypothesis that FoxO-deficiency impedes on neurogenesis via impairment of the mitochondrial compartment.

3.4 Transcription factor FoxG1 – dosage and niche dependent regulator of adult neurogenesis?

In the second part of this thesis the role of the transcription factor FoxG1 in adult neurogenesis was analyzed. Retroviral timeline and stage specific marker analysis revealed a specific expression pattern of FoxG1 in the adult hippocampal neurogenic lineage. FoxG1 is expressed in neural stem cells, transit amplifying progenitors and immature neurons, whereas only a fraction of mature dentate gyrus neurons express FoxG1. Differences were detected in the level of FoxG1 expression between the different stages during the process of neurogenesis. The highest levels of FoxG1 were found in immature neurons, while lower FoxG1 expression was observed in stem cells and transit amplifying progenitors. These observations raised the hypothesis that proper timing and dosage of FoxG1 may be the control of adult hippocampal neurogenesis.

Previous studies revealed that loss or haploinsufficiency of FoxG1 affected multiple steps of postnatal neurogenesis in the hippocampal niche including survival, proliferation, differentiation and migration of postnatally generated granule neurons (Shen et al., 2006; Tian et al., 2012). Here, forced expression of WT FoxG1 and dominant active FoxG1 led to a massive decrease in survival of newborn dentate granule cells. The surviving cells showed a severe impaired morphology. Neuronal differentiation was diminished, while oligodendrogenesis was increased. Thus, both loss and gain of function of FoxG1 have detrimental effects on adult born cells in the dentate gyrus. Collectively the gain and loss of function phenotypes demonstrate not only that FoxG1 is indispensable for adult neurogenesis, but also that the proper timed expression of FoxG1 and the FoxG1 dosage are equally important.

The precise mechanism through which FoxG1 affected fate choice, neuronal morphogenesis, and survival remains to be established. Until now only few FoxG1 target genes have been identified. In the ectoderm of the developing xenopus embryo FoxG1 was shown to regulate positively neuronal differentiation by controlling the expression of NGNR-1 (Neurogenein-related-1) (Bourguignon et al., 1998). Interestingly, the same study revealed opposing effects of FoxG1 in dependency of FoxG1 dosage. High levels of FoxG1 lead to decreased neuronal differentiation as observed in this study, while low doses of FoxG1 promotes neuronal differentiation.

A recent study by Miyoshi and Fishell linked FoxG1 function to morphological transitions of neuronal precursors / immature neurons in cortical development. These authors demonstrated that the dynamic expression of FoxG1 coordinates the integration of multipolar pyramidal neuron precursors into the cortical plate (Miyoshi & Fishell, 2012). FoxG1 is down-regulated at the beginning of the multipolar cell phase and re-expressed when cells exit the multipolar cell phase and enter into the cortical plate. In the absence of down-regulation of FoxG1, migration to the cortical plate was delayed and the laminar identity of the cells was switched; while lack of re-expression of FoxG1 upon entrance into the cortical plate resulted in reversion of cells to the early multipolar phase. Consistent with the importance of proper timing and dosage of FoxG1 in cortical development, tight regulation of the expression level of FoxG1 in the adult hippocampal neurogenic lineage may be crucial for the development of new dentate gyrus neurons. Low expression levels of FoxG1 in progenitor cells might be necessary to allow for neuronal differentiation, which may explain the negative impact of FoxG1 hyperactivity on neuronal fate choice. Moreover, impaired morphological development due to the FoxG1 gain of function in this study may eventually be a consequence of a missing down-regulation.

An interesting finding was that in contrast to the massive effect of FoxG1 on dentate gyrus neurogenesis, FoxG1 gain of function did not lead to any obvious phenotypic changes in SVZ neurogenesis. FoxG1 overexpressing neuroblasts migrated normally along the RMS to the olfactory bulb, where they changed their migration mode and migrated radially towards the neuronal layers of the olfactory bulb. The molecular basis for the differences in the effect of FoxG1 gain of function on adult SVZ and dentate gyrus neurogenesis remains to be determined. Adult SVZ and dentate gyrus neurogenesis share a number of regulatory features and principles; yet, there is growing evidence that each neurogenic zone is also subject to niche specific regulatory factors (Bracko et al., 2012). Such niche specific regulation seems logical as neurogenesis in the adult SVZ and adult hippocampal neurogenesis produces distinct neuronal subtypes: dentate gyrus neurogenesis produces only glutamatergic neurons, while neurogenesis in the SVZ generates a large number of GABAergic, and a comparably small number of dopaminergic and glutamatergic neurons. The transcriptional code underlying the generation of these different neuronal subtypes is likely to be highly distinct and may include and exclude FoxG1 in the case of dentate gyrus neurogenesis and SVZ neurogenesis, respectively. Indeed, haploinsufficiency

of FoxG1 was shown to not affect postnatal SVZ neurogenesis (Shen et al., 2006). Moreover, this study found that while FoxG1 mRNA is expressed in both adult neurogenic niches (Shen et al., 2006), FoxG1 protein is only detectable in the hippocampal neurogenic lineage, indicating that FoxG1 is subject to distinct posttranslational regulation in the adult neurogenic niches. Determining these posttranslational mechanisms as well as their regulation in distinct neuronal subtype lineages and their impact on neuronal development will shed light on the function of FoxG1 in the regulation of adult neurogenesis, especially in the context of niche dependent neuronal cell type differentiation.

3.5 FoxG1 and the congenital form of Rett syndrome

In humans mutations of FoxG1 including disruption of the DNA binding domain, duplications, deletions, frameshift mutations, truncating and missense mutations were found to be associated with the congenital form of Rett syndrome (Ariani et al., 2008; Brunetti-Pierri et al., 2011; Jacob et al., 2009; Kumakura et al., 2013; Le Guen et al., 2011a and 2011b; Mencarelli et al., 2010; Papa et al., 2008; Perche et al., 2013; Takagi et al., 2013). The consequences are microcephaly, epilepsy, severe mental retardation, absent language, dyskinesia, corpus callosum hypogenesis, simplified gyral pattern and reduced white matter volume (Kortüm et al., 2011; Guerrini & Parrini, 2012). Interestingly, the different human mutations in FoxG1 causing the congenital variant of Rett syndrome represent both gain and loss of function mutations and lead to similar phenotypic outcomes, indicating once again that precise FoxG1 dosage and timing are crucial for neurogenesis.

With the results of this study and others some of the phenotypes are at least partially explainable. FoxG1 was reported to be involved in maintaining neural stem cell maintenance in the embryonic forebrain (Fasano et al., 2009; Yadirgi et al., 2011), progenitor proliferation in the telencephalon (Manuel et al., 2011; Yip et al., 2012) and self-renewal of medullablastoma stem cells (Manoranjan et al., 2013); FoxG1 promotes the survival of post-mitotic neurons (Dastidar et al; 2011 and 2012) and coordinates the integration of multipolar pyramidal neuron precursors into the cortical plate (Miyoshi & Fishell, 2012). FoxG1 was shown to promote neurogenesis (Brancaccio et al., 2010). Here, additional insight into the pathophysiology of FoxG1-

dependent Rett-syndrome was provided showing that FoxG1 regulates survival and neuronal differentiation in adult neurogenesis.

The vast majority of Rett-syndrome cases are caused by mutations in the MECP2 gene (Methyl-CpG binding protein 2). Mutations in this gene affect neuronal development and plasticity of inhibitory and excitatory neurons (Fukuda et al., 2005; Matarazzo et al., 2004; Nelson et al., 2011). Interestingly, the present study raises the possibility that FoxG1 mutations may in particular affect neurogenesis of specific neuronal subtypes, e.g. glutamatergic neurons, while leaving neurogenesis of other neuronal subpopulations, such as GABAergic neurons, intact. Investigating such differential effects of FoxG1 mutations on distinct neuronal populations would be of high clinical relevance, in particular as there is emerging evidence that patients with FoxG1 mutations present with clinical features that are distinct from the clinical features of classical Rett-syndrome patients, who carry mutations in MECP2 (Pratt et al., 2013).

3.6 Conclusions

In summary, the first part of the presented study revealed that FoxO transcription factors are modulators of adult hippocampal stem cell maintenance and neurogenesis. They regulate stem cell homeostasis potentially via downstream targets known from the Notch pathway and interfering with other signaling mechanisms like TGFβ and GPR17. The different *in vitro* and *in vivo* results suggest that *in vivo* the effects of loss of FoxO signaling are partially compensated via other pathways like BMP or TGFβ up to mid adulthood. The full impact comes into effect in aging as adult ablation of FoxOs lead to loss of the FoxO deficient cells and decreased proliferation and neurogenesis in aged mice, suggesting that compensating mechanisms were lost during aging or that compensation of the loss of FoxOs was incomplete and therefore resulted in protracted appearance of loss-of-neurogenesis. In addition, indications were acquired that FoxOs play a role in neuronal maturation and survival by maintaining important cellular functions like regulation of mitochondrial ROS production and autophagy.

The second part of the presented study revealed a crucial role for the transcription factor FoxG1 in survival and neuronal differentiation in adult hippocampal neurogenesis. Most importantly, the collected data revealed that the function of FoxG1 is dependent on dosage and timing. Interestingly, manipulations of FoxG1 expression in SVZ neurogenesis did not have major impact on neuronal development, which raises the hypothesis that precise expression of FoxG1 is crucial only for the generation of specific neuronal subtypes.

Taken together, the presented data provided further insight into the regulatory mechanisms underlying stem cell homeostasis and adult neurogenesis. FoxOs and FoxG1 are associated with ageing and neurodegeneration and neurodevelopmental disorders, respectively. Hence, the new insights provided by this work promote further the understanding of the molecular and cell biological basis underlying age-associated brain dysfunction, neurodegeneration and neurodevelopmental disorders and may thereby support the development of new strategies for neural repair.

4 Material and Methods

4.1 Material

4.1.1 Chemicals and reagents

1 kb DNA ladder	New England Biolabs
100 bp DNA ladder	Fermentas
Antibiotic-Antimitotic (100x)	GIBCO/Invitrogen
Accutase	Millipore
Albumin from bovine serum (98%)	Sigma-Aldrich
Ampicillin	Sigma-Aldrich
Atipamezol (Antisedan®)	Pfizer
β-Mercaptoethanol	Sigma
B27 supplement	GIBCO/Invitrogen
BrdU	Sigma
Bovine serum albumin (2 mg/ml)	Pierce
Buprenorphine (Temgesic®)	Essex Pharma
DAPI dilactate	Sigma-Aldrich
DMEM/F-12 Glutamax	GIBCO/Invitrogen
DMEM with high glucose/GlutaMax/Hepes	GIBCO/Invitrogen
DNA agarose	Biozym
dNTPs (10mM)	Fermentas
D-PBS (-$CaCL^2$, -$MgCl^2$)	GIBCO/Invitrogen
EBSS (Earls Balanced Salt Solution)	GIBCO/Invitrogen
EDTA	Sigma-Aldrich
EGF (Epidermal Growth Factor)	Life Tech
EtBr (1 mg/ml)	Roth
EtOH (100 %)	Merck
FCS	GIBCO/Invitrogen
Fentanyl (Fentanyl®)	Janssen-Cilag
FGF-2 (Fibroblast Growth Factor 2)	Pepro Tech
Flumazenil (Anexate®)	Hexal
Geneticin	GIBCO/Invitrogen
HBSS	GIBCO/Invitrogen
HBSS (Hanks Balanced Salt Solution)	GIBCO/Invitrogen

HCl (32 %)	Merck
HEPES (1 M)	GIBCO/Invitrogen
Hyaluronidase	Sigma
Isopropanol (96 %)	Merck
KCl	Merck
Lipofectamine 2000	Invitrogen
Laminin	GIBCO/Invitrogen
Medetomidine (Dormitor®)	Pfizer
MeOH (100 %)	Merck
Midazolam (Dormicum®)	Hoffmann-La Roche
NaAc	Merck
NaOH	Merck
NEAA (100x)	GIBCO/Invitrogen
Normal Donkey Serum	Chemicon
Opti-MEM I Reduced serum medium	GIBCO/Invitrogen
PFA	Roth
Poly-D-Lysine	Sigma
Puromycin	Sigma
RNase A (from bovine pancreas)	Serva
Sodium-Pyruvate (100x)	GIBCO/Invitrogen
Sucrose	Sigma
Tamoxifen	Sigma
Tris-Base	Sigma
Triton X-100	Roth
Trypsin	Sigma
Trypsin-EDTA (0.05 %)	GIBCO/Invitrogen

4.1.2 Enzymes and enzyme buffers

5 PRIME Master Mix (2.5x)	5 PRIME
Antarctic phosphatase (5 U/µl)	New England Biolabs
Antarctic phosphatase buffer	New England Biolabs
Buffer NEB2	New England Biolabs
Buffer NEB4	New England Biolabs

Brilliant II Fast SYBR Green qPCR Master Mix	Agilent
iProof buffer HF (5)	Biorad
iProof polymerase (2U/µl)	Biorad
PmeI	New England Biolabs
SfiI	New England Biolabs
T4 ligase (400 U/µl)	New England Biolabs
T4 ligase buffer with ATP (10x)	New England Biolabs
RevertAid Premium Reverse Transcriptase	Fermentas
RiboLock RNAse I	Fermentas
RT buffer (10x)	Fermentas
DNase	Quiagen
TDD buffer	Quiagen
XbaI	New England Biolabs
XhoI	New England Biolabs

4.1.3 Antibodies

Primary antibodies

β-galactosidase α gt (1:250)	Abcam
β-galactosidase α rb (1:20)	Millipore
BrdU α rat (1:200)	Oxford Biotechnology
DCX α gt (1:250)	Santa Cruz Biotechnologies
FoxO1 α rb (1:500) (ICC)	Cell Signaling
FoxO3 α rb (1:500) (ICC)	Abcam
FoxO3a α rb (1:100) (IHC)	Abcam
GFAP α ms (1:1000)	Santa Cruz Biotechnologies
GFP α chicken (1:500)	Aveslab
Ki67 α rb (1:1000)	Novacastra
Map2(a+b) ms (1:250)	Sigma
Prox1 α rb (1:500)	Chemicon
RFP α rat (1:50)	Prof. Dr. H. Leonhardt, LMU
Sox2 α gt (1:500)	Santa Cruz Biotechnologies
Sox10 α gt (1:200)	Santa Cruz Biotechnologies

Secondary antibodies

Alexa 488 α chicken	Jackson Laboratory
Goat α chicken IgY, Biotin conjugate	Life Technologies
Cy3 α gt	Jackson Laboratory
Cy3 α rat	Jackson Laboratory
Cy3 α rb	Jackson Laboratory
Cy5 α gt	Jackson Laboratory
Cy5 α rb	Jackson Laboratory
Cy5 α ms	Jackson Laboratory
Cy5 α gt	Jackson Laboratory
Fitc α chicken	Jackson Laboratory
Fitc α ms	Jackson Laboratory
Streptavidin, Alexa Fluor® 488 conjugate	Life Technologies

4.1.4 Kits

Fermentas RevertAid	
First Strand cDNA Synthesis Kit	Thermo Fisher Scientific
Lipofectamine™ 2000	Invitrogen
NucleoSpin Plasmid Kit	Machery-Nagel
NucleoSpin® Gel and PCR Clean-up	Machery-Nagel
Pure Yield Plasmid Midiprep System	Promega
Qiashredder	Quiagen
QuikChange® Site-Directed Mutagenesis Kit	Stratagene
RNase-free DNase Set	Quiagen
RNeasy Mini Kit	Quiagen

4.1.5 Oligodeoxynucleotides

Genotyping Primers

FoxO1	forward	5’-GCT TAG AGC AGA GAT GTT CTC ACA TT-3’
FoxO1	reverse	5’-CCA GAG TCT TTG TAT CAG GCA AAT AA-3’
FoxO1	reverse	5’-CAA GTC CAT TAA TTC AGC ACA TTG A-3’

FoxO3	forward	5’-ATT CCT TTG GAA ATC AAC AAA ACT-3’
FoxO3	reverse	5’-TGC TTT GAT ACT ATT CCA CAA ACCC-3’
FoxO3	reverse	5’-AGA TTT ATG TTC CCA CTT GCT TCCT-3’
FoxO4	forward	5’-CTT CTC TGT GGG AAT AAA TGT TTG G-3’
FoxO4	reverse	5’-CTA CTT CAA GGA CAA GGG TGA CAG-3’
FoxO4	reverse	5’-TGA GAA GCC ATT GAA GAT CAG-3’
Glast-CreER	forward	5’-GAGGCACTTGGCTAGGCTCTGAGGA-3’
Glast-CreER	reverse	5’-GAGGAGATCCTGACCGATCAGTTGG-3’
Glast-rerCreER1	forward	5’-GGTGTACGGTCAGTAAATTGGACAT-3’
Rosa26R-R1	forward	5’-CACACCAGGTTAGCCTTTAAGC-3’
Rosa26R-D1	reverse	5’-CAAAGTCGCTCTGAGTTGTTATC-3’
Rosa26R-Mutant	forward	5’- GCGAAGAGTTTGTCCTCA-3’
cDNA Primers		
Foxo1	forward	5’-ACG AGT GGA TGG TGA AGA GC-3’
FoxO1	reverse	5’-CTC TTC TCC GGG GTG ATT TT-3’
FoxO3	forward	5’-GTCATGGGCCACGATAAGTT-3’
FoxO3	reverse	5’-GGGCTGCTAACAGTCTCTGC-3’
FoxO4	forward	5’-CCTCCTGCTGATGTCCTCAT-3’
FoxO4	reverse	5’-TGCTGTGACTCAGGGATCTG-3’
qPCR Primers		
ASCL1	forward	5’-GCAACCGGGTCAAGTTGGT-3’
ASCL1	reverse	5’-GTCGTTGGAGTAGTTGGGGG-3’
Hes1	forward	5’-TTGCCTTTCTCATCCCCAAC-3’
Hes1	reverse	5’-AAGGTGACACTGCGTTAGGA-3’
Hes5	forward	5’-ACCAGCCCAACTCCAAGC-3’
Hes5	reverse	5’-GCCCTCGCTGTAGTCCTG-3’

NFIA	forward	5'-TTGCCATCTCCAAGCACACT-3'
NFIA	reverse	5'-GGTGATGCTGTGTGAATGCT-3'
NFIX	forward	5'-ATGCGGACATCAAACCACTG-3'
NFIX	reverse	5'-TCGCAACTGGAGTCTGTGAT-3'
Primers for cloning		
FoxG1	forward	5'-CAGCTCGAGTGATGCTGGACATGGGAG-3'
FoxG1	reverse	5'-CGTATCTAGAAAAACGTTCACTTACAGTCT-3'
mutFoxG1	forward	5'-CGTGAAGGTACCGTGCCACTACGACGA-3'
mutFoxG1	reverse	5'-TCGTCGTAGTGGCACGGTACCTTCACG-3'

4.1.6 Organisms

1F8 cells (derived from HEK 293 GPG ells)	Provided by the laboratory
C57/Bl6J	Harland Laboratories
E. Coli TOP10	Invitrogen
FoxO1/3/4$^{fl/fl}$	Provided by the laboratory
FoxO1/3/4$^{wt/wt}$	Provided by the laboratory
HEK 293T cells	Provided by the laboratory
Glast::CreER^{T2}/β-gal(Rosa26R)/FoxO1/3/4$^{fl/fl}$	Provided by the laboratory
Glast::CreER^{T2}/β-gal(Rosa26R)/FoxO1/3/4$^{wt/wt}$	Provided by the laboratory

4.1.7 Plasmids

pCAG GFP	expression vector, Amp^r	Zhao et al., 2006
pCAG GFP/CRE	expression vector, Amp^r	Tashiro et al., 2006
pCAG GFP-IRES-Cre	expression vector, Amp^r	Jagasia et al., 2009
pCAG IRES-mitodsRed	expression vector, Amp^r	Provided by the laboratory
pCAG FoxG1-IRES-GFP	expression vector, Amp^r	Provided by the laboratory
pCAG mutFoxG1-IRES-GFP	expression vector, Amp^r	Provided by the laboratory

pCAG RFP	expression vector, Amp^r	Zhao et al., 2006
pKSPS	pexpression vector, Amp^r	Provided by the laboratory

4.1.8 Buffers and solutions

Molecular biology solutions

Agar

Ready made LB agar	32 g/l
Ampicillin	75 µg/ml

TAE (50x)

Tris Base	242.0 g
Glacial acetic acid	57.1 ml
0.5 M EDTA (pH 8.0)	100.0 ml
H_2O	842.9 ml

Solutins for immunohisto- and immunocytochemistry

Blocking solution brain slices

Donkey serum	1.50 ml
10 % Triton X-100	1.25 ml
TBS	50.00 ml

Blocking solution cells

Donkey serum	0.50 ml
10 % Triton X-100	0.50 ml
TBS	50.00 ml

Borate buffer 0.1M (pH 8.5)

Boric acid (MW: 61.83 g/mol)	3.0915 g
H_2O	100 ml

Cryoprotectant solution

Glycin	250 ml
Ethylene glycol	250 ml

0.1 M Phosphate buffer	500 ml
HCl 2N	
32 % HCl	2.49 ml
H_2O	
	9.51 ml
PBS 10x (pH 7.2)	
NaCl	80.0 g
KCl	2.0 g
Na_2PO_4	14.4 g
KH_2PO_4	2.4 g
H_2O	
	800.0 ml
PFA 4% (pH 7.4 at RT)	
PFA (dissolved by heating)	40 g
0.2 M phosphate buffer	500 ml
NaOH	1-2 tablets
H_2O	500 ml
Phosphate buffer 0.2M	
Sodium phosphate monobasic	16.56 g
Sodium phosphate dibasic	65.70 g
H_2O	3 l
Sucrose 30% (4 °C)	
Sucrose	150 g
0.1 M phosphate buffer	500 ml
TBS 10x	
NaCl	80 g NaCl
KCl	2 g
1 M Tris/HCl (pH 7.5)	250 ml
H_2O	750 ml

Solutions for preparing and culturing of mouse neural stem cells

Dissociation media

Solution #1	5 ml
Trypsin	6.7 mg
Hyaluronidase	3.5 mg

Neurosphere media

DMEM F12 Glutamax	500 ml
B27 supplement	10 ml
PSF	5 ml
HEPES	8 mM

Solution #1

HBSS	50 ml
Glucose	2.7 g
HEPES	15 mM
H_2O	up to 500 ml, filter sterilized

Solution #2

HBSS	25 ml
Sucrose	154 g
H_2O	up to 500 ml, filter sterilized

Solution #3

HEPES	20 mM
BSA	20 g
EBSS	up to 500 ml, filter sterilized

Solutions for retrovirus preparation

1F8 medium

DMEM with high glucose/GlutaMax/Hepes	500 ml
FCS	50 ml
Sodium-Pyruvate (100x)	5 ml
Non-Essential-Amino-Acids (100x)	5 ml

Packaging medium	
DMEM with high glucose/GlutaMax/Hepes	500 ml
FCS	50 ml
Transfection medium	
Opti-MEM	500 ml
Viral resuspension buffer – TBS-5	
1 M Tris-HCl, pH7.8	20 ml
5 M NaCl	10.4 ml
1 M KCl	4 ml
1 M $MgCl_2$	2 ml
H_20	fill up to 400 ml, filter sterilized

4.1.9 Other material

24 well plates	Falcon
Aqua-Poly/Mount	Polysciences
Cellstar pipettes	Greiner bio-one
Counting chamber (0.0025 mm^2)	Neubauer
Cover slips	Menzel-Glaser
Cryoblock mounting medium	Medite Medizintechnik GmbH
Microliter syringes	Hamilton
Miniwells (60 wells)	Nunc
PCR tubes	Biozym
Reaction tube 15 ml	Falcon
Reaction tube 50 ml	Falcon
Round bottom tube 14ml	Falcon
Safe lock tube 1.5 ml	Eppendorf
Safe lock tube 2.0 ml	Eppendorf
Superfrost Plus microscope slides	Menzel-Glaser
Surgical disposable scalpels	Braun
Tissue culture dishes	
(100x20 mm)	Falcon
Tissue culture flasks	
(25 m^2, 75 m^2, 175 m^2)	BD BioCoat™

4.1.10 Equipment

Hardware

Centrifuge 5415 D	Eppendorf
Centrifuge 5417 R	Eppendorf
FACStar Plus	Becton Dickinson
Fluorescence microscope DMI 600B	Leica
HeraCell 150 incubator	Kendro
HeraCell Tissue Culture hood	Kendro
Leica SP5 confocal microscope	Leica
Micro4 controller	WPI
Mini Protean® Tetra Cell	Biorad
Nanoliter 2000	WPI
ND-1000 spectrophotometer (Nanodrop)	Peqlab
Powersupply	Biorad
Rotamax 150	Heidolph
Sliding microtome SM 2000R	Leica
Sorvall Evolution High Speed Centrifuge	Thermo Science
Stereotactic Instrument	WPI
Thermomixer comfort	Eppendorf
Zeiss LSM 710 confocal microscope	Zeiss

Software

ImageJ	NIH
Imaris 6.3	Bitplane
LAS AF 2.5	Leica
StepOne 2.0	Applied Biosystems
Vector NTI	Invitrogen
Zen 2010 B SP1	Zeiss

4.2 Methods

4.2.1 Plasmid production

Heat shock transformation of E. coli

With the objective of plasmid amplification, 100 µl competent E. coli cells (TOP10) were transformed with 1 µl of plasmid containing an ampicillin resistance. For this, cells were thawed on ice before DNA was added and incubated on ice for 15 min. Subsequent cells were heat-shocked at 42 °C for 45 sec and immediately placed back on ice for another 15 min. 1 ml LB medium was added and cells were incubated under agitation (350 rpm) at 37 °C for 1 h. After short centrifugation at 13,000 rpm, supernatant except for 100 µl was discarded with which cells were resuspended and plated on agar plates containing 75 µg/ml of ampicillin. Plates were incubated at 37 °C overnight.

Cultivation of bacteria and plasmid isolation

One colony of transformed E. coli (s. above) was picked from the agar plate and transferred into 200 ml LB-medium containing 100 µg/ml ampicillin. Cells were cultured at 350 rpm and 37 °C overnight. Cultures were processed with Pure Yield Plasmid Midiprep System following manufacturer's protocol except for better recovery the volume of resuspension and cell lysis solution were adjusted to 12 instead of 6 ml and of neutralization solution to 15 ml instead of 10 ml. Furthermore the centrifugation step after neutralization was extended to 30 min. For smaller culture volumes (5 ml) the NucleoSpin plasmid kit was used according to manufacture's protocol.

Determination of DNA concentration

Plasmid DNA concentration and quality was measured with a Nanodrop UV-spectrometer.

4.2.2 Molecular cloning

Cloning PCR reaction

Cloning of cDNA was performed by PCR reaction in an Eppendorf Thermocycler using iProof proof reading polymerase. The PCR reaction was set up according to manufacturer's protocol. Primers contained the gene specific 5' and 3' sequences

and specific restriction sites overhangs to allow cloning into the backbone of the shuttle vector pKSPS. Template cDNA was generated from total RNA extracts from the mouse dentate gyrus.

Restriction digest

For a restriction digest 0.5 µg plasmid DNA was mixed with 1 µl of the appropriate enzymes (20 U/µl) (NEB) and 2 µl of the matching buffer. The digest was adjusted to a total volume of 20 µl with water and incubated at 37°C for 2 h.

Analysis of restriction digest by agarose gel electrophoresis and gel purification

To separate and analyze DNA, agarose gel electrophoresis was performed. 1% agarose/TAE-gel was prepared by heating the solution in a microwave oven. To visualize DNA gels were supplemented with 0.02 µl/ml EtBr which allows the detection of nuleic acids at λ = 254 nm. The DNA solution was mixed with 6× loading dye in order to load it on the gel and the DNA fragments were subsequently separated in a constant electric field. The size of the DNA fragments was determined by loading 10 µl of 1 kb DNA ladder (prepared according to the provided protocol) on the gel with the specified digested samples. To isolate the appropriate DNA fragment, the gel was analyzed under UV-light and the correct band was excised with a scalpel. To purify DNA from the gel, NucleoSpin® Gel and PCR Clean-up was used according to the manufacturer's protocol and the DNA was eluted in 15 µl water. The concentration was measured as described above.

Ligation

To perform a ligation 2 µl T4-Ligase and 3 µl Ligase-buffer containing ATP were added to the appropriate mixture of digested backbone and insert. The proper ratio was calculated by the formula:

The reaction was adjusted to 30 µl with sterile water and incubated for 2 h at RT.

Transformation of bacteria with ligation product

To transform the ligated products in bacteria the protocol described before was used, but 15 µL of the ligation were added to bacteria, the heat shock time was extended up to 60 sec and all bacteria were plated on a LB-Amp plate after short centrifugation (1000 rcf).

Identification of positive clones

To identify positive clones, single colonies were picked from the plate and were cultivated in 3 mL overnight at 37 °C. After plasmid isolation, DNA was digested and analyzed by agarose gel electrophoresis.

4.2.3 RNA methods

RNA isolation and DNAse treatment

Total RNA was isolated from cells, micro-dissected dentate gyrus or whole hippocampus, by using RNeasy Mini-Kit according to the manufacturer's protocol. Tissue was homogenized by passing the lysate through a 20-gauge-needle fitted on a 1 mL RNAse-free syringe until complete dissociation. For homogenization of cells Qiashredder colums were used. Possible genomic DNA contamination was eliminated by on-column DNAse treatment using the RNAse-free DNAse-Set according to the manufacturer's protocol. Isolated RNA was eluted in 30 µL RNAse-free water and the concentration determined with a NanoDrop UV-spectrometer. RNA was immediately used for cDNA synthesis or stored at −80 °C.

cDNA synthesis

For cDNA-synthesis 300 ng of total RNA were adjusted with RNAse-free water to a volume of 12.5 µl. Fermentas RevertAid First Strand cDNA Synthesis Kit (Thermo Fisher Scientific) was used according to the manufacturer's protocol. If cDNA was synthesized for cloning, random hexamer primer were used, for quantitative real-time PCR (qPCR) cDNA synthesis was carried out using, oligo(dt)18 primer. cDNA was stored at −20 °C.

Quantitative real-time-PCR (qPCR)

Quantitative RT-PCR was performed using StepOnePlusTM Real-Time PCR System. Brilliant II Fast SYBR Green qPCR Master Mix was used for PCR reactions according to the manufacturer's protocol. qPCR primers were designed using the software's Primer3 (http://primer3.sourceforge.net) and NetPrimer (http://www.premierbiosoft.com). Amplicon sizes ranged from 100-250 bp. Suitability of qPCR Primer was analyzed by evaluation of melting curves and by determination of the efficiency via a standard curve. For quantitative expression analysis, the comparative CT (ΔΔCT) method was applied to determine the relative quantity of

target sequence using a reference sample (control) and an endogenous control target sequence.

4.2.4 Cell culture

Culturing of HEK 293T cells

HEK 293T-cells cells were cultured in DMEM (GIBCO/Invitrogen) supplemented with Antibiotic-Antimycotic (GIBCO/Invitrogen) and FBS (PAA, 100x). Cells were incubated at 37 °C with 5% CO2. 500 ml DMEM were supplemented with 5 mL PSF (GIBCO/Invitrogen) and 55 ml FBS (PAA). For splitting the cells, trypsin with EDTA (0.05%) (GIBCO/Invitrogen) was used.

Calciumchloride transfection

To test functionality of virus plasmids, HEK 293-T-cells were transfected. 50000 cells/well were plated on an uncoated but sterilized 24-well plate with glass cover slips. Transfection was performed on the next day when cells reached 80% confluency. 1 µg of DNA was adjusted to a volume of 547.5 µl sterile water. Then 77.5 µl $CaCl_2$ were added and mixed with a pipette. 625 µl of 2x HBSS were added slowly and drop wise while shaking. After waiting for approximately 3 min, 100 µl of transfection mix was put slowly in each well. Cells were fixed 48 h after transfection.

Preparation of neural stem cells from adult mouse brains

Animals were sacrificed via cervical dislocation, brains were kept in ice-cold PBS, SVZ and HC were isolated under a binocular microscope and kept also in ice-cold PBS. PBS was removed; the tissue was harshly resuspended in 5 ml dissociation media and incubated for a maximum of 30 min at 37°C. After 15 min the tissue was once more harshly resuspended. The dissociation reaction was stopped with 5 ml solution #3. Cells were passed through a 70µm strainer to remove the destroyed tissue. After centrifugation at 1000 rpm for 10 min supernatant was removed and cells resuspended in 10 ml ice-cold solution #2. Cells were centrifuged at 1500 rpm for 10 min, supernatant was removed and cells were resuspended in 2 ml ice-cold solution #3. The 2 ml cell solution was carefully added upon 12 ml ice cold solution #3 and centrifuged at 1000 rpm for 10 min. Supernatant was removed, cells resuspended in 8 ml neurosphere media with 160 µg EGF and FGF-2 (20 µg/ml) and cultured in a 25 m^2 tissue culture flask at 37 °C and 5% CO_2.

Passaging of mouse neural stem cells (neurospheres)

Neurospheres were centrifuged at 500 rpm for 5 min, supernatant (old medium) was removed and cells were resuspended in 1 ml Accutase ant incubated at 37°C for 5 min. After the 5 min cells were harshly resuspended by pipetting up and down to separate the neurospheres in single cells. After centrifugation at 1500 rpm for 5 min cells were washed two times with 5 ml PBS (resuspended in 5 ml PBS, centrifuged at 1500 rpm for 5 min). Cell pellet was resuspended in 1 ml neurosphere media and counted in a counting chamber. The cells were than diluted either in 8 ml (50000 cells, 25 cm^2 tissue culture flask), or in 20 ml (200000 cells, 75 cm^2 tissue culture flask) or in 40 ml (400000 cells, 175 cm^2 tissue culture flask) neurosphere media with 20 µg/ml EGF and FGF-2. Neurospheres were passaged on an average of seven days.

Single cell culture of neural stem cells – single cell neurosphere assay (NSA)

To culture a neurosphere out of a single neural stem cell, split neurospheres were diluted 1 cell/25 µl neurosphere media with 20 µg/ml GF's and seeded into the wells of a 60 well miniwell plate. The miniwell plates were stored in a 15 ml tissue culture plate with 3 ml tissue culture plates filled with Ampuwa to protect the miniwells from dehydration and incubated at 37°C and 5% CO_2. After seeding the cells into the miniwells the miniwells were examined under a binocular microscope/fluorescent microscope and the wells, which contained one, or two cells were marked. After seven days the marked miniwells were again examined under a binocular microscope/fluorescent microscope and the number of formed neurospheres was counted.

96-well-plate neurosphere assay (NSA)

Neurospheres were dissociated into single cells and seeded into wells of a 96-well-plate in a density of 200 cells per 200 µl of medium under proliferative conditions (+ growth factors). A minimum of 3 wells per condition and experimental group was used as technical replicates. After 7 days numbers of formed neurospheres were count under a binocular microscope/fluorescent microscope.

Differentiation of mouse neurospheres

For differentiation experiments 24-well plates with glass covers slips were coated by overnight incubation with 50µg/ml poly-D-Lysine/water at RT, and subsequent incubation with 5 µg/mL Laminin/DPBS at 37 °C overnight.

Neurospheres were dissociated and 100 000 cells/well were seeded in a 24-well plate containing coated cover slips to obtain monolayer cultures. Cells were cultivated without EGF and FGF-2 and fixed with 4% PFA/PBS after 4 days of differentiation.

Immunocytochemistry

After 3 times washing in PBS, cells were blocked with 1% donkey serum and 0.1% Triton-X-100 in PBS for 2h and following incubated with the respective primary antibodies diluted in blocking solution overnight at 4 °C. Cells were washed three times with PBS and blocked again for 30 min, and subsequently incubated with secondary antibodies at 4°C over night. After washing cells once with PBS, cells were put in PBS with Dapi (10 mg/ml) for 5 min and then washed a last time with PBS. Finally, glass cover slips with cells were mounted on slides using Aqua/PolyMount and stored at 4 °C till used for microscopy.

Retroviral transduction of mouse neural stem cells

Mouse neurospheres from FoxO1/3/4$^{fl/fl}$ mice were passaged as described above, cells were counted and resuspended in 2 ml culture medium. Virus particles of an GFP/Cre-expressing retrovirus or an only GFP-expressing retrovirus corresponding to the number of counted cells were added, the cells were incubated at 37°C for 30 min until the virus particles were inactive. 6 ml of culture medium was added for further growth. The infection was controlled after 4 - 7 days via fluorescence microscopy.

Genotyping of mouse neural stem cells

DNA-isolation

Neurospheres were centrifuged at 500 rpm for 5 min, supernatant removed and cells resuspended in 300 µl TE buffer. 300 µl cell lysis buffer (20 mM Tris pH 8.0, 4 mM EDTA, 20 mM NaCl, 1% SDS) containing 20 µl proteinase K (10 mg/ml) were added and incubated at 55°C for at least 5 hours. Afterwards DNA was extracted with 600 µl

Phenol, centrifuged at 13000 rpm for 5 min and the aqueous phase was transferred to a fresh eppendorf tube. DNA was further extracted with 600 µl Chloroform, again centrifuged at 13000 rpm for 5 min and aqueous phase transferred to a fresh eppendorf tube. The precipitation followed with 1.2 ml EtOH 75 mM NaAcetate for 30 min at 4°C. After centrifugation at 12000 rpm for 20 min at 4°C, supernatant was removed and DNA pellet resuspended in TE containing 20 µg/ml RNase A. The DNA was solved over night at 4 °C and stored for further use at -20°C.

PCR

For amplification of the DNA isolated from the cells polymerase chain reaction (PCR) was performed. DreamTaq Green Master Mix was used and prepared after following scheme (Table 4.1).

Table 4.1 Components of PCR Master Mix for genotyping.

[µl]	Per PCR sample
DreamTaq Master Mix 10x	2.5
DreamTaq Polymerase	0.2
$MgCl_2$	0,7
dNTPS (10mM)	0.1
H_2O	19
Fwd Primer (10 µM)	0.5
Fwd Primer (10 µM)	0.5
Rev Primer (10 µM)	0.5
Master Mix	19

For each sample 20 µl of the Master Mix were pipette into a PCR tube. 1 µl of previously prepared DNA (s. above) was added. The DNA fragment of interest to detect either the wildtype gene or the floxed gene or the cut out gene of FoxO1/FoxO3/Foxo4 was partially amplified in a PCR cycler using the corresponding fwd and rev primers (s. 4.1.5). Following PCR program was used (Table 4.2).

Table 4.2 PCR program for cell genotyping.

Step	Temperature [°C]	Duration
Start	95	15 min
32 cycles		
Denaturation	94	30 sec
Hybridisation	55	1 min
Elongation	72	1 min
72.0	6 min	
Stop	4.0	

Analysis by agarose gel electrophoresis

To detect the approx. 100 - 600 bp large DNA fragments, each PCR mix was loaded on a 2 % agarose gel. Per 100 ml gel 1.5 µl EtBr were added. The samples with a total volume of 25 µl were subsequently loaded on the gel together with 6 µl of a 100 bp DNA ladder. DNA fragments were separated by applying a constant electric field (120 V) for 30 - 45 min. The gel was analysed and photographed under UV-light. For the different possible genotypes following PCR product sizes were expected (Table 4.3).

Table 4.3 Expected sizes of the genotyping PCR products

genotype	wildtype [bp]	floxed [bp]	knocked out
FoxO1	115	149	190
FoxO3	100	138	186
FoxO4	313	555	471

4.2.5 FACsorting

Neurospheres, which were infected with either a GFP-expressing or GFP/Cre-expressing retrovirus (as under 4.2.4 described), had to be sorted via FACS (Fluorescence Activated Cell Sorting) to obtain a more or less homogenous GFP-positive cell population. That for neurospheres were passaged according to 4.2.4 and resuspended in 1 ml neurosphere media. The cell sorting was performed at a FacStar Plus FACsorter with the help of Dr. Wolfgang Beisker. After sorting the cells were cultured further as under 4.2.4 described.

4.2.6 Retrovirus preparation

The pCAG GFP, pCAG IRES-GFP, pCAG GFP-IRES-Cre and pCAG RFP retroviruses have been previously described (Jagasia et al., 2009; Tashiro et al., 2006; Zhao et al., 2006). CAG IRES-mitodsRed was generated from the pCAG IRES-GFP vector by replacing the GFP coding sequence with cDNA for mitochondrial targeted Dsred (mitoDsred). For retrovirus-mediated expression of mouse FoxG1 and a mutated form of FoxG1 (point mutation; mutFoxG1) their respective cDNAs were cloned into the pCAG IRES-GFP to generate pCAG FoxG1-IRES-GFP rsp. pCAG mutFoxG1-IRES-GFP. cDNA for mouse FoxG1 was synthesized from RNA isolated from mouse dentate gyrus, cloned via the shuttle vector pKSPS (pBluescript KS modified with a PmeI site near the KpnI site and a SfiI site next to the SacII site; from Fred Gage, Salk Institute, La Jolla, USA) into the retroviral pCAG IRES-GFP cassette. The mutated form of FoxG1 (point mutation; mutFoxG1) was obtained via the QuikChange® Site-Directed Mutagenesis Kit (Stratagene) according to manufacturer's protocol.

Retrovirus production was performed with HEK 293 GPG-1F8 cells (Ory et al., 1996), which constitutively express the gag and pol genes of MMLV. The VSVG gene is under the control of a tetracycline responsive promoter and can be induced upon withdrawal of tetracycline. The viral RNA is encoded by a transiently transfected minimal retroviral expression plasmid containing the 3' and 5' LTR of MMLV, the retroviral packaging signal Ψ, a primer binding site for the retroviral reverse transcriptase and the cDNA encoding the protein of interest. Cells were maintained in 1F8 growth medium under double-selection and Tet-repression: Geneticin (100 mg/ml) to select for integrated MMLV genome, puromycin (2 mg/ml) to select for integrated VSVG and doxycycline (10 µg/ml) to repress expression of the VSVG. For one approach, 150 µg of the retroviral plasmid of interest and 360 µl Lipofectamine 2000 (Invitrogen) both in 9 ml OptiMEM medium were mixed and added to the resuspended cells cultured in 2 to 3 175 cm2 flasks with 30 ml OptiMEM and 10 % FCS. Cells were seeded on six 10 cm plates. One day after transfection, medium was exchanged to packaging medium. Virus-containing supernatant was harvested four times (2 d, 4 d, 6 d and 8 d after transfection) and concentrated by two rounds of ultracentrifugation at 50,000 rcf (Tashiro et al., 2006).

To determine titers of the produced viruses, HEK 293T cells were plated on an uncoated but sterilized 24-well plate with glass cover slips (30000 cells/well). Different wells with cells were transduced 1 h later with the following volumes of virus: 0.01 µl, 0.005 µl. 0.001 µl and 0.0005 µl. Cells were fixed 72 h after transduction and number of colony forming units (cfu) quantified to calculate virus titers. Viral titers ranged between 1.0×10^8 and 1.0×10^{10} cfu × ml^{-1} (cfu ≙ colony forming units).

4.2.7 Animals and stereotactic injections

All experiments were carried out in accordance with the European Communities Council Directive (86/609/EEC). All mice were kept in a normal light dark-cycle (12 hours light/12 hours dark) and had free access to food and water. The age of the mice was 8 weeks. For FoxO1/3/4 loss-of-function experiments, male and female mice (8 weeks) FoxO1/3/4$^{fl/fl}$, FoxO1/3/4$^{wt/wt}$, Glast::CreER^{T2}/β-gal(Rosa26R)/FoxO1/3/4$^{fl/fl}$, Glast::CreER^{T2}/β-gal(Rosa26R)/FoxO1/3/4$^{wt/wt}$) mice (mixed FVBn/C57Bl6J background) were used. All other animal experiments were performed with 8-week-old female C57BL/6J mice.

Animal breeding strategies

FoxO1/3/4$^{fl/fl}$ mice: Mouse line with floxed alleles for FoxO1, FoxO3 and FoxO4 in FVB/N background was kindly obtained from Dr. Ronald A. DePinho (MD Anderson Cancer Center (Houston), University of Texas).

FoxO1/3/4$^{wt/wt}$ mice: FoxO1/3/4$^{fl/fl}$ mice were crossed with C57BL/6J mice. The heterozygous offspring FoxO1/3/4fl/wt was re-crossed with itself and homozygous FoxO1/3/4$^{fl/fl}$ mice and homozygous FoxO1/3/4$^{wt/wt}$ mice were used for further breedings of either FoxO1/3/4$^{fl/fl}$ mice or FoxO1/3/4$^{wt/wt}$ mice.

Glast::CreER^{T2}/β-gal(Rosa26R)/FoxO1/3/4$^{fl/fl}$ mice: FoxO1/3/4$^{fl/fl}$ mice as described previously (Paik et al., 2007) were crossed with Glast::CreER^{T2} (Mori et al., 2006) and Rosa26R beta-galactosidase (β-gal(Rosa26R)) mice (Nakamura et al., 2006).

Glast::CreER^{T2}/β-gal(Rosa26R)/FoxO1/3/4$^{wt/wt}$ mice: Glast::CreER^{T2}/β-gal(Rosa26R)/ FoxO1/3/4$^{fl/fl}$ mice were crossed with FVB/N mice. Heterozygous offspring was further re-crossed to obtain in the end Glast::CreER^{T2}/β-gal(Rosa26R) mice with wildtype alleles for FoxO1, FoxO3 and FoxO4.

Tailclip DNA isolation and genotyping

Tailclips were taken at the age of three weeks. 100 µl of 50 mM NaOH was added and incubated for 20 min at 99°C. After cooling down to 4°C 30 µl of 1 M Tris-HCl pH 7 was added. The resulting DNA mixture was directly used for genotyping or was stored at -20°C until further use.

Genotyping PCRs were performed with the primers described in 4.1.5.

DreamTaq Green Master Mix was used and prepared after following scheme (Table 4.3).

Table 4.3 Components of PCR Master Mix for genotyping.

[µl]	Per PCR sample
DreamTaq Master Mix 10x	2.5
DreamTaq Polymerase	0.2
$MgCl_2$	0,7
dNTPS (10mM)	0.5
H_2O	14.6
Fwd Primer (10 µM)	0.5
Fwd Primer (10 µM)	0.5
Rev Primer (10 µM)	0.5
Master Mix	20

For each sample 20 µl of the Master Mix were pipette into a PCR tube. 5 µl of previously prepared DNA (s. above) was added. Following PCR programs were used for the genotyping PCRs for FoxO1/3/4, Glast::CreER^{T2} and Rosa26R (Tables 4.4 to 4.6).

Table 4.4 PCR program for genotyping of the FoxO1/3/4 loci.

Step	Temperature [°C]	Duration
Start	95	15 min
35 cycles		
Denaturation	94	30 sec
Hybridisation	55	1 min
Elongation	72	1 min
72.0	6 min	
Stop	4.0	

Table 4.5 PCR program for genotyping of the Glast locus.

Step	Temperature [°C]	Duration
Start	94	2 min
35 cycles		
Denaturation	94	20 sec
Hybridisation	55	20 sec
Elongation	72	30 sec
72.0	5 min	
Stop	4.0	

Table 4.6 PCR program for genotyping of the Glast locus.

Step	Temperature [°C]	Duration
Start	95	4 min
35 cycles		
Denaturation	95	30 sec
Hybridisation	50	35 sec
Elongation	72	35 sec
72.0	10 min	
Stop	4.0	

Analysis by agarose gel electrophoresis

To detect the DNA fragments, each PCR mix was loaded on a 2 % agarose gel. Per 100 ml gel 1.5 µl EtBr were added. The samples with a total volume of 25 µl were subsequently loaded on the agarose gel together with 6 µl of a 100 bp DNA ladder. DNA fragments were separated by applying a constant electric field (120 V) for 30 - 45 min. The gel was analysed and photographed under UV-light. For the different possible genotypes following PCR product sizes were expected (Tables 4.7 to 4.9).

Table 4.7 Expected sizes of the genotyping PCR products of the FoxO loci.

genotype	wildtype [bp]	floxed [bp]	knocked out
FoxO1	115	149	190
FoxO3	100	138	186
FoxO4	313	555	471

Table 4.8 Expected sizes of the genotyping PCR products of the Glast locus.

genotype	[bp]
Glast WT	700
Glast::CreER^{T2}	300

Table 4.9 Expected sizes of the genotyping PCR products of the Rosa26 locus.

genotype	[bp]
Rosa26R WT	253
Rosa26R + β-gal gene	300

Tamoxifen injections

Tamoxifen injections were performed intra peritoneal twice a day for 5 consecutive days to induce the KO of FoxO1, FoxO3, and FoxO4 in Glast::CreERT2 / FoxO1/3/4$^{fl/fl}$ / β-gal(Rosa26) mice at an age of 8 weeks.

BrdU injections

For BrdU retention experiments, 50 g per kg bodyweight BrdU/0.9% NaCl was injected intra peritoneal once per day for 3 consecutive days.

Stereotactic injections

For stereotactic injections, mice were deeply anesthetized by injecting 350 µl of the following mixture: 0.05 mg/kg Fentanyl 5 mg/kg Midazolam and 0.5 mg/kg Medetomidine dissolved in 0.9% NaCl. Mice were stereotactically injected at a speed of 250 nl/minute with 0.9 µl the retroviruses with a titer of 2×10^8 cfu × ml^{-1} under standard housing condition and 1×10^8 cfu × ml^{-1} under running condition into the left and right dentate gyrus or RMS (coordinates from bregma for injections into the dentate gyrus: -1.9 anterior/posterior, ±1.6 medial/lateral, -1.9 dorsal/ventral from dura; coordinates from bregma for injections into the RMS: +2.3 mm anterior/posterior, ±0.8 mm medial/lateral, -2.9 mm dorsal/ventral from dura). Anesthesia was antagonized after surgery by injecting 400 µl of the following mixture: 0.1mg/kg Buprenorphine, 2.5 mg/kg Atipamezol and 0.5 mg/kg Flumazenil dissolved in 0.9% NaCl.

4.2.8 Tissue procedures

Animals were sacrificed using CO_2. Animals were transcardially perfused with approximately 100 ml PBS (pH 7.4) for 5 min followed by approximately 100 ml 4% paraformaldehyde (PFA/PBS) at the respective time points. Post fixation was performed in 4% PFA/PBS for 12 h at 4 °C and brains were subsequently transferred to a 30% sucrose solution. 50 µm and 100 µm thick coronal or sagittal brain sections were produced using a sliding microtome. Sections were stored in a cryoprotectant solution at −20 °C until further use.

4.2.9 Histology procedures

Appropriate free floating sections for staining were collected in 0.1 M phosphate buffer and rinsed 3 times (each 15 min) in TBS or PBS. Sections were blocked in TBS or PBS supplemented with 3% donkey serum and 0.25% Triton-X-100 for 2 h and then incubated with primary antibodies dissolved in blocking solution at 4 °C for 72 h. After washing 3 times in TBS or PBS (each 15 min) and blocking for 30 min, sections were incubated in blocking solution containing secondary antibodies over night at 4°C. Sections were rinsed again 3 times in TBS or PBS, one wash step containing Dapi (10 mg/ml). Sections were mounted using SuperFrost microscope slides and Aqua/PolyMount and stored at 4 °C.

For BrdU detection, sections were pretreated with 2 N HCl for 30 min at 37 °C followed by incubation in 0.1 M borate buffer two times for each 15 min and 90 min washing in TBS or PBS before staining.

4.2.10 Phenotyping of cells

To phenotype genetically manipulated cells, transduced cells were evaluated for the expression of stage specific markers. At least 50-100 cells from 4-6 sections of the same regions from at least 3 different animals were analyzed. For BrdU retention experiments, number of BrdU positive cells was quantified and the size of the dentate gyrus measured in 4-6 different sections from at least 3 animals.

4.2.11 Morphology analysis

Global morphology analysis

To analyze the overall size of a large number of cells, confocal images of the dentate gyrus from several sections were obtained with a 40x oil objective using a Leica TCS Sp5 confocal microscope (step size 0.8 µm, resolution 1024×1024). 50 double-transduced cells expressing the fluorescent markers (GFP and mitodsRed) per animal from at least 3 different animals were analyzed by measuring the maximum extension of the cell (distance soma to end of longest dendrite) and the maximum possible extension (distance soma to hippocampal fissure). By this normalizing the analysis to the specific hippocampus position. The cumulative distribution of the measured ratios was compared.

Cell specific analysis of cell length and complexity

To analyze detailed cell morphology, confocal images of double-transduced cells expressing the fluorescent markers (GFP and mitodsRed) were obtained with a 63x glycerol objective using Leica TCS Sp5 confocal microscope (step size 0.3 µm, resolution 1024×1024). 100 µm sections from the same hippocampal position were used to avoid differences due to truncated cells and different positioning, respectively. 15-20 cells per group from at least 3 different animals were analyzed. 3D reconstructions were obtained by using the Filament Tracer tool in Imaris and values for total dendritic length, number of branch points and number of sholl intersections compared.

Morphological analysis of synaptic integration

To analyze morphological synaptic integration of transduced cells, confocal images of at least 3 dendrites in the mid-third of the molecular layer from 3 different double-transduced cells from at least 3 different animals expressing the fluorescent markers (GFP and mito-dsRed) were obtained with a 63x glycerol objective using a Zeiss LSM 710 confocal microscope (step size 0.3 µm, resolution 1024x1024, 5x zoom). The GFP signal was enhanced in immunohistochemistry via sequential antibody stainings for GFP α chicken, goat α chicken IgY Biotin-conjugated and Streptavidin cconjugated Alexa 488. Length of dendrites was measured using ImageJ and number of dendritic spines quantified. Spine number was normalized to dendritic length and compared. To analyze maturation of spines, number of mushroom spines (spine head > 0.6 µm) was quantified and percentage of total spine number calculated.

Analysis of mitochondrial volume and number

Mitochondria volumes were analyzed by reconstruction of mitochondria using the surface tool in Imaris in the same confocal images that were used for the morphology analyses. Mitochondria number and volume was reconstructed from the mito-dsRed fluorescence. Laser intensity was set to the same signal saturation.

4.2.12 Statistics

Graphs show values ± standard deviation (SD). Significance was determined in general with Student's t-test or certain experiments with Two-Way-Anova and indicated with * for $p < 0.05$, ** for $p < 0.01$ and *** for $p < 0.001$.

5 References

Ables, J.L., Decarolis, N.A., Johnson, M.A., Rivera, P.D., Gao, Z., Cooper, D.C., Radtke, F., Hsieh, J. & Eisch, A.J. (2010): Notch1 is required for maintenance of the reservoir of adult hippocampal stem cells. *J. Neurosci.*, **30**, 10484-10492.

Ahn, S. & Joyner, A.L. (2005): In vivo analysis of quiescent adult neural stem cells responding to Sonic hedgehog. *Nature*, **437**, 894-897.

Altman, J. (1962): Are new neurons formed in the brains of adult mammals? *Science*, **135**,1127–1128.

Altman, J. (1963): Autoradiographic investigation of cell proliferation in the brains of rats and cats. Postnatal growth and differentiation of the mammalianss brain, with implications for a morphological theory of memory. *Anat. Rec.*, **145**, 573-581.

Altman, J. & Das, G.D. (1965): Autoradiographic and histological evidence of postnatal hippocampal neurogenesis in rats. *J. Comp. Neurol.*, **124**, 319-335.

Altman, J, & Das, G.D. (1966): Autoradiographic and histological studies of postnatal neurogenesis I. A longitudinal investigation of the kinetics, migration and transformation of cells incorporating tritiated thymidine in neonate rats, with special reference to postnatal neurogenesis in some brain regions. *J. Comp. Neurol.*, **126**, 337-390.

Altman, J. (1969): Autoradiographic and histological studies of postnatal neurogenesis IV. Cell proliferation and migration in the anterior forebrain, with special reference to persisting neurogenesis in the olfactory bulb. *J. Comp. Neurol.*, **137**, 433-458.

Alvarez-Buylla, A., & Garcia-Verdugo, J.M. (2002): Neurogenesis in adult subventricular zone. *J. Neurosc.*, **22**, 629-634.

Amaral, D. G. & Witter, M. P. (1989): The three-dimensional organization of the hippocam- pal formation: a review of anatomical data. *Neuroscience*, **31**, 571–591.

Andelman, F., Hoofien, D., Goldberg, I., Aizenstein, O. & Neufeld, M.Y. (2010): Bilateral hippocampal lesion and a selective impairment of the ability for mental time travel. *Neurocase*, **16**, 426-35.

Andersen, P. (2007): The hippocampus book. Oxford: Oxford Univ. Pr.

Anselmi, C.V., Malovini, A., Roncarati, R., Novelli, V., Villa, F., Condorelli, G., Bellazzi, R. & Puca, A.A. (2009): Association of the FOXO3A locus with extreme longevity in a southern Italian centenarian study. *Rejuvenation Res.*, **12**, 95-104.

Arden, K.C. (2007): FoxOs in tumor suppression and stem cell maintenance. *Cell*, **128**, 235-237.

Ariani F, Hayek G, Rondinella D, Artuso R, Mencarelli MA, Spanhol-Rosseto A, Pollazzon M, Buoni S, Spiga O, Ricciardi S, Meloni I, Longo I, Mari F, Broccoli V, Zappella M, Renieri A. (2008): FOXG1 is responsible for the congenital variant of Rett syndrome. *Am J Hum Genet.*, **83**, 89-93.

Bahi-Buisson, N., Nectoux, J., Girard, B., Van Esch, H., De Ravel, T., Boddaert, N., Plouin, P., Rio, M., Fichou, Y., Chelly, J. & Bienvenu, T. (2010): Revisiting the phenotype associated with FOXG1 mutations: two novel cases of congenital Rett variant. *Neurogenetics*, **11**, 241-249.

Bakker, W.J., Blázquez-Domingo, M., Kolbus, A., Besooyen, J., Steinlein, P., Beug, H., Coffer, P.J., Löwenberg, B., von Lindern, M. & van Dijk, T.B. (2004): FoxO3a regulates erythroid differentiation and induces BTG1, an activator of protein arginine methyl transferase 1. *J. Cell Biol.*, **164**, 175-84.

Barry, G., Piper, M., Lindwall, C., Moldrich, R., Mason, S., Little, E., Sarkar, A., Tole, S., Gronostajski, R.M. & Richards, L.J. (2008): Specific glial populations regulate hippocampal morphogenesis. *J. Neurosci.*, **28**, 12328-12340.

Battista, D., Ferrari, C.C., Gage, F.H. & Pitossi, F.J. (2006): Neurogenic niche modulation by activated microglia: transforming growth factor beta increases neurogenesis in the adult dentate gyrus. *Eur. J. Neurosci.*, **23**, 83-93.

Beckervordersandforth, R., Tripathi, P., Ninkovic, J., Bayam, E., Lepier, A., Stempfhuber, B., Kirchhoff, F., Hirrlinger, J., Haslinger, A., Lie, D.C., Beckers, J., Yoder, B., Irmler, M. & Götz, M. (2010): In vivo fate mapping and expression analysis reveals molecular hallmarks of prospectively isolated adult neural stem cells. *Cell Stem Cell*, **7**, 744-758.

Belluizzi, O., Benedusi, M., Ackman, J. & LoTurco, J.J.(2003): Electrophysiological differentiation of new neurons in the olfactory bulb. *J. Neurosci.*, **23**, 10411-10418.

Bertrand, N., Castro, D.S. & Guillemot, F. (2002): Proneural genes and the specification of neural cell types. *Nat. Rev. Neurosci.*, **3**, 517-530.

Besson, A., Dowdy, S.F. & Roberts, J.M. (2008): CDK inhibitors: cell cycle regulators and beyond. *Dev. Cell*, **14**, 159–169.

Biggs, W.H. 3rd, Meisenhelder, J., Hunter, T., Cavenee, W.K. & Arden, K.C. (1999): Protein kinase B/Akt-mediated phosphorylation promotes nuclear exclusion of the winged helix transcription factor FKHR1. Proc. Natl. Acad. Sci. USA, 22, 7421-7426.

Bonaguidi, M.A., Peng, C., McGuire, T., Falciglia, G., Gobeske, K.T., Czeisler, C. & Kessler, J.A. (2008): Noggin expands neural stem cells in the adult hippocampus. *J. Neurosci.*, **28**, 9194-91204.

Bonaguidi, M.A., Wheeler, M.A., Shapiro, J.S., Stadel, R.P., Sun, G.J., Ming, G.L. & Song, H. (2011): In vivo clonal analysis reveals self-renewing and multipotent adult neural stem cell characteristics. *Cell*, **145**, 1142-55.

Bourguignon, C., Li, J. & Papalopulu, N. (1998): XBF-1, a winged helix transcription factor with dual activity, has a role in positioning neurogenesis in Xenopus competent ectoderm. *Development*, **125**, 4889-4900.

Bracko, O., Singer, T., Aigner, S., Knobloch, M., Winner, B., Ray, J., Clemenson, G.D. Jr., Suh, H., Couillard-Despres, S., Aigner, L., Gage, F.H. & Jessberger, S. (2012): Gene expression profiling of neural stem cells and their neuronal progeny reveals IGF2 as a regulator of adult hippocampal neurogenesis. *J. Neurosci.*, **32**, 3376-3387.

Brancaccio, M., Pivetta, C., Granzotto, M., Filippis, C. & Mallamaci, A. (2010): Emx2 and Foxg1 inhibit gliogenesis and promote neuronogenesis. *Stem Cells*, **28**, 1206-1218.

Brandt, M.D., Jessberger, S., Steiner, B., Kronenberg, G., Reuter, K., Bick-Sander, A., von der Behrens, W. & Kempermann, G. (2003): Transient calretinin expression defines early postmitotic step of neuronal differentiation in adult hippocampal neurogenesis of mice. *Mol. Cell Neurosci.*, **24**, 603-613.

Breunig, J.J., Silbereis, J., Vaccarino, F.M., Sestan, N. & Rakic, P. (2007): Notch regulates cell fate and dendrite morphology of newborn neurons in the postnatal dentate gyrus. *Proc. Natl. Acad. Sci. USA*, **104**, 20558–20563.

Brown, J., Cooper-Kuhn, C.M., Kempermann, G., Van Praag, H., Winkler, J., Gage, F.H. & Kuhn, H.G. (2003): Enriched environment and physical activity stimulate hippocampal but not olfactory bulb neurogenesis. *Europ. J. Neurosci.*, **17**, 2042–2046.

Brunet, A., Bonni, A., Zigmond, M.J., Lin, M.Z., Juo, P., Hu, L.S., Anderson, M.J., Arden, K.C., Blenis, J. & Greenberg, M.E. (1999): Akt promotes cell survival by phosphorylating and inhibiting a Forkhead transcription factor. *Cell*, **96**, 857-868.

Brunet, A., Sweeney, L.B., Sturgill, J.F., Chua, K.F., Greer, P.L., Lin, Y., Tran, H., Ross, S.E., Mostoslavsky, R., Cohen, H.Y., Hu, L.S., Cheng, H.L., Jedrychowski, M.P., Gygi, S.P., Sinclair, D.A., Alt, F.W. & Greenberg, M.E. (2004): Stress-dependent regulation of FOXO transcription factors by the SIRT1 deacetylase. *Science*, **303**, 2011–2015.

Brunetti-Pierri, N., Paciorkowski, A.R., Ciccone, R., Della Mina, E., Bonaglia, M.C., Borgatti, R., Schaaf, C.P., Sutton, V.R., Xia, Z., Jelluma, N., Ruivenkamp, C., Bertrand, M., de Ravel, T.J., Jayakar, P., Belli, S., Rocchetti, K., Pantaleoni, C., D'Arrigo, S., Hughes, J., Cheung S.W., Zuffardi, O. & Stankiewicz, P. (2011): Duplications of FOXG1 in 14q12 are associated with developmental epilepsy, mental retardation, and severe speech impairment. *Eur. J. Hum. Genet.*, **19**, 102-107.

Brunk, U.T. & Terman, A. (2002): The mitochondrial-lysosomal axis theory of aging: accumulation of damaged mitochondria as a result of imperfect autophagocytosis. *Eur. J. Biochem.*, **269**, 1996-2002.

Buckwalter, M.S., Yamane, M., Coleman, B.S., Ormerod, B.K., Chin, J.T., Palmer, T. & Wyss-Coray, T. (2006): Chronically increased transforming growth factor-beta1 strongly inhibits hippocampal neurogenesis in aged mice. *Am. J. Pathol.*, **169**, 154-164.

Calnan, D.R. & Brunet, A. (2008): The FoxO code. *Oncogene*, **27**, 2276-2288.

Cecchi, G.A., Petreanu, L.T., Alvarez-Buylla, A., & Magnasco, M.O. (2001). Unsupervised learning and adaptation in a model of adult neurogenesis. *J. Comput. Neurosci.*, ***11***, 175-182.

Chan, D.C. (2006): Mitochondrial fusion and fission in mammals. *Annu. Rev. Cell. Dev. Biol.*, **22**, 79-99.

Chen, H., Thiagalingam, A., Chopra, H., Borges, M.W., Feder, J.N., Nelkin, B.D., Baylin, S.B. & Ball, D.W. (1997): Conservation of the Drosophila lateral inhibition pathway in human lung cancer: a hairy-related protein (HES-1) directly represses achaete-scute homolog-1 expression. *Proc. Natl. Acad. Sci. USA*, **94**, 5355-5360.

Cheng, A., Hou, Y. & Mattson, M.P. (2010): Mitochondria and neuroplasticity. *ASN Neuro.*, **2**, e00045.

Christensen, R., de la Torre-Ubieta, L., Bonni, A. & Colón-Ramos, D.A. (2011): A conserved PTEN/FOXO pathway regulates neuronal morphology during C. elegans development. *Development*, **138**, 5257-5267.

Chung, W.J., Kindler, S., Seidenbecher, C. & Garner, C.C. (1996): MAP2a, an alternatively spliced variant of microtubule associated protein 2. *J. Neurochem.*, **66**, 1273-1281.

Clelland, C.D., Choi, M., Romberg, C., Clemenson, G.D. Jr., Fragniere, A., Tyers, P., Jessberger, S., Saksida, L.M., Barker, R.A., Gage, F.H. & Bussey, T.J. (2009): A functional role for adult hippocampal neurogenesis in spatial pattern separation. *Science*, **325**, 210-213.

Couillard-Despres, S., Winner, B., Schaubeck, S., Aigner, R., Vroemen, M., Weidner, N., Bogdahn, U., Winkler, J., Kuhn, H.G. & Aigner, L. (2005): Doublecortin expression levels in adult brain reflect neurogenesis. *Eur. J. Neurosci.*, **21**, 1-14.

Cowles, M.W., Brown, D.D., Nisperos, S.V., Stanley, B.N., Pearson, B.J. & Zayas, R.M. (2013): Genome-wide analysis of the bHLH gene family in planarians identifies factors required for adult neurogenesis and neuronal regeneration. *Development*, **140**, 4691-4702.

Creer, D.J., Romberg, C., Saksida, L.M., van Praag, H. & Bussey, T.J. (2010): Running enhances spatial pattern separation in mice. *Proc. Natl. Acad. Sci. USA*, **107**, 2367-2372.

Danesin, C., Peres, J.N., Johansson, M., Snowden, V., Cording, A., Papalopulu, N. & Houart, C. (2009): Integration of telencephalic Wnt and hedgehog signaling center activities by Foxg1. *Dev Cell.*, **16**, 576-587.

Dastidar, S.G., Landrieu, P.M. & D'Mello, S.R. (2011): FoxG1 promotes the survival of postmitotic neurons. *J. Neurosci.*, **31**, 402-413.

Dastidar, S.G., Narayanan, S., Stifani, S. & D'Mello, S.R. (2012): Transducin-like enhancer of Split-1 (TLE1) combines with Forkhead box protein G1 (FoxG1) to promote neuronal survival. *J. Biol. Chem.*, **287**, 14749-14759.

David, L., Mallet, C., Keramidas, M., Lamandé, N., Gasc, J.M., Dupuis-Girod, S., Plauchu, H., Feige, J.J. & Bailly, S. (2008): Bone morphogenetic protein-9 is a circulating vascular quiescence factor. *Circ. Res.*, **102**, 914-922.

David, D.J., Samuels, B.A., Rainer, Q., Wang, J.W., Marsteller, D.,Mendez, I., Drew, M., Craig, D.A., Guiard, B.P., Guilloux, J.P., Artymyshyn, R.P., Gardier, A.M., Gerald, C., Antonijevic, I.A., Leonardo, E.D. & Hen, R. (2009): Neurogenesis-dependent and –independent effects of fluoxetine in an animal model of anxiety/depression. *Neuron*, **62**, 479–493.

de la Torre-Ubieta, L., Gaudillière, B., Yang, Y., Ikeuchi, Y., Yamada, T., DiBacco, S., Stegmüller, J., Schüller, U., Salih, D.A., Rowitch, D., Brunet, A. & Bonni, A. (2010): A FOXO-Pak1 transcriptional pathway controls neuronal polarity. *Genes Dev.*, **24**, 799-813.

DeCarolis, N.A., Mechanic, M., Petrik, D., Carlton, A., Ables, J.L., Malhotra, S., Bachoo, R., Götz, M., Lagace, D.C. & Eisch, A.J. (2013): In vivo contribution of nestin- and GLAST-lineage cells to adult hippocampal neurogenesis. *Hippocampus*, **23**, 708-719.

Deneen, B., Ho, R., Lukaszewicz, A., Hochstim, C.J., Gronostajski, R.M. & Anderson, D.J. (2006): The transcription factor NFIA controls the onset of gliogenesis in the developing spinal cord. *Neuron*, **52**, 953-68.

Deng, W., Saxe, M.D., Gallina, I.S. & Gage, F.H. (2009): Adult-born hippocampal dentate granule cells undergoing maturation modulate learning and memory in the brain. *J. Neurosci.*, **29**, 532-542.

Dijkers, P.F., Medema, R.H., Lammers, J.W., Koenderman, L. & Coffer, P.J. (2000): Expression of the pro-apoptotic Bcl-2 family member Bim is regulated by the forkhead transcription factor FKHR-L1. *Curr. Biol.*, **10**, 1201–1204.

Dijkers, P.F., Medema, R.H., Pals, C., Banerji, L., Thomas, N.S., Lam, E.W., Burgering, B.M., Raaijmakers, J.A., Lammers, J.W., Koenderman, L. & Coffer, P.J. (2000a): Forkhead transcription factor FKHR-L1 modulates cytokine-dependent transcriptional regulation of p27(KIP1). Mol. Cell Biol., 20, 9138-9148.

Doetsch, F. & Alvarez-Buylla, A. (1996): Network of tangential pathways for neuronal migration in adult mammalian brain. *Proc. Natl. Acad. Sci. USA*, **93**, 14895–14900.

Doetsch, F., García-Verdugo, J.M. & Alvarez-Buylla, A. (1997): Cellular composition and three-dimensional organization of the subventricular germinal zone in the adult mammalian brain. *J. Neurosci.*, **17**, 5046-5061.

Doetsch, F., Verdugo, J.M.G., Caille, I., Alvarez-Buylla, A., Chao, M.V. & Casaccia-Bonnefil, P. (2002): Lack of the cell-cycle inhibitor p27Kip1 results in selective increase of transit-amplifying cells for adult neurogenesis. *J. Neurosci.*, **22**, 2255-2264.

Doetsch, F., & Hen, R. (2005). Young and excitable: the function of new neurons in the adult mammalian brain. *Curr. Opin. Neurobiol.*, **15**, 121-128.

Duan, X., Chang, J.H., Ge, S., Faulkner, R.L., Kim, J.Y., Kitabatake, Y., Liu, X.B., Yang, C.H., Jordan, J.D., Ma D.K., Liu, C.Y., Ganesan, S., Cheng, H.J., Ming, G.L., Lu, B. & Song, H. (2007): Disrupted-In-Schizophrenia 1 regulates integration of newly generated neurons in the adult brain. *Cell*, **130**, 1146–1158.

Duggan, C.D., DeMaria, S., Baudhuin, A., Stafford, D. & Ngai, J. (2008): Foxg1 is required for development of the vertebrate olfactory system. *J. Neurosci.*, **28**, 5229-5239.

Guillemot, F. (2007): Spatial and temporal specification of neural fates by transcription factor codes. *Development*, **134**, 3771-3780.

Ehm, O., Göritz, C., Covic, M., Schäffner, I., Schwarz, T.J., Karaca, E., Kempkes, B., Kremmer, E., Pfrieger, F.W., Espinosa, L., Bigas, A., Giachino, C., Taylor, V., Frisén, J. & Lie, D.C. (2010): RBPJkappa-dependent signaling is essential for long-term maintenance of neural stem cells in the adult hippocampus. *J. Neurosci.*, **30**, 13794-807.

Eidinoff, M.L., Cheong, L., Rich, M.A. (1959): Incorporation of unnatural pyrimidine bases into deoxyribonucleic acid of mammalian cells. *Science*, **129**, 1550-1551.

Ekholm, S. V., & Reed, S.I. (2000): Regulation of G(1) cyclin-dependent kinases in the mammalian cell cycle. *Curr. Opin. Cell Biol.*, **12**, 676-684.

Eng, L. F., Vanderhaeghen, J. J., Bignami, A., and Gerstl, B. (1971): An acidic protein isolated from fibrous astrocytes. *Brain Res.*, **28**, 351-354.

Eriksson, P.S., Perfilieva, E., Bjork-Eriksson, T., Alborn, A.M., Nordborg, C., Peterson, D.A., Gage, F.H. (1998): Neurogenesis in the adult human hippocampus. *Nat. Med.*, **4**, 1313-1317.

Essers, M.A., Weijzen. S., de Vries-Smits, A.M., Saarloos, I., de Ruiter, N.D., Bos, J.L. & Burgering, B.M. (2004): FOXO transcription factor activation by oxidative stress mediated by the small GTPase Ral and JNK. EMBO J., **23**, 4802-4812.

Ewan, K.B., Oketch-Rabah, H.A., Ravani, S.A., Shyamala, G., Moses, H.L. & Barcellos-Hoff, M.H. (2005): Proliferation of estrogen receptor-alpha-positive mammary epithelial cells is restrained by transforming growth factor-beta1 in adult mice. *Am. J. Pathol.*, **167**, 409-417.

Fasano, C.A., Phoenix, T.N., Kokovay, E., Lowry, N., Elkabetz, Y., Dimos, J.T., Lemischka, I.R., Studer, L. & Temple, S. (2009): Bmi-1 cooperates with Foxg1 to maintain neural stem cell self-renewal in the forebrain. *Genes Dev.*, **23**, 561-574.

Favaro, R., Valotta, M., Ferri, A.L., Latorre, E., Mariani, J., Giachino, C., Lancini, C., Tosetti, V., Ottolenghi, S., Taylor, V. & Nicolis, S.K. (2009): Hippocampal development and neural stem cell maintenance require Sox2-dependent regulation of Shh. *Nat. Neurosci.*, **12**, 1248-1256.

Ferri, A.L., Cavallaro, M., Braida, D., Di Cristofano, A., Canta, A., Vezzani, A., Ottolenghi, S., Pandolfi, P.P., Sala, M., DeBiasi, S. & Nicolis, S.K. (2004): Sox2 deficiency causes neurodegeneration and impaired neurogenesis in the adult mouse brain. *Development*, **131**, 3805-3819.

Finkel, T. & Holbrook, N.J. (2000): Oxidants, oxidative stress and the biology of ageing. *Nature*, **408**, 239-247.

Flachsbart, F., Caliebe, A., Kleindorp, R., Blanché, H., von Eller-Eberstein, H., Nikolaus, S., Schreiber, S. & Nebel, A. (2009): Association of FOXO3A variation with human longevity confirmed in German centenarians. *Proc. Natl. Acad. Sci. USA*, **106**, 2700-2705.

Flanders, K.C., Kim, E.S. & Roberts, A.B. (2001): Immunohistochemical expression of Smads1-6 in the 15-day gestation mouse embryo: signaling by BMPs and TGF-βs. *Dev. Dyn.*, **220**, 141-154.

Fukuda, S., Kato, F., Tozuka, Y., Yamaguchi, M., Miyamoto, Y., & Hisatsune, T. (2003). Two distinct subpopulations of nestin-positive cells in adult mouse dentate gyrus. *J. Neurosci.*, **23**, 9357–9366.

Fukuda, T., Itoh, M., Ichikawa, T., Washiyama, K. & Goto, Y. (2005): Delayed maturation of neuronal architecture and synaptogenesis in cerebral cortex of Mecp2-deficient mice. *J. Neuropathol. Exp. Neurol.*, **64**, 537-544.

Furukawa-Hibi, Y., Yoshida-Araki, K., Ohta, T., Ikeda, K. & Motoyama, N. (2002): FoxO forkhead transcription factors induce G2-M checkpoint in response to oxidative stress. *J. Bio. Chem.*, **277**, 26729-26732.

Furukawa-Hibi, Y., Kobayashi, Y, Cen, C. & Motoyama, N. (2005): FoxO transcription factors in cell-cycle regulation and the response in oxidative stress. *Antioxidants & Redox Signaling*, **7**, 752-760.

Furuyama, T., Nakazawa, T., Nakano, I. & Mori, N. (2000): Identification of the differential distribution patterns of mRNA and consensus binding sequences for mouse DAF-16 homologues. *Biochem. J.*, **349**, 629-634.

Furuyama, T., Kitayama, K., Shimoda, Y., Ogawa, M., Sone, K., Yoshida-Araki, K., Hisatsune, H., Nishikawa, S., Nakayama, K., Ikeda, K., Mozoyama, N. & Mor, N. (2004): Abnormal angiogenesis in FoxO1 (Fkhr)- deficient mice. *J. Biol. Chem.*, **279**, 34741-34749.

Gage, F.H. (2000): Mammalian neural stem cells. *Science*, **287**, 1433-1438.

Gage, F.H., Kempermann, G. & Song, H. (2008) Adult neurogenesis. Cold Spring Harbor, NY: Cold Spring Harbor Laboratory Press.

Gao, Z., Ure, K., Ables, L., Lagace, D.C., Nave, K.A:, Goebbels, S., Eisch, A.J. & Hsieh, J. (2009): NeuroD1 is essemtial for the survival and maturation of adult-born neurons. *Nat. Neurosci.*, **12**, 1090-1092.

Gao, Z., Ure, K., Ding, P., Nashaat, M., Yuan, L., Ma, J., Hammer, R.E. & Hsieh, J. (2011): The master negative regulator REST/NRSF controls adult neurogenesis by restraining the neurogenic program in quiescent stem cells. J. Neurosci., 31, 9772-9786.

Ge S, Goh EL, Sailor KA, Kitabatake Y, Ming GL, Song H. (2006): GABA regulates synaptic integration of newly generated neurons in the adult brain. *Nature*, **439**, 589–593.

Ge, S., Yang, C.H., Hsu, K.S., Ming, G.L. & Song, H. (2007): A critical period for enhanced synaptic plasticity in newly generated neurons of the adult brain. Neuron, *2007*, **54**, 559-566.

Ge, S., Sailor, K.A., Ming, G.L. & Song, H. (2008): Synaptic integration and plasticity of new neurons in the adult hippocampus. *J. Physiol.*, **586**, 3759-3765.

Gil-Perotin, S., Haines, J.D., Kaur, J., Marin-Husstege, M., Spinetta, M.J., Kim, K.H., Duran-Moreno, M., Schallert, T., Zindy, F., Roussel, M.F., Garcia-Verdugo, J.M. & Casaccia, P. (2011): Roles of p53 and p27(Kip1) in the regulation of neurogenesis in the murine adult subventricular zone. *Eur. J. Neurosci.*, **34**, 1040-1052.

Gilbert, P.E., Kesner, R.P. & Lee, I. (2001): Dissociating hippocampal subregions: double dissociation between dentate gyrus and CA1. *Hippocampus*, **11**, 626-636.

Gilley, J., Coffer, P.J. & Ham, J. (2003): FOXO transcription factors directly activate bim gene expression and promote apoptosis in sympathetic neurons. *J. Cell Biol*., **162**, 613–622.

Gold, A.E.,& Kesner, R.P. (2005): The role of the CA3 subregion of the dorsal hippocampus in spatial pattern completion in the rat. *Hippocampus*, **15**, 808–814.

Gómez-Pinilla, F., Dao, L. & So, V. (1997): Physical exercise induces FGF-2 and its mRNA in the hippocampus. *Brain Research*, **764**, 1–8.

Gómez-Skarmeta, J.L., de la Calle-Mustienes, E., Modolell, J. & Mayor, R. (1999): Xenopus brain factor-2 controls mesoderm, forebrain and neural crest development. *Mech. Dev.*, **80**, 15-27.

Gould, E., Reeves, A.J., Fallah, M., Tanapat, P., Gross, C.G. & Fuchs, E. (1999a): Hippocampal neurogenesis in adult old world primates. *Proc. Natl. Acad. Sci. USA*, **69**, 5263-5267.

Grasby, P.M., Frith, C.D., Friston, K., Frackowiak, R.S. & Dolan, R.J. (1993): Activation of the human hippocampal formation during auditory-verbal long-term memory function. *Neurosci. Lett.*, **163**, 185-188.

Greer, E.L., Oskoui, P.R., Banko, M.R., Maniar, J.M., Gygi, M.P., Gygi, S.P., Brunet, A. (2007): The energy sensor AMP-activated protein kinase directly regulates the mammalian FOXO3 transcription factor. *J. Biol. Chem.*, **282**, 30107-30119.

Groszer, M., Erickson, R., Scripture-Adams, D.D., Lesche, R., Trumpp, A., Zack, J.A., Kornblum, H.I., Liu X, & Wu, H. (2001): Negative regulation of neural stem/progenitor cell proliferation by the Pten tumor suppressor gene in vivo. *Science*, **7**, 2186-2189.

Guerrini, R. & Parrini, E. (2012): Epilepsy in Rett syndrome, and CDKL5- and FOXG1-gene-related encephalopathies. *Epilepsia*, **53**, 2067-2078.

Hanashima, C., Shen, L., Li ,S.C. & Lai, E. (2002): Brain factor-1 controls the proliferation and differentiation of neocortical progenitor cells through independent mechanisms. *J. Neurosci.*, **22**, 6526–6536.

Hanashima, C., Li, S.C., Shen, L., Lai, E. & Fishell, G. (2004): Foxg1 suppresses early cortical cell fate. *Science*, **303**, 56–59.

Hannenhalli, S. & Kaestner, K.H. (2009): The evolution of Fox genes and their role in development and disease. *Nat. Rev. Genet.*, **10**, 233-240.

Harris, L., Dixon, C., Cato, K., Heng, Y.H., Kurniawan, N.D., Ullmann, J.F., Janke, A.L., Gronostajski, R.M., Richards, L.J., Burne, T.H. & Piper M. (2013): Heterozygosity for nuclear factor one x affects hippocampal-dependent behaviour in mice. *PLoS One*, **8**, e65478.

Hastings, N.B. & Gould, E. (1999): Rapid extension of axons into the CA3 region by adult-generated granule cells. *J. Comp. Neurol.*, **41**, 146-154.

Hatini, V., Tao, W. & Lai, E. (1994): Expression of winged helix genes, BF-1 and BF-2, define adjacent domains within the developing forebrain and retina. *J. Neurobiol.*, **25**, 1293-309.

Hatini, V., Huh, S.O., Herzlinger, D., Soares, V.C. & Lai, E. (1996): Essential role of stromal mesenchyme in kidney morphogenesis revealed by targeted disruption of Winged Helix transcription factor BF-2. *Genes Dev.*, **10**, 1467-1478.

Heng, Y.H., McLeay, R.C., Harvey, T.J., Smith, A.G., Barry, G., Cato, K., Plachez, C., Little, E., Mason, S., Dixon, C., Gronostajski, R.M., Bailey, T.L., Richards, L.J. & Piper, M. (2012): NFIX Regulates Neural Progenitor Cell Differentiation During Hippocampal Morphogenesis. *Cereb. Cortex.*, doi:10.1093/cercor/bhs307.

Ho, K.K., Myatt, S.S. & Lam, E.W. (2008): Many forks in the path: cycling with FoxO. *Oncogene*, **27**, 2300–2311.

Hodge, R.D., Kowalczyk, T.D., Wolf, S.A., Encinas, J.M., Rippey, C., Enikolopov, G., Kempermann, G. & Hevner, R.F. (2008): Intermediate progenitors in adult hippocampal neurogenesis: Tbr2 expression and coordinate regulation of neuronal output. *J. Neurosci.*, **28**, 3707-3717.

Hosaka, T., Biggs, W.H., 3rd, Tieu, D., Boyer, A.D., Varki, N.M., Cavenee, W.K., & Arden, K.C. (2004): Disruption of forkhead transcription factor (FOXO) family members in mice reveals their functional diversification. *Proc. Natl. Acad. Sci. USA*, **101**, 2975-2980.

Huber, C., Marschallinger, J., Tempfer, H., Furtner, T., Couillard-Despres, S., Bauer, H.C., Rivera, F.J. & Aigner, L. (2011): Inhibition of leukotriene receptors boosts neural progenitor proliferation. *Cell. Physiol. Biochem.*, **28**, 793-804.

Huynh, M.A., Ikeuchi, Y., Netherton, S., de la Torre-Ubieta, L., Kanadia, R., Stegmüller, J., Cepko, C., Bonni, S. & Bonni, A. (2011): An isoform-specific SnoN1-FOXO1 repressor complex controls neuronal morphogenesis and positioning in the mammalian brain. *Neuron*, **69**, 930-44.

Ihrie, R.A. & Alvarez-Buylla, A. (2011): Lake-front property: a unique germinal niche by the lateral ventricles of the adult brain. *Neuron*, **70**, 674-86.

Imayoshi, I., Sakamoto, M., Yamaguchi, M., Mori, K. & Kageyama, R. (2010): Essential roles of Notch signaling in maintenance of neural stem cells in developing and adult brains. *J. Neurosci.*, **3**, 3489-3498.

Iwano, T., Masuda, A., Kiyonari, H., Enomoto, H. & Matsuzaki, F. (2012): Prox1 postmitotically defines dentate gyrus cells by specifying granule cell identity over CA3 pyramidal cell fate in the hippocampus. *Development*, **139**, 3051-62.

Jacob, F.D., Ramaswamy, V., Andersen, J. & Bolduc, F.V. (2009): Atypical Rett syndrome with selective FOXG1 deletion detected by comparative genomic hybridization: case report and review of literature. *Eur. J. Hum. Genet.*, **17**, 1577-1581.

Jacobs, T., Causeret, F., Nishimura, Y.V., Terao, M., Norman, A., Hoshino, M. & Nikolić, M. (2007): Localized activation of p21-activated kinase controls neuronal polarity and morphology. *J. Neurosci.*, **27**, 8604-8615.

Jagasia, R., Steib, K., Englberger, E., Herold, S., Faus-Kessler, T., Saxe, M., Gage, F.H., Song, H. & Lie, D.C. (2009): GABA-cAMP response element-binding protein signaling regulates maturation and survival of newly generated neurons in the adult hippocampus. *J. Neurosci.*, **29**, 7966-7977.

Jankovski, A. & Sotelo, C. (1996): Subventricular zone-olfactory bulb migratory pathway in the adult mouse: cellular composition and specificity as determined by heterochronic and heterotopic transplantation. *J. Comp. Neurol*., **371**, 376–396.

Jankowsky, J.L., Melnikova, T., Fadale, D.J., Xu, G.M., Slunt, H.H., Gonzales, V., Younkin, L.H., Younkin, S.G., Borchelt, D.R. & Savonenko, A.V. (2005): Environmental enrichment mitigates cognitive deficits in a mouse model of Alzheimer's disease. *J. Neurosci.*, **25**, 5217–5224.

Jarriault, S., Brou, C., Logeat, F., Schroeter, E.H., Kopan, R. & Israel, A. (1995): Signalling downstream of activated mammalian Notch. *Nature*, **377**, 355-358.

Jarriault, S., Le Bail, O., Hirsinger, E., Pourquié, O., Logeat, F., Strong, C.F., Brou, C., Seidah, N.G. & Isra, I.A. (1998): Delta-1 activation of notch-1 signaling results in HES-1 transactivation. *Mol. Cell. Biol.*, **18**, 7423-7431.

Jessberger, S., Nakashima, K., Clemenson, G.D. Jr., Mejia, E., Mathews, E., Ure, K., Ogawa, S., Sinton, C.M., Gage, F.H. & Hsieh, J. (2007): Epigenetic modulation of seizure-induced neurogenesis and cognitive decline. *J. Neurosci.*, **27**, 5967-5975.

Jessberger, S., Clark, R.E., Broadbent, N.J., Clemenson, G.D. Jr., Consiglio, A., Lie, D.C., Squire, L.R. & Gage F.H. (2009): Dentate gyrus-specific knockdown of adult neurogenesis impairs spatial and object recognition memory in adult rats. *Learn. Mem*., **16**, 147–154.

Jin, K., Sun, Y., Xie, L., Batteur, S., Mao, X.O., Smelick, C., Logvinova, A. & Greenberg, D.A. (2003): Neurogenesis and aging: FGF-2 and HB-EGF restore neurogenesis in hippocampus and subventricular zone of aged mice. *Aging Cell*, **2**, 175-183.

Kaestner, K.H., Knochel, W. & Martinez, D.E. (2000): Unified nomenclature for the winged helix/forkhead transcription factors. *Genes Dev.*, **14**, 142-146.

Kageyama, R. & Nakanishi, S. (1997): Helix-loop-helix factors in growth and differentiation of the vertebrate nervous system. *Curr. Opin. Genet. Dev.*, **7**, 659-665.

Kageyama, R., Ohtsuka, T. & Kobayashi, T. (2007): The Hes gene family: repressors and oscillators that orchestrate embryogenesis. *Development*, **134**, 1243-1251.

Kandasamy, M., Couillard-Despres, S., Raber, K.A., Stephan, M., Lehner, B., Winner, B., Kohl, Z., Rivera, F.J., Nguyen, H.P., Riess, O., Bogdahn, U., Winkler, J., von Hörsten, S. & Aigner, L. (2010): Stem cell quiescence in the hippocampal neurogenic niche is associated with elevated transforming growth factor-beta signaling in an animal model of Huntington disease. *J. Neuropathol. Exp. Neurol.*, **69**, 717-728.

Kandyba, E., Hazen, V.M., Kobielak, A., Butler, S.J. & Kobielak, K. (2013): Smad1&5 but not Smad8 establish stem cell quiescence which is critical to transform the premature hair follicle during morphogenesis towards the Postnatal State. *Stem Cells*, doi: 10.1002/stem.1548.

Kaplan, M.S. & Hinds, J.W. (1977): Neurogenesis in the adult rat: electron microscopic analysis of light radioautographs. *Science*, **197**, 1092-1104.

Kappeler, C., Saillour, Y., Baudoin, J.P., Tuy, F.P., Alvarez, C., Houbron, C., Gaspar, P., Hamard, G., Chelly, J., Métin, C. & Francis, F. (2006): Branching and nucleokinesis defects in migrating interneurons derived from doublecortin knockout mice. *Hum. Mol. Genet.*, **15**, 1387-1400.

Kato, T., Yokouchi, K., Fukushima, N., Kawagishi, K., Li, Z. & Moriizumi, T. (2001): Continual replacement of newly-generated olfactory neurons in adult rats. *Neurosci. Lett.* **307**, 17-20.

Kawauchi, S., Kim, J., Santos, R., Wu, H.H., Lander, A.D. & Calof, A.L. (2009a): Foxg1 promotes olfactory neurogenesis by antagonizing Gdf11. *Development*, **136**, 1453-1464.

Kawauchi, S., Santos, R., Kim, J., Hollenbeck, P.L., Murray, R.C. & Calof, A.L. (2009b): The role of foxg1 in the development of neural stem cells of the olfactory epithelium. *Ann. NY Acad. Sci.*, **1170**, 21-27.

Kee, N., Sivalingam, S., Boonstra, R. &Wojtowicz, J.M. (2002): The utility of Ki-67 and BrdU as proliferative markers of adult neurogenesis. *Journal of Neuroscience Methods*, **115**, 97–105.

Kempermann, G., Kuhn, H.G. & Gage, F.H. (1997a): More hippocampal neurons in adult mice living in an enriched environment. *Nature*, **386**, 493-495.

Kempermann, G., Kuhn, H.G. & Gage, F.H. (1997b): Genetic influence on neurogenesis in the dentate gyrus of adult mice. *Proc. Natl. Acad. Sci. USA*, **94**, 10409-10414.

Kempermann, G., Jessberger, S., Steiner, B., & Kronenberg, G. (2004). Milestones of neuronal development in the adult hippocampus. *Trends. Neurosci.*, **27**, 447-452.

Kenyon, C., Chang, J., Gensch, E., Rudner, A. & Tabtiang, R. (1993): A C. elegans mutant that lives twice as long as wild type. *Nature*, **366**, 461-464.

Kim, J.Y., Duan, X., Liu, C.Y., Jang, M.H., Guo, J.U., Pow-anpongkul, N., Kang, E., Song, H. & Ming, G.L. (2009): DISC1 regulates new neuron development in the adult brain via modulation of AKT-mTOR signaling through KIAA1212. *Neuron*, **63**, 761–773.

Kippin, T.E., Martens, D.J. & van der Kooy, D. (2005): p21 loss compromises the relative quiescence of forebrain stem cell proliferation leading to exhaustion of their proliferation capacity. *Genes Dev.*, **19**, 756-767.

Kitamura, Y.I., Kitamura, T., Kruse, J.P., Raum, J.C., Stein, R., Gu, W. & Accili, D. (2005): FoxO1 protects against pancreatic beta cell failure through NeuroD and MafA induction. *Cell Metab.*, **2**, 153-163.

Kitamura, T., Kitamura, Y.I., Funahashi, Y., Shawber, C.J., Castrillon, D.H., Kollipara, R., DePinho, R.A., Kitajewski, J. & Accili, D. (2007): A Foxo/Notch pathway controls myogenic differentiation and fiber type specification. *J. Clin. Invest.*, **117**, 2477-2485.

Kitamura, T., Saitoh, Y., Takashima, N., Murayama, A., Niibori, Y., Ageta, H., Sekiguchi, M., Sugiyama, H. & Inokuchi, K. (2009): Adult neurogenesis modulates the hippocampus-dependent period of associative fear memory. *Cell*, **139**, 814-827.

Komatsu, M., Waguri, S., Chiba, T., Murata, S., Iwata, J., Tanida, I., Ueno, T., Koike, M., Uchiyama, Y., Kominami, E. & Tanaka, K. (2006): Loss of **autophagy** in the central nervous system causes neurodegeneration in mice. *Nature*, **441**, 880-884.

Komatsu, M., Wang, Q.J., Holstein, G.R., Friedrich, V.L. Jr., Iwata, J., Kominami, E., Chait, B.T., Tanaka, K. & Yue, Z. (2007): Essential role for **autophagy** protein Atg7 in the maintenance of axonal homeostasis and the prevention of axonal degeneration. *Proc. Natl. Acad. Sci. USA*, **104**, 14489-14494.

Kops, G.J., de Ruiter, N.D., De Vries-Smits, A.M., Powell, D.R., Bos, J.L., Burgering, B.M. (1999): Direct control of the Forkhead transcription factor AFX by protein kinase B. *Nature*, **398**, 630-634.

Kops, G.J., Dansen, T.B., Polderman, P.E., Saarloos, I., Wirtz, K.W., Coffer, P.J., Huang, T.T., Bos, J.L., Medema, R.H. & Burgering, B.M. (2002): Forkhead transcription factor FOXO3a protects quiescent cells from oxidative stress. *Nature*, **419**, 316–321.

Kornack, D.R. & Rakic, P. (1999): Continuation of neurogenesis in the hippocampus of the adult macaque monkey. *Proc. Natl. Acad. Sci. USA*, **96**, 5768-5773.

Kortüm, F., Das, S., Flindt, M., Morris-Rosendahl, D.J., Stefanova, I., Goldstein, A., Horn, D., Klopocki, E., Kluger, G., Martin, P., Rauch, A., Roumer, A., Saitta, S., Walsh, L.E., Wieczorek, D., Uyanik, G., Kutsche, K. & Dobyns, W.B. (2011): The core FOXG1 syndrome phenotype consists of postnatal microcephaly, severe mental retardation, absent language, dyskinesia, and corpus callosum hypogenesis. *J. Med. Genet.*, **48**, 396-406.

Kress, T.R., Cannell, I.G., Brenkman, A.B., Samans, B., Gaestel, M., Roepman, P., Burgering, B.M., Bushell, M., Rosenwald, A. & Eilers, M. (2011): The MK5/PRAK kinase and Myc form a negative feedback loop that is disrupted during colorectal tumorigenesis. *Mol. Cell.*, **41**, 445-457.

Krzisch, M., Sultan, S., Sandell, J., Demeter, K., Vutskits, L. & Toni, N. (2013): Propofol anesthesia impairs the maturation and survival of adult-born hippocampal neurons. *Anesthesiology*, **118**, 602-610.

Kron, M.M., Zhang, H., Parent, J.M. (2010): The developmental stage of dentate granule cells dictates their contribution to seizure-induced plasticity. *J. Neurosci.*, **30**, 2051–2059.

Kuhn, H.G., Winkler, J., Kempermann, G., Thal, L.J. & Gage, F.H. (1997): Epidermal growth factor and fibroblast growth factor-2 have different effects on neural progenitors in the adult rat brain. *J. Neurosci.*, **17**, 5820-5829.

Kumakura, A., Takahashi, S., Okajima, K. & Hata, D. (2013): A haploinsufficiency of FOXG1 identified in a boy with congenital variant of Rett syndrome. *Brain Dev.*, **7604**, 287-288.

Kuwabara, T., Hsieh, J., Muotri, A., Yeo, G., Warashina, M., Lie, D.C., Moore, L., Nakashima, K., Asashima, M. & Gage, F.H. (2009): Wnt-mediated activation of NeuroD1 and retro-elements during adult neurogenesis. *Nat. Neurosci.*, **12**, 1097-1105.

Lai, K., Kaspar, B.K., Gage, F.H. & Schaffer, D.V. (2003): Sonic hedgehog regulates adult neural progenitor proliferation in vitro and in vivo. *Nat. Neurosci.*, **6**, 21-27.

Lauri, S.E., Bortolotto, Z.A., Bleakman, D., Ornstein, P.L., Lodge, D., Isaac, J.T., & Collingridge, G.L. (2001). A critical role of a facilitatory presynaptic kainate receptor in mossy fiber LTP. *Neuron*, **32**, 697-709.

Lavado, A., Lagutin, O.V., Chow, L.M., Baker, S.J. & Oliver, G. (2010): Prox1 is required for granule cell maturation and intermediate progenitor maintenance during brain neurogenesis. *PLoS Bio.,* **8**, e1000460.

Le Belle, J.E., Orozco, N.M., Paucar, A.A., Saxe, J.P., Mottahedeh, J., Pyle, A.D., Wu, H. & Kornblum, H.I. (2011): Proliferative neural stem cells have high endogenous ROS levels that regulate self-renewal and neurogenesis in a PI3K/Akt-dependant manner. *Cell Stem Cell*, **8**, 59-71.

Le Guen, T., Bahi-Buisson, N., Nectoux, J., Boddaert, N., Fichou, Y., Diebold, B., Desguerre, I., Raqbi, F., Daire, V.C., Chelly, J. & Bienvenu, T. (2011a): A FOXG1 mutation in a boy with congenital variant of Rett syndrome. *Neurogenetics*, **12**, 1-8.

Le Guen, T., Fichou, Y., Nectoux, J., Bahi-Buisson, N., Rivier, F., Boddaert, N., Diebold, B., Héron, D., Chelly, J. & Bienvenu, T. (2011b): A missense mutation within the fork-head domain of the forkhead box G1 Gene (FOXG1) affects its nuclear localization. *Hum. Mutat.*, **3**, 2026-2035.

Lehmann, O.J., Sowden, J.C., Carlsson, P., Jordan, T., & Bhattacharya, S.S. (2003): Fox's in development and disease. *Trends Genet.*, **19**, 339-344.

Lei, H. & Quelle, F.W. (2009): FoxO transcription factors enforce cell cycle checkpoints and promote survival of hematopoietic cells after DNA damage. *Mol. Cancer Res.*, **7**, 1294-1303.

Leutgeb, J.K., Leutgeb, S., Moser, M.B. & Moser, E.I. (2007): Pattern separation in the dentate gyrus and CA3 of the hippocampus. *Science*, **16**, 961-966.

Levine, B., Sinha, S. & Kroemer, G. (2008): Bcl-2 family members: dual regulators of apoptosis and **autophagy**. *Autophagy*, **4**, 600-606.

Li, Y., Wang, W.J., Cao, H., Lu, J., Wu, C., Hu, F.Y., Guo, J., Zhao, L., Yang, F., Zhang, Y.X., Li, W., Zheng, G.Y., Cui, H., Chen, X., Zhu, Z., He, H., Dong, B., Mo, X., Zeng, Y. & Tian, X.L. (2009): Genetic association of FOXO1A and FOXO3A with longevity trait in Han Chinese populations. *Hum. Mol. Genet.*, **18**, 4897-4904.

Lim, D.A., Tramontin, A.D., Trevejo, J.M., Herrera, D.G,, García-Verdugo, J.M. & Alvarez-Buylla, A. (2000): Noggin antagonizes BMP signaling to create a niche for adult neurogenesis. *Neuron*, **28**, 713-726.

Liu, Q.A. & Shio, H. (2008): Mitochondrial morphogenesis, dendrite development, and synapse formation in cerebellum require both Bcl-w and the glutamate receptor delta2. *PLoS Genet.*, **4**, e1000097.

Liu, C., Teng, Z.Q., Santistevan, N.J., Szulwach, K.E., Guo, W., Jin, P. & Zhao X. (2010): Epigenetic regulation of miR-184 by MBD1 governs neural stem cell proliferation and differentiation. *Cell Stem Cell*, **6**, 433-44.

Lois, C., Garcia-Verdugo, J.M. & Alvarez-Buylla, A. (1996): Chain migration of neuronal precursors. *Science*, **271**, 978–981.

Luo, Y., Shan, G., Guo, W., Smrt, R.D., Johnson, E.B., Li, X., Pfeiffer, R.L., Szulwach, K.E., Duan, R., Barkho, B.Z., Li, W., Liu, C., Jin, P. & Zhao, X. (2010): Fragile x mental retardation protein regulates proliferation and differentiation of adult neural stem/progenitor cells. *PLoS Genet.*, **6**, e1000898.

Luukko, K., Ylikorkala, A. & Mäkelä, T.P. (2001): Developmentally regulated expression of Smad3, Smad4, Smad6 and Smad7 involved in TGF-beta signaling. *Mech. Dev.*, **101**, 209-212.

Ma, D.K., Kim, W.R., Ming, G.L. & Song, H. (2009): Activity-dependent extrinsic regulation of adult olfactory bulb and hippocampal neurogenesis. *Ann. NY Acad. Sci.*, **1170**, 664-673.

Malmersjö, S., Rebellato, P., Smedler, E., Planert, H., Kanatani, S., Liste, I., Nanou, E., Sunner, H., Abdelhady, S., Zhang, S., Andäng, M., El Manira, A., Silberberg, G., Arenas, E. & Uhlén, P. (2013): Neural progenitors organize in small-world networks to promote cell proliferation. *Proc. Natl. Acad. Sci. USA*, **110**, 1524-1532.

Mammucari, C., Milan, G., Romanello, V., Masiero, E., Rudolf, R., Del, P.P., Burden, S.J., Di, L.R., Sandri, C., Zhao, J., Goldberg, A.L., Schiaffino, S. & Sandri, M. (2007): FoxO3 controls autophagy in skeletal muscle in vivo. *Cell Metab.*, **6**, 458–471.

Mannella, C,A. (2008): Structural diversity of mitochondria: functional implications. *Ann. NY Acad. Sci.*, **1147**, 171-179.

Manoranjan, B., Wang, X., Hallett, R.M., Venugopal, C., Mack, S.C., McFarlane, N., Nolte, S.M., Scheinemann, K., Gunnarsson, T., Hassell, J.A., Taylor, M.D., Lee, C., Triscott, J., Foster, C.M., Dunham, C., Hawkins, C., Dunn, S.E. & Singh, S.K. (2013): FoxG1 interacts with Bmi1 to regulate self-renewal and tumorigenicity of medulloblastoma stem cells. *Stem Cells*, **31**, 1266-1277.

Manuel, M., Martynoga, B., Yu, T., West, J.D., Mason, J.O. & Price, D.J. (2010): The transcription factor Foxg1 regulates the competence of telencephalic cells to adopt subpallial fates in mice. *Development*, **137**, 487-497.

Manuel, M.N., Martynoga, B., Molinek, M.D., Quinn, J.C., Kroemmer, C., Mason, J.O. & Price, D.J. (2011): The transcription factor Foxg1 regulates telencephalic progenitor proliferation cell autonomously, in part by controlling Pax6 expression levels. *Neural. Dev.*, **6**, 9.

Marín-Burgin, A., Mongiat, L.A., Pardi, M.B. & Schinder, A.F. (2012): Unique processing during a period of high excitation/inhibition balance in adult-born neurons. *Science*, **335**, 1238-1242.

Martynoga, B., Mateo, J.L., Zhou, B., Andersen, J., Achimastou, A., Urbán, N., van den Berg, D., Georgopoulou, D., Hadjur, S., Wittbrodt, J., Ettwiller, L., Piper, M., Gronostajski, R.M. & Guillemot, F. (2013): Epigenomic enhancer annotation reveals a key role for NFIX in neural stem cell quiescence. *Genes Dev.*, **27**, 1769-1786.

Marqués-Torrejón, M.Á., Porlan, E., Banito, A., Gómez-Ibarlucea, E., Lopez-Contreras, A.J., Fernández-Capetillo, O., Vidal, A., Gil, J., Torres, J. & Fariñas, I. (2013): Cyclin-dependent kinase inhibitor p21 controls adult neural stem cell expansion by regulating Sox2 gene expression. *Cell Stem Cell*, **3**, 88-100.

Matarazzo, V., Cohen, D., Palmer, A.M., Simpson, P.J., Khokhar, B., Pan, S.J. & Ronnett, G.V. (2004): The transcriptional repressor Mecp2 regulates terminal neuronal differentiation. *Mol. Cell. Neurosci.*, **27**, 44–58.

McBride, H.M., Neuspiel, M. & Wasiak, S. (2006): Mitochondria: more than just a powerhouse. *Curr. Biol.*, **16**, 551-560.

Medema, R.H., Kopsm G.J., Bosm J.L. & Burgering, B.M. (2000): AFX-like Forkhead transcription factors mediate cell-cycle regulation by Ras and PKB through p27kip1. *Nature*, **404**, 782-787.

Melrose, H.L., Dächsel, J.C., Behrouz, B., Lincoln, S.J., Yue, M., Hinkle, K.M., Kent, C.B., Korvatska, E., Taylor, J.P., Witten, L., Liang, Y.Q., Beevers, J.E., Boules, M., Dugger, B.N., Serna, V.A., Gaukhman, A., Yu, X., Castanedes-Casey, M., Braithwaite, A.T., Ogholikhan, S., Yu, N., Bass, D., Tyndall, G., Schellenberg, G.D., Dickson, D.W., Janus, C. & Farrer, M.J. (2010): Impaired dopaminergic neurotransmission and microtubule-associated protein tau alterations in human LRRK2 transgenic mice. *Neurobiol. Dis.*, **40**, 503–517.

Mencarelli, M.A., Spanhol-Rosseto, A., Artuso, R., Rondinella, D., De Filippis, R., Bahi-Buisson, N., Nectoux, J., Rubinsztajn, R., Bienvenu, T., Moncla, A., Chabrol, B., Villard, L., Krumina, Z., Armstrong, J., Roche, A., Pineda, M., Gak, E., Mari, F., Ariani, F. & Renieri, A. (2010): Novel FOXG1 mutations associated with the congenital variant of Rett syndrome. *J. Med. Genet.*, **47**, 49-53.

Menn, B., Garcia-Verdugo, J.M., Yaschine, C., Gonzalez-Perez, O., Rowitch, D. & Alvarez-Buylla, A. (2006): Origin of oligodendrocytes in the subventricular zone of the adult brain. *J. Neurosci.*, **26**, 7907-7918.

Miller, J.F., Neufang, M., Solway, A., Brandt, A., Trippel, M., Mader, I., Hefft, S., Merkow, M., Polyn, S.M., Jacobs, J., Kahana, M.J. & Schulze-Bonhage A. (2013): Neural activity in human hippocampal formation reveals the spatial context of retrieved memories. *Science*, **342**, 1111-1114.

Ming, G.L. & Song, H. (2011): Adult neurogenesis in the mammalian brain: significant answers and significant questions. *Neuron*, **70**, 687-702.

Mira, H., Andreu, Z., Suh, H., Lie, D.C., Jessberger, S., Consiglio, A., San Emeterio, J., Hortigüela, R., Marqués-Torrejón, M.A., Nakashima, K., Colak, D., Götz, M., Fariñas, I. & Gage, F.H. (2010): Signaling through BMPR-IA regulates quiescence and long-term activity of neural stem cells in the adult hippocampus. *Cell Stem Cell*, **7**, 78-89.

Mirescu C., & Gould, E. (2006): Sress and adult neurogenesis. *Hippocampus*, **16**, 233-238.

Mitra, K., Wunder, C., Roysam, B., Lin, G. & Lippincott-Schwartz, J. (2009): A hyperfused mitochondrial state achieved at G1-S regulates cyclin E buildup and entry into S phase. *Proc. Natl. Acad. Sci. USA*, **106**, 11960–11965.

Miyamoto, K., Araki, K.A., Naka, K., Arai, F., Takubo, K., Yamazaki, S., Matsuoka, S., Miyamoto, T., Ito, K., Ohmura, M., et al. (2007): Foxo3a is essential for maintenance of the hematopoietic stem cell pool. *Cell Stem Cell*, **1**, 101–112.

Miyazono, K., Kamiya, Y. & Morikawa, M. (2010): Bone morphogenetic protein receptors and signal transduction. *J. Biochem.*, **147**, 35–51.

Miyoshi, G. & Fishell, G. (2012): Dynamic FoxG1 expression coordinates the integration of multipolar pyramidal neuron precursors into the cortical plate. *Neuron*, **74**, 1045-1058.

Molofsky, A.V., Slutsky, S.G., Joseph, N.M., He, S., Pardal, R., Krishnamurthy, J., Sharpless, N.E. & Morrison, S.J. (2006): Increasing p16INK4a expression decreases forebrain progenitors and neurogenesis during ageing. *Nature*, **443**, 448-452.

Mori, T., Tanaka, K., Buffo, A., Wurst, W., Kühn, R. & Götz, M. (2006): Inducible gene deletion in astroglia and radial glia--a valuable tool for functional and lineage analysis. *Glia*, **54**, 21-34.

Murphy, D.B., Wiese, S., Burfeind, P., Schmundt, D., Mattei, M.G., Schulz-Schaeffer, W. & Thies, U. (1994): Human brain factor 1, a new member of the fork head gene family. *Genomics*, **21**, 551-557.

Nakae, J., Kitamura, T., Kitamura, Y., Biggs, W.H. 3rd, Arden, K.C. & Accili, D. (2003): The forkhead transcription factor Foxo1 regulates adipocyte differentiation. *Dev. Cell*, **4**, 119-129.

Nakamura, T., Colbert, M.C. & Robbins, J. (2006): Neural crest cells retain multipotential characteristics in the developing valves and label the cardiac conduction system. *Circ. Res.*, **98**, 1547-1554.

Nakashiba, T., Cushman, J.D., Pelkey, K.A., Renaudineau, S., Buhl, D.L., McHugh, T.J., Rodriguez Barrera, V., Chittajallu, R., Iwamoto, K.S., McBain, C.J., Fanselow. M.S. & Tonegawa, S. (2012): Young dentate granule cells mediate pattern separation, whereas old granule cells facilitate pattern completion. *Cell*, **30**, 188-201.

Nelson, E.D., Bal, M., Kavalali, E.T. & Monteggia, L.M. (2011): Selective impact of MeCP2 and associated histone deacetylases on the dynamics of evoked excitatory neurotransmission. *J. Neurophysiol.*, **106**, 193-201.

Nieto, M., Schuurmans, C., Britz, O. & Guillemot, F. (2001): Neural bHLH genes control the neuronal versus glial fate decision in cortical progenitors. *Neuron*, **29**, 401-413.

Niu, W., Zou, Y., Shen, C. & Zhang, C.L. (2011): Activation of postnatal neural stem cells requires nuclear receptor TLX. J. Neurosci., 31, 13816-13828.

Nuber, S., Petrasch-Parwez, E., Winner, B., Winkler, J., von Hörsten, S., Schmidt, T., Boy, J., Kuhn, M., Nguyen, H.P., Teismann, P., Schulz, J.B., Neumann, M., Pichler, B.J., Reischl, G., Holzmann, C., Schmitt, I., Bornemann, A., Kuhn, W., Zimmermann, F., Servadio, A. & Riess, O. (2008): Neurodegeneration and motor dysfunction in a conditional model of Parkinson's disease. *J. Neurosci.*, **28**, 2471–2484.

Ohtsuka, T., Sakamoto, M., Guillemot, F. & Kageyama, R. (2001): Roles of the basic helix-loop-helix genes Hes1 and Hes5 in expansion of neural stem cells of the developing brain. *J. Biol. Chem.*, **276**, 30467-30474.

Ory, D.S., Neugeboren, B.A. & Mulligan, R.C. (1996): A stable human-derived packaging cell line for production of high titer retrovirus/vesicular stomatitis virus G pseudotypes. Proc. *Natl. Acad. Sci. USA*, **93**, 11400-11406.

Paik, J.H., Kollipara, R., Chu, G., Ji, H., Xiao, Y., Ding, Z., Miao, L., Tothova, Z., Horner, J.W,, Carrasco, D.R., Jiang. S,, Gilliland, D.G., Chin, L., Wong, W.H., Castrillon, D.H. & DePinho, R.A. (2007): FoxOs are lineage-restricted redundant tumor suppressors and regulate endothelial cell homeostasis. *Cell*, **128**, 309-323.

Paik, J.H., Ding, Z., Narurkar, R., Ramkissoon, S., Muller, F., Kamoun, W.S., Chae, S.S., Zheng, H., Ying, H., Mahoney, J., Hiller, D., Jiang, S., Protopopov, A., Wong, W.H., Chin, L., Ligon, K.L. & DePinho, R.A. (2009): FoxOs cooperatively regulate diverse pathways governing neural stem cell homeostasis. *Cell Stem Cell*, **5**, 540-53.

Paling, N.R., Wheadon, H., Bone, H.K. & Welham, M.J. (2004): Regulation of embryonic stem cell self-renewal by phosphoinositide 3-kinase-dependent signaling. *J. Biol. Chem.*, **279**, 48063-48070.

Palmer, T.D., Willhoite, A.R., & Gage F.H. (2000): Vascular niche for adult hippocampal neurogenesis. *J. Comp. Neurol*., **425**, 479–494.

Papa, F.T., Mencarelli, M.A., Caselli, R., Katzaki, E., Sampieri, K., Meloni, I., Ariani, F., Longo, I., Maggio, A., Balestri, P., Grosso, S., Farnetani, M.A., Berardi, R., Mari, F. & Renieri, A. (2008): A 3 Mb deletion in 14q12 causes severe mental retardation, mild facial dysmorphisms and Rett-like features. *Am. J. Med. Genet. A*, **146A**, 1994-1998.

Pauley, S., Lai, E. & Fritzsch, B. (2006): Foxg1 is required for morphogenesis and histogenesis of the mammalian inner ear. *Dev Dyn.*, **235**, 2470-2482.

Perche, O., Haddad, G., Menuet, A., Callier, P., Marcos, M., Briault, S. & Laudier, B. (2013): Dysregulation of FOXG1 pathway in a 14q12 microdeletion case. *Am. J. Med. Genet. A*, **161**, 3072-3077.

Peretto, P., Merighi, A., Fasolo, A., & Bonfanti, L. (1997): Glial tubes in the rostral migratory stream of the adult rat. *Brain. Res. Bull.*, **42**, 9–21.

Piper, M., Barry, G., Hawkins, J., Mason, S., Lindwall, C., Little, E., Sarkar, A., Smith, A.G., Moldrich, R.X., Boyle, G.M., Tole, S., Gronostajski, R.M., Bailey, T.L. & Richards, L.J. (2010): NFIA controls telencephalic progenitor cell differentiation through repression of the Notch effector Hes1. *J. Neurosci.*, **30**, 9127-9139.

Pratt, D.W., Warner, J.V. & Williams, M.G. (2013): Genotyping FOXG1 Mutations in Patients with Clinical Evidence of the FOXG1 Syndrome. *Mol. Syndromol.*, **3**, 284-287.

Qu, Q., Sun, G., Li, W., Yang, S., Ye, P., Zhao, C., Yu, R.T., Gage, F.H., Evans, R.M. & Shi, Y. (2010): Orphan nuclear receptor TLX activates Wnt/beta-catenin signalling to stimulate neural stem cell proliferation and self-renewal. Nat Cell Biol., 12, 31-40.

Ramon y Cajal, S. (1928): Degeneration and regeneration of the nervous system. Oxford Univ Press.

Ren, H., Orozco, I.J., Su, Y., Suyama, S., Gutiérrez-Juárez, R., Horvath, T.L., Wardlaw, S.W., Plum, L., Arancio, O. & Accili, D. (2012): G protein-coupled purinergic receptor GPR17 mediates orexigenic effects of FoxO1 in AgRP neurons. *Cell*, **149**, 1314–1326.

Rena G, Guo S, Cichy SC, Unterman TG, Cohen P. (1999): Phosphorylation of the transcription factor forkhead family member FKHR by protein kinase B. *J. Biol. Chem.*, **274**, 17179-17183.

Renault, V.M., Rafalski, V.A., Morgan, A.A., Salih, D.A., Brett, J.O., Webb, A.E., Villeda, S.A., Thekkat, P.U., Guillerey, C., Denko, N.C., Palmer, T.D., Butte, A.J. & Brunet, A. (2009): FoxO3 regulates neural stem cell homeostasis. *Cell Stem Cell*, **5**, 527-539.

Reynolds, B.A., Tetzlaff, W. & Weiss, S. (1992): A multipotent EGF-responsive striatal embryonic progenitor cell produces neurons and astrocytes. *J. Neurosci.*, **12**, 4565-4574.

Reynolds, B.A. & Weiss, S. (1996): Clonal and population analyses demonstrate that an EGF-responsive mammalian embryonic CNS precursor is a stem cell. *Dev Biol.*, **175**, 1-13.

Richards, L.J., Kilpatrick, T.J., and Bartlett, P.F. (1992): De novo generation of neuronal cells from the adult mouse brain. *Proc. Natl. Acad. Sci. USA*, **89**, 8591–8595.

Rietze, R.L., Valcanis, H., Brooker, G.F., Thomas, T., Voss, A.K., Bartlett, P.F. (2001): Purification of a pluripotent neural stem cell from the adult mouse brain. *Nature*, **412**, 736-739.

Rossi, D.J., Jamieson, C.H., & Weissman, I.L. (2008): Stems cells and the pathways to aging and cancer. *Cell*, **22**, 681-696.

Roth, M., Bonev, B., Lindsay, J., Lea, R., Panagiotaki, N., Houart, C. & Papalopulu, N. (2010): FoxG1 and TLE2 act cooperatively to regulate ventral telencephalon formation. *Development*, **137**, 1553-1562.

Sahay, A., Scobie, K.N., Hill, A.S., O'Carroll, C.M., Kheirbek, M.A., Burghardt, N.S., Fenton, A.A., Dranovsky, A. & Hen R. (2011a): Increasing adult hippocampal neurogenesis is sufficient to improve pattern separation. *Nature*, **28**, 466-470.

Sahay, A., Wilson, D.A. & Hen, R. (2011b): Pattern separation: a common function for new neurons in hippocampus and olfactory bulb. *Neuron*, **70**, 582-8.

Salih, D.A., Rashid, A.J., Colas, D., de la Torre-Ubieta, L., Zhu, R.P., Morgan, A.A., Santo, E.E., Ucar, D., Devarajan, K., Cole, C.J., Madison, D.V., Shamloo, M., Butte, A.J., Bonni, A., Josselyn, S.A. & Brunet, A. (2012): FoxO6 regulates memory consolidation and synaptic function. *Genes Dev.*, **26**, 2780-2801.

Salminen, A., Kaarniranta, K. & Kauppinen, A. (2013): Crosstalk between Oxidative Stress and SIRT1: Impact on the Aging Process*. Int. J. Mol. Sci.*, **14**, 3834-3859.

Santarelli, L., Saxe, M., Gross, C., Surget, A., Battaglia, F., Dulawa, S., Weisstaub, N., Lee, J., Duman, R., Arancio, O., Belzung, C. & Hen, R. (2003): Requirement of hippocampal neurogenesis for the behavioral effects of antidepressants. *Science*, **301**, 805–809.

Schmidt, M., Fernandez de Mattos, S., van der Horst, A., Klompmaker, R., Kops, G.J., Lam, E.W., Burgering, B.M. & Medema, R.H. (2002): Cell cycle inhibition by FoxO forkhead transcription factors involves downregulation of cyclin D. Mol. Cell Biol., 22, 7842-7852.

Schmidt-Hieber, C., Jonas, P. & Bischofberger, J. (2004): Enhanced synaptic plasticity in newly generated granule cells of the adult hippocampus. *Nature*, **429**, 184-187.

Scholzen, T. & Gerdes, J. (2000): The Ki-67 protein: from the known and the unknown. *J. Cell. Physiol.*, **182**, 311–322.

Scoville, W.B., Milner, B. (1957): Loss of recent memory after bilateral hippocampal lesions. *J. Neurol. Neurosurg. Psychiatry*, **20**, 11-21.

Sengupta, A., Molkentin, J.D. & Yutzey, K.E. (2009): FoxO transcription factors promote autophagy in cardiomyocytes. *J. Biol. Chem.*, **284**, 28319–28331.

Seri , B., Garcia-Verdugo, J.M., McEwen, B.S. & Alvarez-Buylla, A. (2001): Astrocytes Give Rise to New Neurons in the Adult Mammalian Hippocampus. *J. Neurosci.*, **21**, 7153–7160.

Seoane, J., Le, H.V., Shen, L., Anderson, S.A. & Massague, J. (2004): Integration of smad and forkhead pathways in the control of neuroepithelial and glioblastoma cell proliferation. *Cell*, **117**, 211–223.

Shen, L., Nam, H., Song, P., Moore, H. & Anderson, S.A. (2006): FoxG1 Haploinsufficiency Results in Impaired Neurogenesis in the Postnatal Hippocampus and Contextual Memory Deficits. *Hippocampus*, **16**, 875-890.

Sherr, C.J. (1996): Cancer cell cycles. *Science*, **274**, 1672-1677.

Sherr, C.J. & Roberts, J.M. (1999): CDK inhibitors: positive and negative regulators of G1-phase progression. *Genes Dev.*, **13**, 1501-1512.

Shi, Y., Lie, D.C, Taupin, P., Nakashima, K., Ray, J., Yu, R.T., Gage, F.H. & Evans, R.M. (2004): Expression and function of orphan nuclear receptor TLX in adult neural stem cells. *Nature*, **427**, 78–83.

Shimozaki, K., Zhang, C.L., Suh, H., Denli, A.M., Evans, R.M. & Gage, F.H. (2012): SRY-box-containing gene 2 regulation of nuclear receptor tailless (Tlx) transcription in adult neural stem cells. *J. Biol. Chem.*, **287**, 5969-5978.

Sholl, D.A. (1953): Dendritic organization in the neurons of the visual and motor cortices of the cat. *J. Anat.*, **87**, 387-406.

Shu, T., Butz, K.G., Plachez, C., Gronostajski, R.M. & Richards, L.J. (2003): Abnormal development of forebrain midline glia and commissural projections in Nfia knock-out mice. *J. Neurosci.*, **23**, 203-212.

Simons, B.D., and Clevers, H. (2011): Strategies for homeostatic stem cell selfrenewal in adult tissues. *Cell*, **145**, 851-862.

Smrt, R.D., Eaves-Egenes, J., Barkho, B.Z., Santistevan, N.J., Zhao, C., Aimone, J.B., Gage, F.H. & Zhao, X. (2007): Mecp2 deficiency leads to delayed maturation and altered gene expression in hippocampal neurons. *Neurobiol. Dis.*, **27**, 77-89.

Snyder, J.S., Kee, N. & Wojtowicz, J.M. (2001): Effects of adult neurogenesis on synaptic plasticity in the rat dentate gyrus. *J. Neurophysiol.*, **85**, 2423–2431.

Snyder, J.S., Hong, N.S., McDonald, R.J. & Wojtowicz, J.M. (2005): A role for adult neurogenesis in spatial longterm memory. *Neuroscience*, **130**, 843–852.

Song, J., Zhong, C., Bonaguidi, M.A., Sun, G.J., Hsu, D., Gu, Y., Meletis, K., Huang, Z.J., Ge, S., Enikolopov, G., Deisseroth, K., Luscher, B., Christian, K.M., Ming, G.L. & Song, H. (2012): Neuronal circuitry mechanism regulating adult quiescent neural stem-cell fate decision. *Nature*, **489**, 150-154.

Song, J., Sun, J., Moss, J., Wen, Z., Sun, G.J., Hsu, D., Zhong, C., Davoudi, H., Christian, K.M., Toni, N., Ming, G.L. & Spng, H. (2013): Parvalbumin interneurons mediate neuronal circuitry-neurogenesis coupling in the adult hippocampus. *Nat. Neurosci.*, **16**, 1728-1730.

Spalding, K.L., Bergmann, O., Alkass, K., Bernard, S., Salehpour, M., Huttner, H.B., Boström, E., Westerlund, I., Vial, C., Buchholz, B.A., Possnert, G., Mash, D.C., Druid, H. & Frisén, J. (2013): Dynamics of hippocampal neurogenesis in adult humans. *Cell*, **153**, 1219-1227.

Steib, K.A. (2013): The function of mitochondrial dynamics, content and localization during adult hippocampal neurogenesis. http://nbn-resolving.de/urn/resolver.pl?urn:nbn:de:bvb:91-diss-20130913-1162497-0-1

Subramanian, L., Sarkar, A., Shetty, A.S., Muralidharan, B., Padmanabhan, H., Piper, M., Monuki, E.S., Bach, I., Gronostajski, R.M., Richards, L.J. & Tole, S. (2011): Transcription factor Lhx2 is necessary and sufficient to suppress astrogliogenesis and promote neurogenesis in the developing hippocampus. *Proc. Natl. Acad. Sci. USA*, **108**, 265-274.

Sun, J., Sun, J., Ming, G.L. & Song, H. (2011): Epigenetic regulation of neurogenesis in the adult mammalian brain. *Eur. J. Neurosci.*, **33**, 1087-1093.

Sunters, A., Madureira, P.A., Pomeranz, K.M., Aubert, M., Brosens, J.J., Cook, S.J., Burgering, B.M., Coombes, R.C. & Lam, E.W. (2006): Paclitaxel-induced nuclear translocation of FOXO3a in breast cancer cells is mediated by c-Jun NH2-terminal kinase and Akt. *Cancer Res.*, **66**, 212-220.

Takagi, M., Sasaki, G., Mitsui, T., Honda, M., Tanaka, Y. & Hasegawa, T. (2013): A 2.0 Mb microdeletion in proximal chromosome 14q12, involving regulatory elements of FOXG1, with the coding region of FOXG1 being unaffected, results in severe developmental delay, microcephaly, and hypoplasia of the corpus callosum. *Eur. J. Med. Genet.*, **56**, 526-528.

Tang, E.D., Nuñez, G., Barr, F.G. & Guan, K.L. (1999): Negative regulation of the forkhead transcription factor FKHR by Akt. *J. Biol. Chem.*, **274**, 16741-16746.

Tani, M., Hayakawa, H., Yasuda, T., Nihira, T., Hattori, N., Mizuno, Y. & Mochizuki, H. (2010): Ectopic expression of a-synuclein affects the migration of neural stem cells in mouse subventricular zone. *J. Neurochem.*, **115**, 854–863.

Tao, W. & Lai, E. (1992): Telencephalon-restricted expression of BF-1, a new member of the HNF-3/fork head gene family, in the developing rat brain. *Neuron*, **8**, 957–966.

Tashiro, A., Zhao, C. & Gage, F.H. (2006): Retrovirus-mediated single-cell gene knockout technique in adult newborn neurons in vivo. *Nat. Protoc.*, **1**, 3049-3055.

Tashiro, A., Sandler, V.M., Toni, N., Zhao, C. & Gage, F.H. (2006a): NMDA-receptor-mediated, cell-specific integration of new neurons in adult dentate gyrus. *Nature*, **442**, 929–933.

Tian, C., Gong, Y., Yang Y., Shen, W.,Wang, K., Liu, J., Xu, B., Zhao, J. & Zhao, C. (2012): Foxg1 Has an Essential Role in Postnatal Development of the Dentate Gyrus. *J. Neurosc.*, **32**, 2931-2949.

Tomita, K., Moriyoshi, K., Nakanishi, S., Guillemot, F. & Kageyama, R. (2000): Mammalian achaete-scute and atonal homologs regulate neuronal versus glial fate determination in the central nervous system. *EMBO J.*, **19**, 5460-5472.

Toni, N., Teng, E.M., Bushong, E.A., Aimone, J.B., Zhao, C., Consiglio, A., van Praag, H., Martone, M.E., Ellisman, M.H. & Gage, F.H. (2007): Synapse formation on neurons born in the adult hippocampus. *Nat. Neurosci.*, **10**, 727-734.

Toni, N., Laplagne, D.A., Zhao, C., Lombardi, G., Ribak, C.E., Gage, F.H. & Schinder, A.F. (2008): Neurons born in the adult dentate gyrus form functional synapses with target cells. *Nat. Neurosci.*, **11**, 901–907.

Tothova, Z., Kollipara, R., Huntly, B.J., Lee, B.H., Castrillon, D.H., Cullen, D.E., McDowell, E.P., Lazo-Kallanian, S., Williams, I.R., Sears, C., et al. (2007): FoxOs are critical mediators of hematopoietic stem cell resistance to physiologic oxidative stress. *Cell*, **128**, 325–339.

Tozuka, Y., Fukuda, S., Namba, T., Seki, T. & Hisatsune, T. (2005): GABAergic Excitation Promotes Neuronal Differentiation in Adult Hippocampal Progenitor Cells. *Neuron*, **47**, 803–815.

Tran, H., Brunet, A., Grenier, J.M., Datta, S.R., Fornace, A.J., DiSTefano, P.S. et al. (2002): DNA repair pathway stimulated by the forkhead transcription factor FoxO3a through the Gadd45 protein. *Science*, **296**, 530-534.

Trejo, J.L., Carro, E. & Torres-Aleman, I. (2001): Circulating Insulin-Like Growth Factor I mediates exercise-induced increases in the number of new neurons in the adult hippocampus. *J. Neurosci.*, **21**, 1628–1634.

Tsai, W.B., Chung, Y.M., Takahashi, Y., Xu, Z. & Hu, M.C. (2008): Functional interaction between FOXO3a and ATM regulates DNA damage response. *Nat. Cell Biol.*, **10**, 460-467.

Tuteja, G. & Kaestner, K.H. (2007a): SnapShot: forkhead transcription factors I. *Cell*, **130**, 1160.

Tuteja, G. & Kaestner, K.H. (2007b): Forkhead transcription factors II. *Cell*, **5,** 192.

United Nations (2013): http://esa.un.org/unpd/wpp/index.htm.

van der Heide, L.P., Hoekman, M.F. & Smidt, M.P. (2004): The ins and outs of FoxO shuttling: mechanisms of FoxO translocation and transcriptional regulation. *Biochem. J.*, **380**, 297-309.

van der Horst, A., de Vries-Smits, A.M., Brenkman, A.B., van Triest, M.H., van den Broek, N., Colland, F., Maurice, M.M. & Burgering, B.M. (2006): FOXO4 transcriptional activity is regulated by monoubiquitination and USP7/HAUSP. *Nat. Cell Biol*., **8**, 1064-1073.

van der Horst, A. & Burgering, B.M. (2007): Stressing the role of FoxO proteins in lifespan and disease. Nat. Rev. Mol. Cell. Biol., 8, 440-450.

van Praag, H., Christie, B.R., Sejnowski, T.J. & Gage, F.H. (1999a): Running enhances neurogenesis, learning, and long-term potentiation in mice. Proc. *Nat. Acad. Sci. USA*, **96**, 13427–13431.

van Praag, H., Kempermann, G. & Gage, F.H. (1999b): Running increases cell proliferation and neurogenesis in the adult mouse dentate gyrus. *Nat. Neurosci.*, **2**, 266–270.

Vanneste, J. & van den Bosch de Aguilar, P. (1981): Mitochondrial alterations in the spinal ganglion neurons in ageing rats. *Acta Neuropathol.*, **54**, 83–87.

Verret, L., Jankowsky, J.L., Xu, G.M., Borchelt, D.R. & Rampon, C. (2007): Alzheimer's-type amyloidosis in transgenic mice impairs survival of newborn neurons derived from adult hippocampal neurogenesis. *J. Neurosci.*, **27**, 6771-6780.

Wachs, F.P., Couillard-Despres, S., Engelhardt, M., Wilhelm, D., Ploetz, S., Vroemen, M., Kaesbauer, J., Uyanik, G., Klucken, J., Karl, C., Tebbing, J., Svendsen, C., Weidner, N., Kuhn, H.G., Winkler, J. & Aigner, L. (2003): High efficacy of clonal growth and expansion of adult neural stem cells. *Lab Invest.*, **83**, 949-962.

Wachs, F.P., Winner, B., Couillard-Despres, S., Schiller, T., Aigner, R., Winkler, J., Bogdahn, U. & Aigner, L. (2006): Transforming growth factor-beta1 is a negative modulator of adult neurogenesis. *J. Neuropathol. Exp. Neurol.*, **65**, 358-370.

Wang, R., Dineley, K.T., Sweatt, J.D. & Zheng, H. (2004): Presenilin 1 familial Alzheimer's disease mutation leads to defective associative learning and impaired adult neurogenesis. *Neuroscience*, **126**, 305–312.

Wang, M.C., Bohmann, D. & Jasper, H. (2005): JNK extends life span and limits growth by antagonizing cellular and organism-wide responses to insulin signaling. *Cell*, **121**, 115-125.

Wang, X., Chen, W.R. & Xing, D. (2012): A pathway from JNK through decreased ERK and Akt activities for FOXO3a nuclear translocation in response to UV irradiation. *J. Cell. Physiol.*, **227**, 1168-1178.

Wang, K., Long, B., Jiao, J.Q., Wang, J.X., Liu, J.P., Li, Q. & Li, P.F. (2012a): miR-484 regulates mitochondrial network through targeting Fis1. *Nat. Commun.*, **3**, 781.

Wang, C., Liang, C.C., Bian, Z.C., Zhu, Y. & Guan, J.L. (2013): FIP200 is required for maintenance and differentiation of postnatal neural stem cells. *Nat. Neurosci.*, **16**, 532-542.

Webb, A.E., Pollina, E.A., Vierbuchen, T., Urbán, N., Ucar, D., Leeman, D.S., Martynoga, B., Sewak, M., Rando, T.A., Guillemot, F., Wernig, M. & Brunet, A. (2013): FOXO3 shares common targets with ASCL1 genome-wide and inhibits ASCL1-dependent neurogenesis. *Cell Rep.*, **4**, 477-491.

Weigel, D., Jürgens, G., Küttner, F., Seifert, E. & Jäckle, H. (1989): The homeotic gene fork head encodes a nuclear protein and is expressed in the terminal regions of the Drosophila embryo. *Cell*, **57**, 645-658.

Winner, B., Lie, D.C., Rockenstein, E., Aigner, R., Aigner, L., Masliah, E., Kuhn, H.G. & Winkler, J. (2004): Human wild-type alpha-synuclein impairs neurogenesis. *J. Neuropathol. Exp. Neurol.*, **63**, 1155–1166.

Winner, B., Melrose, H.L., Zhao, C., Hinkle, K.M., Yue, M., Kent, C., Braithwaite, A.T., Ogholikhan, S., Aigner, R., Winkler, J., Farrer, M.J. & Gage, F.H. (2011): Adult neurogenesis and neurite outgrowth are impaired in LRRK2 G2019S mice. *Neurobiol. Dis.*, **41**, 706–716.

Winocur, G., Wojtowicz, J.M., Sekeres, M., Snyder, J.S. & Wang, S. (2006): Inhibition of neurogenesis interferes with hippocampus-dependent memory function. *Hippocampus*, **16**, 296–304.

Xuan, S., Baptista, C.A., Balas, G., Tao, W., Soares, V.C. & Lai, E. (1995): Winged helix transcription factor BF-1 is essential for the development of the cerebral hemispheres. *Neuron*, **14**, 1141–1152.

Yadirgi, G., Leinster, V., Acquati, S., Bhagat, H., Shakhova, O. & Marino, S. (2011): Conditional activation of Bmi1 expression regulates self-renewal, apoptosis, and differentiation of neural stem/progenitor cells in vitro and in vivo. *Stem Cells*, **29**, 700-712.

Yalcin, S., Zhang, X., Luciano, J.P., Mungamuri, S.K., Marinkovic, D., Vercherat, C., Sarkar, A., Grisotto, M., Taneja, R. & Ghaffari, S. (2008): Foxo3 is essential for the regulation of ataxia telangiectasia mutated and oxidative stress-mediated homeostasis of hematopoietic stem cells. *J. Biol. Chem.*, **283**, 25692-25705.

Yanagita, M. (2005): BMP antagonists: their roles in development and involvement in pathophysiology. *Cytokine Growth Factor Rev.*, **16**, 309-17.

Yilmaz, O.H., Valdez, R., Theisen, B.K., Guo, W., Ferguson, D.O., Wu, H. & Morrison, S.J. (2006): Pten dependence distinguishes haematopoietic stem cells from leukaemia-initiating cells. *Nature*, **441**, 475-482.

You, H., Pellegrini, M., Tsuchihara, K., Yamamoto, K., Hacker, G., Erlacher, M., Villunger, A., & Mak, T.W. (2006): FOXO3a-dependent regulation of Puma in response to cytokine/growth factor withdrawal. *J. Exp. Med.*, **203**, 1657–1663.

Yuan, Z., Becker, E.B., Merlo, P., Yamada, T., DiBacco, S., Konishi, Y., Schaefer, E.M. & Bonni, A. (2008): Activation of FOXO1 by Cdk1 in cycling cells and postmitotic neurons. *Science*, **319**, 1665-1668.

Zhang, C.L., Zou, Y., Yu, R.T., Gage, F.H. & Evans, R.M. (2006): Nuclear receptor TLX prevents retinal dystrophy and recruits the corepressor atrophin1. *Genes Dev.*, **20**, 1308-1313.

Zhang, C.L., Zou, Y., He, W., Gage, F.H. & Evans, R.M. (2008): A role for adult TLX-positive neural stem cells in learning and behaviour. Nature, 451, 1004-1007.

Zhao, C., Teng, E.M., Summers, R.G., Ming, G.L. & Gage, F.H. (2006): Distinct Morphological Stages of Dentate Granule Neuron Maturation in the Adult Mouse Hippocampus. *J. Neurosc.*, **26**, 3-11.

Zhao, J., Nassar, M.A., Gavazzi, I. & Wood, J.N. (2006a): Tamoxifen-inducible NaV1.8-CreERT2 recombinase activity in nociceptive neurons of dorsal root ganglia. *Genesis*, **44**, 364-371.

Zhao, M., Li, D., Shimazu, K., Zhou, Y.X., Lu, B. & Deng, C.X. (2007): Fibroblast growth factor receptor-1 is required for long-term potentiation, memory consolidation, and neurogenesis. *Biol. Psychiatry*, **62**, 381–390.

Zhao, J., Brault, J.J., Schild, A., Cao, P., Sandri, M., Schiaffino, S., Lecker, S.H. & Goldberg, A.L. (2007a): FoxO3 Coordinately Activates Protein Degradation by the Autophagic/Lysosomal and Proteasomal Pathways in Atrophying Muscle Cells. *Cell Metab.*, **6**, 472–483.

Zhao, C., Deng, W., & Gage, F.H. (2008): Mechanisms and functional Implications of adult neurogenesis. *Cell*, **132**, 645–660.